DENDRITIC NEUROTRANSMITTER RELEASE AND ITS MODULATION IN ACCESSORY OLFACTORY BULB CIRCUITS

by

Jason Brian Castro

BS, BA University of Rochester, 2000

Submitted to the Graduate Faculty of

Art and Sciences in partial fulfillment

of the requirements for the degree of

Doctor of Philosophy

University of Pittsburgh

2008

UNIVERSITY OF PITTSBURGH

FACULTY OF ARTS AND SCIENCES

This dissertation was presented

by

Jason Castro

It was defended on

10 March 2008

and approved by

Justin Crowley, Ph.D., Biology, Carnegie Mellon University

Bard Ermentrout, Ph.D., Mathematics, University of Pittsburgh

Karl Kandler, Ph.D., Neurobiology, University of Pittsburgh

External Examiner: Gordon Shepherd, MD, DPhil, Neurobiology, Yale University

Dissertation Chair: Steve Meriney, Ph.D., Neuroscience, University of Pittsburgh

Dissertation Advisor: Nathan Urban, Ph.D., Biology, Carnegie Mellon University

DENDRITIC NEUROTRANSMITTER RELEASE AND ITS MODULATION IN ACCESSORY OLFACTORY BULB CIRCUITS

Jason Castro, PhD

University of Pittsburgh, 2008

Dendrites are classically regarded as the brain's "listeners," while neuronal output is thought to be the exclusive privilege of the axon. Although we now appreciate the complexity of dendritic integration, the role of dendrites as output structures has received less attention. This is becoming an increasingly important topic, as the list of cell types with release competent dendrites continues to grow.

One boon of coupling dendritic activity to dendritic release is that outputs from a single neuron – typically thought to occur from fixed sites with stereotyped dynamics – may occur for signals of varying spatial extent, timecourse, and release efficacy. In essence, dendritic output may "inherit" the same diversity characteristic of events in excitable dendrites. Here I studied dendritic transmitter output and its modulation in cells of the accessory olfactory bulb – a CNS structure critical for processing species-specific chemical signals called pheromones. Because of the stereotypy of its inputs, the prevalence of dendritic transmitter release from its cells, and its well-defined outputs, the AOB offers a superb model system for studying the integrative and output properties of dendrites.

I first characterized basic excitable properties of the apical dendrites of mitral cells (the principal AOB neurons), and observed that they conduct non-decremental action potentials (APs). In addition to APs, these dendrites were also found to support compartmentalized, synaptically-evoked calcium spikes. Both APs and local spikes were triggers of dendritic

glutamate release and feedback inhibition, suggesting that neuronal output can be flexibly routed to particular populations of postysynaptic cells. I next asked whether the relative efficacy of particular dendritic events as triggers of transmitter release can be altered, as this could provide an additional level of control over single neuron output. I found that metabotropic glutamate receptors (mGluRs) play a key role in controlling dendritic output from AOB mitral cells and an obligatory role in concomitant feedback inhibition. This work culminates with the demonstration of a new principle of neuronal signaling: the ability of mGluRs to gate a transition between phasic and tonic dendritic transmitter release. Taken in total, these results extend our understanding of how the outputs from single neurons are controlled.

PREFACE

The work presented herein is based on several manuscripts that are published or in review. Two publications were truncated to form the body of work shown in chapter 2. These are:

Urban, N.N. and Castro, J.B. (2005) Tuft calcium spikes in accessory olfactory bulb mitral cells. *J. Neurosci* 25(20): 5024-8.

Castro, J.B. and Urban, N.N. Local dendritic calcium spikes in tufts of accessory olfactory bulb mitral cells evoke neurotransmitter release. *In review, Neuron*.

Chapter 3 is a modified version of:

Castro, J.B., Hovis, K.R., and Urban, N.N. (2007) Recurrent dendrodendritic inhibition of accessory olfactory bulb mitral cells requires activation of group I metabotropic glutamate receptors. J. Neurosci 27(21): 5664-71.

Chapter 4 is based on:

Castro, J.B., and Urban, N.N. MGluR activation selectively enhances graded glutamate release from mitral cell dendrites. *Under revision, Neuron*.

ACKNOWLEDGEMENTS

First and foremost, I wish to thank my parents for their their constant support and for encouraging me always follow my heart. Even when the trials of science and graduate school seemed mysterious to them, they stood by me and offered their words of wisdom. This is for you.

My advisor, Nathan Urban, must also be thanked up front. From my first days in the lab, Nathan treated me as a colleague. He always let me find my own way and pursue the projects I found most interesting or fruitful. In addition to this freedom I felt I had as a student, I also always knew that I could count on Nathan's support, insight, and complete involvement in my work. In many respects, Nathan serves as my model of what a scientist and mentor should be – I am proud to come out of his lab and to have been his student.

Steve Meriney, my committee chair, introduced me to neurophysiology years before graduate school when I was a summer undergraduate fellow, and convinced me that Pittsburgh was a great place to live and do science. His calm and careful approach to work has been a great inspiration, and I still try to emulate it. I am also indebted to the other members of my committee – Karl Kandler, Justin Crowley, and Bard Ermentrout - for their invaluable insight and advice at many points during graduate school. I would also like to thank my outside examiner, Gordon Shepherd, for being involved in my thesis defense – it was a great privilege to share my work with him and hear his perspectives.

Many friends and colleagues have made my years in graduate school memorable and exciting ones. Abigail Kalmbach always lent an ear and open arms when I was confused or frustrated, and I am unlikely to forget our bar-b-queing adventures. Vikrant Kapoor – a fellow graduate student in Nathan's lab – was a great friend and "rigmate" for these last few years. We talked equal parts life and science, and I learned much (in both domains) from him. Krishnan "the Raji" Padmanabhan was also a partner in crime for all of grad school. He was a steadfast friend during difficult and challenging times, and consistently enlightened me with his insights into science and art. I will miss our many conversations at strange hours.

My graduate years were spent almost entirely in the Great Hall of Brain Science (the "GHBS") – a wonderful melting pot of personalities and intellectual styles tucked away in the

basement of Mellon Institute. I truly felt like I was part of something special and exciting when I showed up for work, and will miss the company of kindred spirits in the GHBS.

Finally, I would like to acknowledge the individuals who helped me with the work presented in this thesis. Nathan Urban first discovered and characterized the tuft calcium spikes described in the early part of Chapter 2. The electron microscopy data shown in Chapter 2 was collected by Matt Angle - an undergraduate in Nathan's lab – under the guidance of Joe Suhan. Ken Hovis contributed to the work on recurrent inhibition (Chapter 3), and did some of the experiments to determine whether DHPG was acting via mGluR1 or mGluR5. Sam Behseta and Rob Kass suggested the use of BARS (Bayesian Adaptive Regression Splines) for testing the statistical independence of two functions (Chapter 4).

This work was supported financially by an NSF IGERT grant, an NIH training grant, and an NRSA predoctoral fellowship.

LIST OF ABBREVIATIONS

AOB – Accessory olfactory bulb

AOS – Accessory olfactory system

AP – Action potential

BAP – Backpropagating action potential

BNST – Bed nucleus of the stria terminalis

CNS – Central nervous system

DAG – Diacyl-glycerol

EPP – End plate potential

GC – Granule cell

HVA – high voltage activated

LH – Leutenizing hormone

LHRH – Leutenizing hormone releasing hormone

LVA – low voltage activated

mCoA – medial cortical amygdala

mGluR – Metabotropic glutamate receptor

MHC – Major histocompatability complex

MOB – Main olfactory bulb

MPO – Medial preoptic (nucleus)

MUP – Major Urinary Protein

NAOT – Nucleus of the accessory olfactory tract

ON – Olfactory nerve

ORN – Olfactory receptor neuron

OSN – Olfactory sensory neuron

PG – Periglomerular (cell)

PMN – premammillary nucleus

pmCoA – posteromedial cortical amygdala

SN – substantia nigra

SON – Supra-optic nucleus

TRP – Transient receptor potential

VMN – ventromedial nucleus

VN – Vomeronasal nerve

VNE – Vomeronasal epithelium

VNO – Vomeronasal organ

VNx – Vomeronasal nerve lesion

VRN – Vomeronasal receptor neuron

VSN – Vomeronasal sensory neuron

TABLE OF CONTENTS

LIST OF FIGURES

1.0 INTRODUCTION

1.1 PHEROMONE DETECTION AND THE VOMERONASAL SYSTEM

The abilities to detect, discriminate, and respond to chemicals with appropriate behaviors are critical to survival. Although chemosensation is sometimes regarded as an aesthetic or "supplemental" sense in humans, chemical compounds and mixtures are the principal cues most animals use to identify objects ranging from food to prey to potential mates. Clearly, being able to differentiate between such stimuli is adaptive, and evolution has selected for dedicated sensory systems to process information about both volatile and nonvolatile environmental chemicals.

Chemical sensation in most mammals is mediated by two parallel olfactory systems - the main olfactory system (MOS), and the vomeronasal (or accessory olfactory) system (AOS). Early comparative approaches suggested that the AOS evolved in terrestrial animals as a specialization for detecting nonvolatile odorants (Broman, 1920), but more recent findings – especially of vomeronasal structures in fully-aquatic amphibians (Eisthen et al., 1994) - contradict this idea. More modern comparisons between the MOS and AOS emphasize differences in their relative response specificities, particularly for natural, ethological stimuli. Typically, the MOS is thought to function as a general-purpose chemical analyzer that detects a broad range of chemically diverse stimuli, while the AOS responds to a comparatively small set of (mostly nonvolatile) chemicals, called pheromones, that convey species-specific messages to elicit pre-programmed behaviors or endocrine responses (reviewed in (Dulac and Torello, 2003)). Although recent work has shown important exceptions to this strict dichotomy (Sam et

al., 2001;Schaefer et al., 2001;Trinh and Storm, 2004;Xu et al., 2005;Kobayakawa et al., 2007), it remains useful for interpreting physiological differences between MOS and AOS receptors, cells, and neural circuits.

The appeal of studying AOS function is that its processing stream is strikingly compressed: only two or three synapses separate the vomeronasal periphery from presumed effector structures, such as the amygdala and hypothalamus, and few centrifugal projections feed back to earlier AOS processing areas (Kevetter and Winans, 1981;Meisami and Bhatnagar, 1998). How is information about pheromones, which include complex and specific chemical blends, integrated in such a short trisynaptic circuit? The answer may partially lie in the specialized synaptic interactions that occur among neurons of the accessory olfactory bulb (AOB) – the first CNS structure in the AOS pathway.

One of the striking aspects of AOB organization is its subdivision into small-scale functional circuits defined by local synaptic interactions between the dendrites of principal neurons and interneurons (Taniguchi and Kaba, 2001;Jia et al., 1999a). It has been suggested that these synaptic motifs, sometimes described as "microcircuits" (Shepherd, 1978;Murphy et al., 2005), allow small sub-neuronal networks to perform complex operations even in the absence of somatic spikes. One major boon of such fine-scaled processing is that compartmentalized and prolonged dendritic integration can occur in principal neurons prior to spike initiation. Thus, dendritic integration and transmitter release processes that introduce such a "safety factor" for axonal spiking may be critical for brain structures where small numbers of spikes (or low rates of spiking) are likely to be behaviorally relevant. Since AOB principal neurons have low basal firing rates, and can take seconds to respond to stimuli (Luo and Katz, 2004), it is likely that AOB synaptic processing is tailored to ensure "accuracy," possibly at the expense of speed.

The remainder of this introduction has three major goals. The first is to describe behavioral and ethological aspects of AOS function to illustrate biological computations at the center of AOS processing. The second is to summarize what is known about AOS anatomy, physiology, and function, with an emphasis on features most relevant for AOS sensitivity and selectivity. The third is to describe attributes of dendritic excitability and synaptic transmission – particularly dendrodendritic transmission – that are likely critical to AOS and AOB function.

1.1.1 Role of the vomeronasal system in pheromonally mediated behaviors

1.1.1.1 Lesion studies

The earliest controlled studies on mammalian vomeronasal function were done by Powers and Winans in 1975. In previous work, these investigators had shown that infusions of $ZnSO_4$ in the main olfactory epithelium of hamsters resulted in widespread degeneration of main olfactory bulb (MOB) glomeruli, with relatively little diminishment of sexual (mounting) behavior in male hamsters (Powers and Winans, 1973;Borer et al., 1974). By contrast, deafferentation of the vomeronasal nerve (VN) produced pronounced deficits in mounting, and complete bulbectomy (which disrupts processing by *both* the MOS and AOS) eliminated male sexual responses altogether.

Subsequent work by these same investigators and others indicated that the vomeronasal-dependent effects on sexual behavior were likely due to release of pituitary hormones. Coquelin et al (1984) indirectly investigated the effect of vomeronasal activity on hypothalamic/pituitary function by monitoring blood plasma-levels of leutenizing hormone (LH) in sexually experienced males. Elevations of LH in VN-lesioned (VNx) animals were elicited by direct exposure to females, but not by female urine, while in sham animals both stimuli evoked a reflexive LH surge. In addition, it was also shown that sexual activity in VNx animals could be restored by injections of leutenizing hormone releasing hormone (LHRH), and that the LH promoting, vomeronasal dependent effects of urine were isolated in a high-molecular weight fraction (Clancy et al., 1984).

The above studies describe examples of "releaser" effects of pheromones, in which exposure to particular chemicals leads to immediately observable behaviors (mounting, aggression, avoidance, etc.). In addition to such short-latency, transient effects, pheromones can also induce "primer" responses, in which endocrine or reproductive state is altered over longer time scales without necessarily producing overt behaviors. The best studied examples of primer pheromone responses include the Whitten effect – in which estrus is advanced among unisexually grouped females (Kaneko et al., 1980), and the Bruce effect - in which pregnancy is aborted when recently mated females are exposed to pheromones of a non-stud male (Bruce and Parrott, 1960). Although releaser effects were documented before primer effects, their

dependence on vomeronasal function was demonstrated relatively late. While investigating the neural basis of the Bruce effect, Lloyd-Thomas and Keverne discovered that the Bruce effect persisted after lesions of the main olfactory epithelium. By contrast, destruction of the vomeronasal organ eliminated the ability of male pheromones to block pregnancy (Lloyd-Thomas and Keverne, 1982). Later studies by Kaba et al showed that temporary infusions of lignocaine into the accessory olfactory bulb of recently mated females disrupted the Bruce effect, such that stud-male pheromones were capable of blocking pregnancy(Kaba and Keverne, 1988).

Taken together, these early studies on both releaser and primer pheromones argued for a basic theory of mammalian vomeronasal function in which specific urine compounds activate the vomeronasal system, which in turn leads to changes in endocrine state to elicit innate sexual and courtship behaviors.

1.1.1.2 Genetic knockout studies

Many of the claims made in this early work were re-investigated recently using molecular approaches. The benefit of these techniques is that they allow functional ablation of VNO efferents without the interpretive complications associated with partial or incomplete VN lesions, or post-operative scarring and ischemia. Such selective dissociation of main versus accessory olfactory system function was made possible by the fortuitous discovery that vomeronasal receptor neurons (VRNs) use a transduction mechanism unrelated to that in main olfactory receptor neurons (Berghard et al., 1996;Liman et al., 1999).

By knocking out the TRP2C gene in mice, which encodes a cation-selective channel expressed only in VRNs and the testes, Stowers et al (2002)., and Leypold et al (2002) showed dramatic changes in a number of innate rodent behaviors. Specifically, TRP2C-/- male mice showed reduced intruder aggression, and indiscriminate mounting of both males and females. Likewise, TRP2C-/- female mice showed reduced maternal aggression and, surprisingly, mounting of conspecific males. This has lead to a revised view of accessory olfactory function in which the vomeronasal organ is not seen as responsible for actively triggering sexual behaviors, but rather exerts top-down discriminatory control over latent sexual behaviors (Kimchi et al., 2007).

1.1.2 The nature of pheromonal stimuli

The term 'pheromone' was originally coined by Karlson and Luscher in 1959 to describe substances "released by an individual, and received by another individual of the same species, in whom they activate specific physiological or behavioural responses." Pheromones were proposed to include compounds that functioned as sexual attractants, and early-on were described by analogy with hormones. Like hormones, they were presumed to be biologically active at minute concentrations, and were believed to influence behavior principally through activation of the hypothalamus and pituitary. The original Karlson – Luscher definition of pheromones was largely operational though, and left open the question of their physical and chemical identity.

1.1.2.1 Simple compounds

The earliest successes in establishing a strong correspondence between distinct chemicals and robust, pre-programmed behaviors were in insects, with the work of Butenandt being most notable. In a series of painstaking experiments that pre-dated gas chromatography or mass spectometry, Butenandt and colleagues determined that a single 16-carbon alcohol, later named bombykol, was responsible for the sexual attractiveness of pheromones released from the scent sacs of the female silkworm moth, Bombyx Mori (Butenandt et al., 1961b;Butenandt et al., 1961a). In addition to providing the first pheromone structure, Butendant's work also highlighted the extraordinary sensitivity and selectivity of pheromone detection: synthesized compounds closely related to Bombykol failed to elicit sensitive responses in a bioassay, while the active Bombykol fraction was effective at concentrations as low as 10^{-9} μg/L.

Since this work, several "simple" mammalian pheromones have been isolated and synthesized from urine as well as facial and anogenital glands. These substances range from small single molecules, to small peptides, to large (~20 kDA) proteins. The first mammalian pheromone identified was dimethyl-disulfide, found in the active fraction of hamster vaginal secretions, which was capable attracting conspecific males (Singer et al., 1976). Similar, simple compounds have also been found to elicit innate responses in other mammals. The nipple-search behavior of rabbit pups during parturition, for example, was shown to be dependent on the single

chemical 2 methyl- but- 2 enal (Teicher et al., 1980;Schaal et al., 2003), and the single chemical (methylthio)methylthione (MTMT) can enhance the attractiveness of male urine to female mice (Lin et al., 2005).

1.1.2.2 Chemical mixtures as pheromones

Later work by Novotny et al. described the first example of mammalian multi-component pheromones (Novotny et al., 1984;Novotny et al., 1985). These investigators synthesized two androgen dependent compounds from male mouse urine (2-sec-butyl dihydrothiazole (SBT), and dehydro-exo-brevicomin (DHB)), and tested their efficacy in eliciting male aggression when added to the urine of castrated males. Interestingly, castrated male urine alone, or urine spiked with each compound alone failed to promote male aggression. Urine spiked with both components in approximately equal amounts, however, was nearly as effective as urine from control mice. There also appear to be sex and age-dependent effects in the processing of these chemicals. SBT or DHB alone can accelerate the onset of puberty in young females, while a mixture of the two compounds induces estrus in mature females.

In the studies described above, the pheromonally active fraction was generally found to contain small organic compounds. This raised basic questions about questions about whether vomeronasal function is involved in these behaviors, since physical considerations suggest that pheromones should be nonvolatile (the vomeronasal organ is a blind-end fluid filled tube, and stimuli are delivered to it via an active pumping mechanism through the vomeronasal duct). Moreover, recent work indicates that detection of pheromones conveying information about strain and gender in mice requires direct physical contact (Luo et al., 2003).

Some of the earliest work investigating VN-dependent behaviors suggested that pheromonally active components of urine were contained in a high molecular-weight fraction (Clancy et al., 1984). In addition, initial work by Vandenbergh and Lombardi partially isolated a mammalian pheromone and found it to be "heat labile, nondialysable, precipitatable with ammonium sulphate, and […] not extractable in ether," indicating it was likely proteinaceous (Vandenbergh et al., 1975). One resolution of this apparent discrepancy came with the discovery of aphrodisin, a 17 kDA lipocalin isolated from hamster vaginal discharges that was found to arouse males (Singer et al., 1986b). Later work indicated that aphrodisin was only one of many so-called Major Urinary Proteins (MUPs) – a highly polymorphic protein family that showed

strain specific expression in mice (Bocskei et al., 1992). Recent estimates indicate that MUPs may constitute up to 99% of the protein content of rodent urine (Humphries et al., 1999).

1.1.2.3 Pheromones conveying individual identity

The discovery of MUPs ushered in a renewed interest in vomeronasal function, since these proteins appeared to be a candidate non-volatile, multi-component stimulus set whose differential expression could convey information about strain, gender, and possibly individual identity among mice (Sherborne et al., 2007;Cheetham et al., 2007). There is still some debate over whether MUPs are themselves pheromonal stimuli, or merely carriers of smaller molecules that actually convey biological signals (Chamero et al., 2007). In the initial discovery of aphrodisin, care was taken to remove possible ligands in tests of its biological efficacy, suggesting its direct role as a pheromone (Singer et al., 1986a). Later work called this into question, and investigations of the tertiary structure of lipocalins showed a potential ligand binding groove in its beta barrel (Bocskei et al., 1991; Bocskei et al., 1992). Very recent work has again suggested that MUPs can elicit pheromone-like effects in the absence of bound ligands (Chamero et al., 2007).

A parallel line of research has expanded the repertoire of pheromone-mediated behaviors to include identification of individuality among conspecifics. Work by Yamakazi, Beauchamp and others showed that the urine-odors of mice were strain-dependent, and could be discriminated by mice in a Y-maze behavioral test (Yamazaki and Beauchamp, 2007;Yamazaki et al., 1988;Yamazaki et al., 1984;Yamazaki, 1982). Moreover, it was found that the critical determinant of individuality was conveyed by the H2 locus of the major histocompatibility complex (MHC)- a diverse gene family involved in immuno-recognition.

Regardless of the specifics of how individuality is conveyed, these studies indicate that the neural circuitry underlying pheromone detection has considerable “resolving power”, and is capable of remarkably fine discriminations. Because of the large and differential expression of MUPs, and the high variability at the H2 MHC locus, it is unlikely that individual identity is conveyed by single compounds. Rather, these studies argue for a system capable of resolving subtle differences in the individual components of a multi-dimensional stimulus blend. The ability to do this has been demonstrated in a number of species, with the most well studied examples again being in insects. Carpenter ants, for example are able to differentiate nestmates

from non-nestmates by detecting differences in the ratios of ~ 20 cuticular hydrocarbons (Ozaki et al., 2005), while certain species of moth only respond to precise mixtures of compounds in a pheromone blend (Hildebrand, 1995). Evidence of such phenomena in mammals is intriguing, though somewhat less abundant. During parturition, lactating sheep are able to recognize their own lambs though olfactory cues (Keverne and Brennan, 1996). In addition, one recent report suggests that female elephants respond preferentially to particular chiral mixtures of frontalin enantiomers present in secretions from males (Greenwood et al., 2005).

1.2 ORGANIZATION OF THE VOMERONASAL SYSTEM

1.2.1 Vomeronasal organ

The best-studied structures of the vomeronasal/accessory olfactory system are the vomeronasal organ (VNO) and the accessory olfactory bulb. The VNO, first discovered by Jacobson in 1813 (Broman, 1920), is a blind-end capsule located, in rodents, in the ventral aspect of the nasal septum. This structure contains a sensory receptor epithelium which, when viewed in coronal section, appears crescent-shaped with its concave aspect oriented toward a midline lumen. Running rostro-caudally along the lumen is a blood vessel that can regulate the relative pressure inside the vomeronasal cavity, controlling ligand access to the epithelium. Unlike the main olfactory epithelium in the nasal cavity, which can have relatively passive access to volatile stimuli, vomeronasal stimuli must be actively delivered to the VNE via a pumping mechanism regulated both by behavioral state (likely via adrenergic input) and seasonally (Meredith and O'Connell, 1979). Artificial stimulation of the nasopalatine nerve is also sufficient to activate the pumping mechanism (Meredith and O'Connell, 1979). Because of this requirement for active stimulus sampling, and the fact that many pheromonal stimuli are non-volatile, vomeronasal sensation in rodents is believed to require direct physical contact between the snout and a pheromone source (but see (Trinh and Storm, 2003)).

1.2.2 Sensory neurons and stimulus transduction

The vomeronasal epithelium is composed of two distinct layers of bipolar sensory neurons. Neurons in both layers extend a single long dendrite oriented toward the VNO lumen, which terminates in a knob studded with microvilli – the sites of stimulus transduction. As is the case with ORNs, VRNs are believed to each express only a single receptor type (Vassar et al., 1993;Mombaerts, 2004). Sensory neurons in the apical portion of the epithelium (closest to the lumen) express receptors of the V1R family, and project their axons centrally to the anterior aspect of the accessory olfactory bulb (Fig. 1, (Jia et al., 1997)). The V1Rs number about 150, and can be subdivided into 12 families on the basis of sequence homology (Dulac and Axel, 1995;Del Punta et al., 2000). Intriguingly, the relative genomic distances between these families may be represented centrally in the AOB as spatial distances between glomeruli – discrete sites of VRN axon termination (Wagner et al., 2006b). Targeted deletion of two V1R subfamilies (the V1Ra's and the V1Rb's) in mice has recently been shown to eliminate physiological and behavioral responses to select putative pheromones (Del Punta et al., 2002a).

Neurons in the basal portion of the epithelium express a different family of receptors, known as V2Rs (numbering ~ 50-100), and project to the posterior aspect of the AOB (Jia et al., 1997). Far less is known about the V2Rs, and no genome-wide draft exists yet for these receptors. Although both V1Rs and V2Rs encode 7 transmembrane G-Protein coupled receptors (GPCRs), they share little homology with each other, or with odorant receptors. V2Rs are notable for having large extracellular N-terminal domains, which are argued to be important for the detection of MUPs or small peptides signaling individuality via MHC profile (Ryba and Tirindelli, 1997;Tirindelli et al., 1998).

Likewise, the transduction mechanism between VRNs and ORNs differ substantially. ORN transduction is dependent on a variant of Gα known as G_{olf}, and uses adenyl cyclase III as a second messenger to activate cyclic nucleotide gated channels (Reed, 1992;Ronnett et al., 1993;Ronnett and Snyder, 1992), while VRN transduction is mediated by $G\alpha_o$ in V1R expressing cells, and $G\alpha_i$ in V2R expressing cells (Berghard et al., 1996;Berghard and Buck, 1996). In addition, VRN transduction uses diacyl-glycerol (DAG) as a second messenger to activate a nonspecific cation conductance mediated by TRP2C channels (Lucas et al., 2003). Relatively little comparative physiology has been done to explore differences in the intrinsic

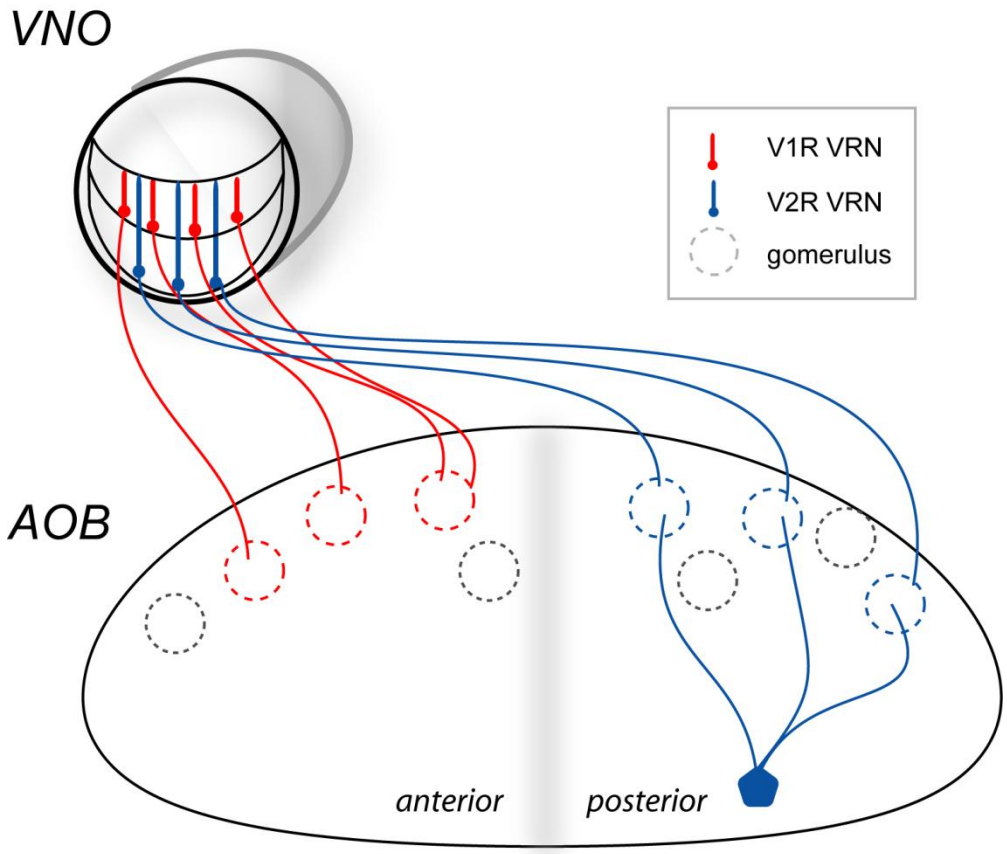
VNO
V1R VRN
V2R VRN
gomerulus
AOB
anterior
posterior

Figure 1. Inputs to the accessory olfactory bulb. AOB inputs originate in the vomeronasal organ (VNO), which contains a two-layered sensory epithelium. The apical layer of this epithelium contains vomeronasal receptor neurons (VRNs) expressing receptors from the V1R family (red). These receptor neurons project axons to the anterior aspect of the AOB, where they terminate in discrete regions of neuropil called glomeruli (dashed circles). The basal layer of the vomeronasal epithelium contains sensory neurons expressing receptors from the V2R family, which differs substantially from the V1Rs (described in text). V2R-expressing **receptor** neurons project to the posterior AOB. The principal neurons of the AOB are mitral cells (blue), which project several principal neurons to distinct glomeruli. All of the excitatory VRN input to a given mitral cell occurs onto its dendritic tufts, in the glomerular layer.

excitability of ORNs and VRNs, with the notable exception of work by Liman and Corey (1996). The most intriguing difference between these two receptor-neuron types is in their responses to steady current injection: ORNs fire only a handful of spikes immediately following stimulation and rapidly undergo depolarization block, while VRNs have a near-linear F-I curve. This observation is also supported by multi-electrode recordings from the VNE showing that VRN responses to increasing concentrations of urine are non-adapting and well described by a first-order kinetic model relating ligand binding to firing rate (Holy et al., 2000).

The most conspicuous feature of VRNs is their extraordinary response specificity. Unlike ORNs, which typically respond to broad panels of related odorants, individual VRNs appear to be activated by only a single ligand (Leinders-Zufall et al., 2000). Moreover, this specificity appears to be independent of ligand concentration. In experiments in which VRN calcium dynamics were monitored *in vitro* in Fura-loaded VNE slices, presentation of single pheromones activated well-defined subsets of VRNs that were invariant over several orders of magnitude of stimulus concentration. Moreover, no single VRN appeared to respond to more than one pheromone. These and related data have been used to argue that pheromone processing in the vomeronasal system relies a labeled line coding strategy in which the activity of particular nerve fibers unambiguously conveys information about presence of particular stimuli (Luo and Katz, 2004). Although more work is required before concluding that this is in general true, the specificity of VRN responses greatly simplifies the interpretation of experiments investigating integration and processing by neurons postsynaptic to VRNs (see **sections 1.2.3 & 1.2.4**).

1.2.3 Inputs to the AOB

The axons of VRNs fasciculate, coarse through the cribrifrom plate via the dorsal aspect of the main olfactory bulb, and enter the accessory olfactory bulb as the vomeronasal nerve. Once in the AOB, VRN axons defasciculate in to multiple bundles which each converge onto small, roughly spherical regions of neuropil called glomeruli (reviewed in Meisami and Bhatnagar, 1998). There are several hundred AOB glomeruli in rodents, which range in diameter from 30-50 microns- somewhat smaller (and less well-defined) than those observed the main

olfactory bulb. Although glomeruli are sites of axonal convergence, this convergence factor is estimated to be ~ 10 fold smaller than in the MOB, and may be an important factor in determining the sensitivity and selectivity of AOB function. Golgi histology also suggests that patterns of axon termination within single glomeruli can be variable: labeled VSN axons can either innervate a glomerulus densely and homogenously, or in a small sub-glomerular domain. The function of these different innervation patterns remains unknown (Takami and Graziadei, 1990;Takami and Graziadei, 1991).

At present there is some debate on the molecular homogeneity of VRNs that innervate a single glomerulus. Early work using transgenic mice, in which axons of a single receptor class were modified to express LacZ, showed small, punctate regions within single LacZ+ glomeruli that were NCAM (or synaptotagmin) positive, but LacZ negative, suggesting that axons of multiple receptor types terminated within single glomeruli (Belluscio et al., 1999). More recent work has suggested that afferents to a given AOB glomerulus are from VRNs all of the same type (Del Punta et al., 2002b). In general, the axons of a single VRN type project to between 10-20 glomeruli, and there appears to be somewhat less stereotypy in the AOB glomerular map than in the main olfactory bulb (Belluscio et al., 1999).

1.2.4 Intrinsic circuitry of the AOB

Postsynaptic to VRNs are mitral cells, the principal AOB neurons. The somata of these cells are between 10 and 20 micrometers long, and are notable for extending multiple (between 2-10), smooth principal dendrites (Figs. 2 & 3), each of which terminates in a glomerulus in a ramified structure known as a tuft. In contrast to pyramidal cells or other CNS neurons, which receive inputs diffusely across their dendritic trees, glutamatergic input to AOB mitral cells occurs only at their tufts. Moreover, the inputs to a given tuft are in principle known: each mitral cell tuft integrates the convergent input from axons of a single (or few) receptor type(s).

Mitral cell morphology remains relatively poorly studied (in the AOB, at least), though Graziadei and colleagues have suggested a rudimentary classification scheme for these cells. At the coarsest level, these researchers first described the glomerular arbors of AOB mitral cell dendrites as either simple or complex. Most (~70%) arbors were simple – that is, composed of a

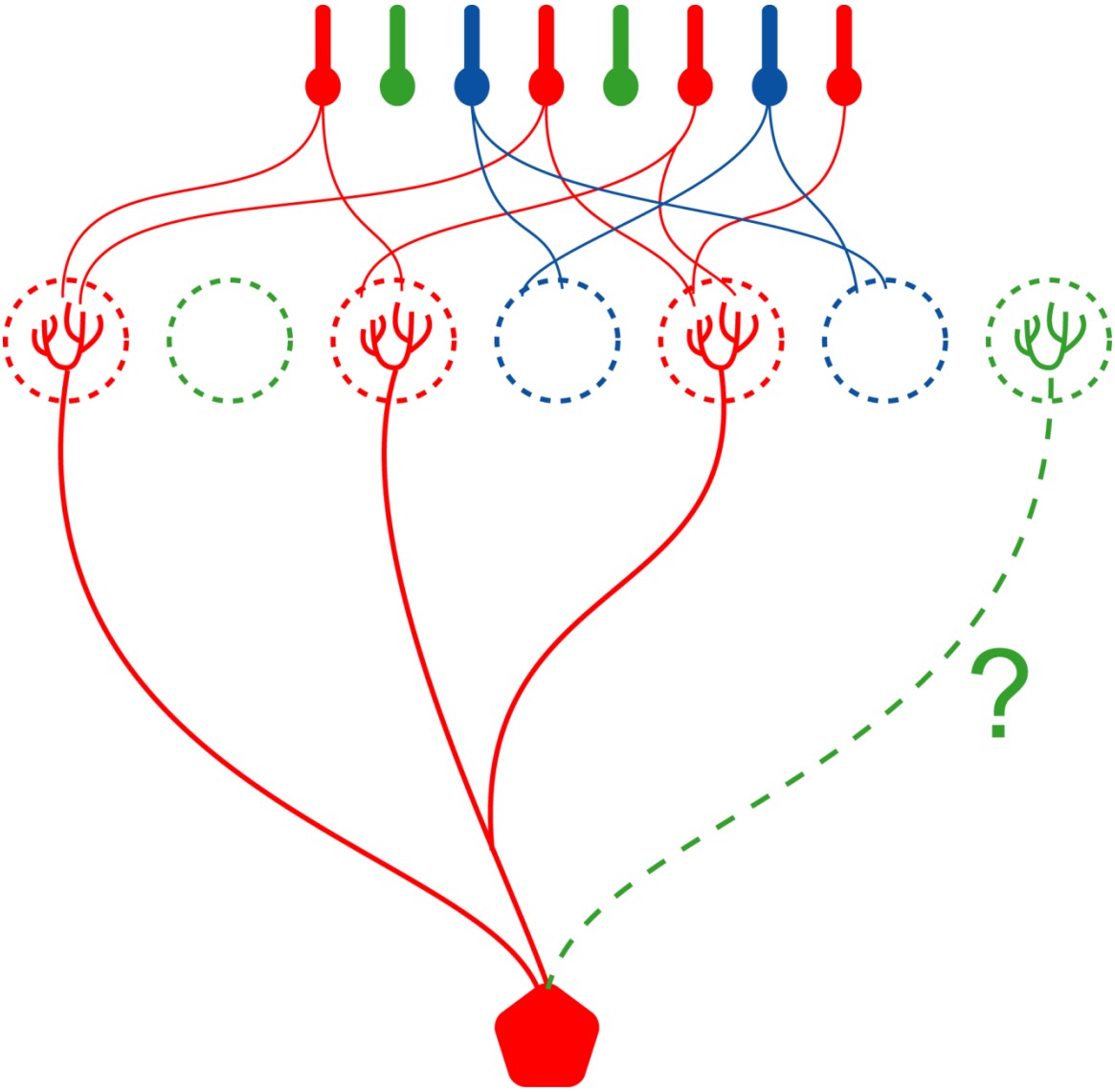

Figure 2. Homotypic and heterotypic connectivity of AOB mitral cells. Glomeruli (dashed circles) are sites of axonal convergence of vomeronasal receptor neurons (cells at the top of the figure). Each glomerulus receives input from receptor neurons expressing the same receptor type (indicated by the color of the receptors shown at the top of the figure), and is hence a discrete region dedicated to processing "labeled" information from a molecularly homogeneous population of receptors. There are at present two models described for patterns of mitral cell-glomerulus connectivity: homotypic connectivity, and heterotypic connectivity. Under the homotypic connectivity hypothesis, all of the principal dendrites from a given *mitral cell* (shown at bottom) contact glomeruli receiving inputs from the same receptor type (shown as red dendrites terminating in red glomeruli). The heterotypic connectivity hypothesis asserts that mitral cell principal dendrites may receive inputs from glomeruli innervated by different receptor types (green dashed dendrite).

single tuft - while the remaining glomerular arbors were formed by two or more tufts converging on a common glomerulus (Takami and Graziadei, 1990;Takami and Graziadei, 1991). In addition to these gross termination patterns, mitral cells were also found to differ considerably in the fine structure of their tufts, which were divided into three groups: baskets (small, or ovoid shaped tufts), balls of yarn (large tufts with looped dendrites), and bushes (dense tufts with irregular processes). Interestingly, these investigators found considerable heterogeneity in the glomerular volume occupied by a single tuft, with some tufts sequestered in sub-glomerular domains, and others filling their target glomerulus completely. No work to date has followed up on the physiological consequences of these variable termination patterns.

One issue that has garnered attention recently is the question of whether all the tufts of a given mitral cell contact glomeruli of the same molecular identity – that is, receiving inputs from the same receptor type. There are no definitive answers to this question yet, and the answer may depend in part on which receptors (V1R or V2R, or specific families within these classes) are studied. Work from the Mombaerts lab (Del Punta et al., 2002b) has recently offered support for a so-called homotypic connectivity model, in which the principal dendrites of a given mitral cell all project to glomeruli of the same molecular identity (Fig. 2). By contrast, earlier work from this same lab (Rodriguez et al., 1999), as well as more recent work from the Dulac lab (Wagner et al., 2006b), suggests that mitral cell dendrites terminate in more than one type of glomerulus (Fig.2). In the original terminology proposed by Mombaerts, this was described as heterotypic connectivity.

Regardless of which of these models is correct, the multiglomerular dendritic projections of AOB mitral cells offers a superb opportunity to investigate and test hypotheses on the local control of synaptic integration on small spatial scales and within well-defined dendritic compartments. Perhaps the most intriguing aspect of heterotypic connectivity is that it provides a ready anatomical means by which single mitral cells could integrate information about multi-component pheromone blends. Under this scheme, mitral cells may operate as "blend detectors" that receive information about different stimulus components. Consistent with this, recent *in-vivo* work by Katz and Luo (2003) has shown that some single mitral cells respond only to particular combinations of strain and gender. Since it is unlikely that single, ultraspecific molecules convey information about both sex and strain, one possibility is that information about multidimensional pheromones is integrated at the level of single mitral cells, across their multiple tufts.

a


1
2
3
4
5
6
50 µm

b

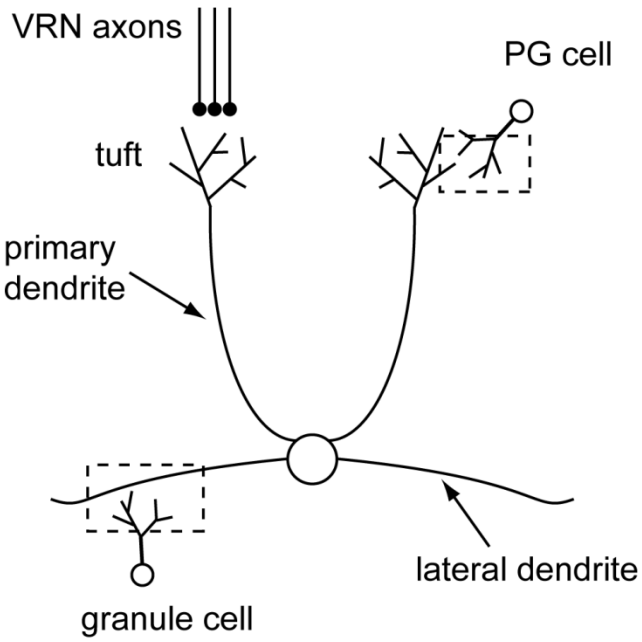
VRN axons
PG cell
tuft
primary dendrite
lateral dendrite
granule cell

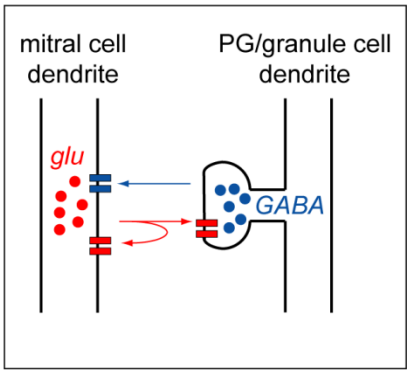
mitral cell dendrite
PG/granule cell dendrite
glu
GABA

Figure 3. Intrinsic circuitry of the AOB. a) Neurolucida reconstruction of an AOB mitral cell showing its numerous principal dendrites. Putative individual tufts are numbered. **b)** All of the excitatory vomeronasal receptor neuron (VRN) input to a given mitral cell occurs at its tufts, up to several hundred microns from the soma. Both the primary and lateral dendrites of mitral cells form reciprocal dendrodendritic synapses with local interneurons (PG cells and granule cells). The dendrites of periglomerular (PG) cells form synapses with mitral cell tufts, while the dendrites of granule cells form synapses with mitral cell lateral dendrites. Sites of dendrodendritic communication are demarcated by the dashed boxes, and are schematized in the box on the right. *Boxed Region:* Excitation of a mitral cell dendrite evokes dendritic glutamate release, which can be detected by AMPA/NMDA receptors on the same dendrite, or by receptors on a postsynaptic interneuron. Glutamatergic excitation of the PG/granule cell dendrite can in turn evoke GABA release from these interneurons to inhibit mitral cells in a local and reciprocal fashion.

The dendrites of AOB mitral cells are presynaptic to two major classes of local interneurons: periglomerular (PG) cells, and granule cells. Mitral cells communicate with both interneuron types via reciprocal dendrodendritic synapses. The ultrastructure and physiology of these atypical synapses have been studied extensively in the MOB, but are far less well described for the AOB. Thus, the data described in the remainder of this section (**1.2.4.**) are from MOB, and their relevance for AOB function is assumed by homology, unless otherwise noted. Anatomically, reciprocal connections are observed as the close apposition of two regions of dendritic membrane (mitral cell and interneuron) with a pair of oppositely oriented synapses separated by a few hundred nanometers (Rall et al., 1966;Price and Powell, 1970a;Price and Powell, 1970b). The synapse from the mitral cell to interneuron is asymmetric, (Gray type 1), while the neighboring 'partner' synapse – from interneuron to mitral cell – is typically symmetric (Gray type 2). Glutamate released from mitral cell dendrites depolarizes postsynaptic interneurons, which in turn locally inhibit mitral cell dendrites by release of GABA (Jia et al., 1999b;Taniguchi and Kaba, 2001). Properties of dendritic excitability and dendritic release relevant to the function of this synapse are discussed in **section 1.3.**

In the MOB, the somata of PG cells are arranged in semilunar shells around glomeruli, though in the AOB, these shells are somewhat less distinct and concentrated along the deeper aspect of the glomerular layer (closer to mitral cell somata). PG cells generally have short axons (Pinching and Powell, 1971a;Pinching and Powell, 1971b;Pinching and Powell, 1971c), and are typically GABA-ergic and/or Dopaminergic (Halasz et al., 1982;Gall et al., 1987;Kosaka et al., 1988;Maher and Westbrook, 2008). Several patterns of dendritic arborization have been described for these cells, with a common morphology being the partial filling of a single glomerulus by a claw-like dendritic tree. PG cell physiology has not been studied in great detail, but it is known that these cells support low-threshold spikes (McQuiston and Katz, 2001), which are mediated in part by an L-type Calcium channel (Murphy et al., 2005). In addition to receiving input from mitral cell dendrites, some PG cells also receive direct sensory neuron innervation (Kasowski et al., 1999;Toida et al., 2000), and can participate in triadic synaptic interactions with sensory nerve terminals and mitral cell tufts. PG cells may play a particularly important role in the integration of VSN inputs by AOB mitral cells, since they are effectively positioned to deliver tuft-specific inhibition. One possibility is that each tuft of a multitufted

mitral cell is associated with relatively independent sets of PG cells, allowing each tuft to operate as an independent processing module.

Granule cells (GCs) occupy a distinct layer in both the main and accessory olfactory bulb, and their physiology and functions are far better characterized than for periglomerular cells. The spiny dendrites of these axon-lacking cells extend into the external plexiform layer, where they make GABA-ergic synaptic contacts with the lateral dendrites of mitral cells. In the MOB, there are approximately ~ 100 GCs for each mitral cell (Shepherd, Shepherd, 2004). Although this number is thought to be significantly smaller in the AOB (Meisami and Bhatnagar, 1998), the inhibition provided by AOB granule cells is known to play a critical role in certain pheromonally mediated behaviors (Kaba et al, 1994).

Granule cells can mediate both self (recurrent) inhibition of MOB mitral cells, and lateral inhibition between mitral cells (Rall et al., 1966;Yokoi et al., 1995). In the AOB, self inhibition via granule cells is argued to be critical for the induction of pheromonal memories, and pharmacological manipulations of this inhibition have been shown to facilitate the induction of such memories (Kaba et al, 1994). Lateral inhibition between AOB mitral cells has not yet been documented, and our own observations suggest that inhibitory connections between mitral cells are exceedingly rare, if present at all. In dozens of recordings from mitral-mitral pairs in the AOB, we have never observed lateral inhibition between mitral cells. One explanation for this is that granule cell connections between mitral cells are present but highly specific, and hence difficult to observe in blind paired recordings. Another possibility is that granule cells are only synaptically connected to single (or very few) mitral cells, and mediate mitral self-inhibition exclusively. This view is consistent with some anecdotal observations that lateral dendrites of AOB mitral cells have only a limited radial extent.

1.2.5 Efferent and centrifugal pathways

Given the work of Luo and Katz (2003) describing selective mitral cell responses for complex stimuli, AOB outputs presumably carry sufficient information to directly drive pheromonally-mediated behaviors that rely on discriminations of sex and strain. Consistent with this, AOB

mitral cells are immediately presynaptic to “effector” structures that exert a powerful influence on neuroendocrine state.

Axons of AOB mitral cells leave the bulb as part of the lateral olfactory tract, and become thinly myelinated, or non-myelinated close to their sites of termination. These axons terminate in several archicortical structures, including the medial cortical amygdala (m-CoA), the posteromedial cortical amygdala (pm-CoA), and the nucleus of the accessory olfactory tract (NAOT)(Meredith, 1998). These structures are often grouped together as the “vomeronasal amygdala,” since they are the only amygdala structures to receive direct vomeronasal input. Most of the work investigating the targets of AOB efferents has been done in reptiles, and has revealed considerable variability in the inter-connections between amygdala subdivisions and the AOB. In hamsters, one of few mammals in which these connections were studied, the pm-CoA was found to project reciprocally to the AOB granule cell layer (Kevetter and Winans, 1981;Halpern and Martinez-Marcos, 2003). The other major feedback/centrifugal projection to the AOB is a noradrenergic input from the locus coeruleus - which is believed to alter granule cell excitability in ways critical for certain learned, pheromonally-mediataed behaviors (Brennan and Keverne, 1997).

Efferents of the vomeronasal amygdala project to several hypothalamic regions, including the preoptic, ventromedial, premammillary, and supraoptic nuclei (Kevetter and Winans, 1981;reviewed in Halpern and Martinez-Marcos, 2003;Bian et al., 2008). Among these nuclei, the medial preoptic area has been the focus of particular interest since it is one of few brain regions containing neurons that secrete LHRH into the hypopheseal portal vasculature to control the synthesis and release of leutenizing hormone (LH) by the anterior pituitary (Wu et al., 1997). This organization is appealing from the perspective of one studying AOB function, since a feed-forward disynaptic pathway emanating from the AOB is apparently directly linked to the production of LH, and, presumably, changes in behavioral state. It is worth noting, however, that recent studies have suggested revisions to this relatively simple, feedfoward view of pheromonal processing (Boehm et al., 2005;Yoon et al., 2005).

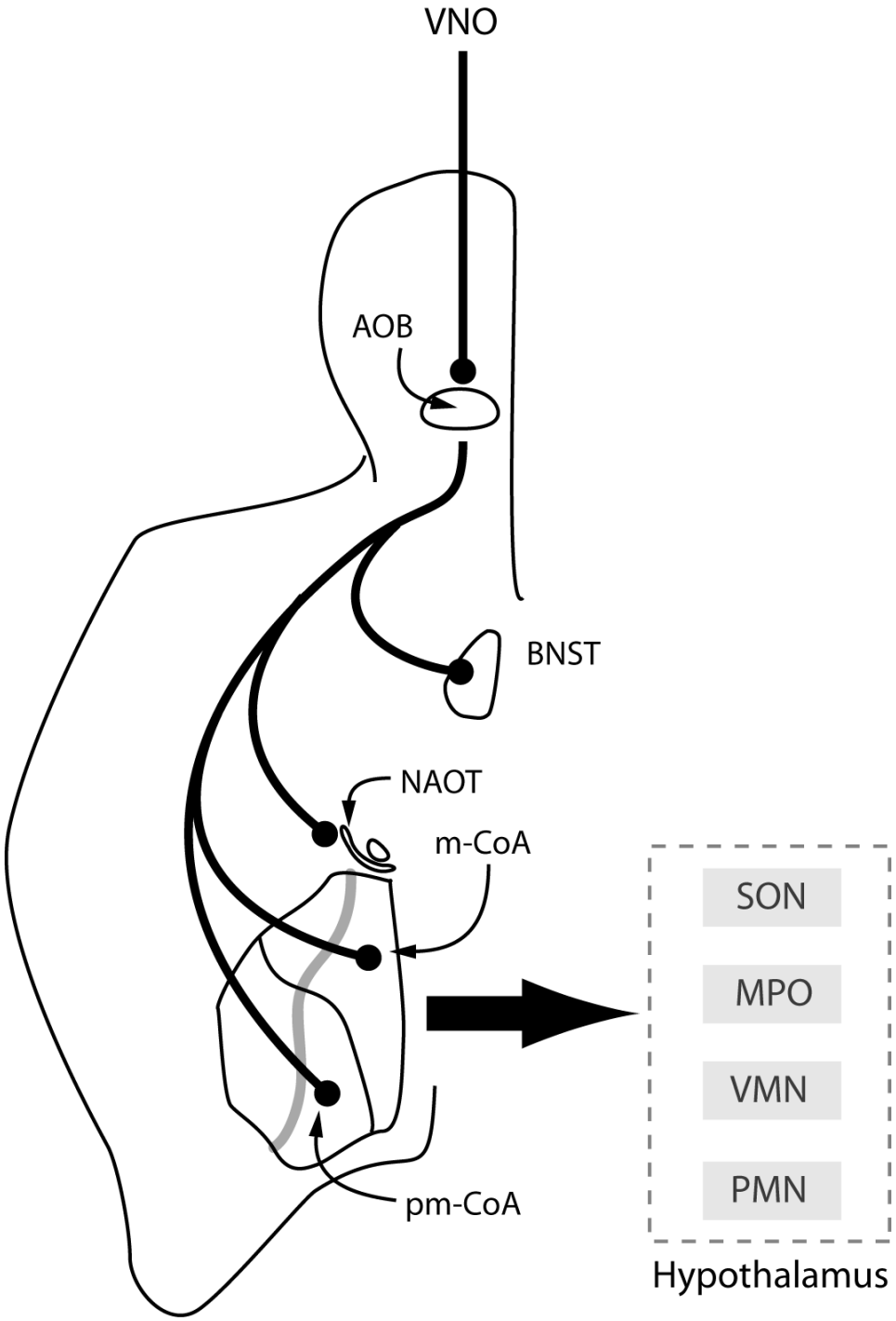
VNO
AOB
BNST
NAOT
m-CoA
pm-CoA
SON
MPO
VMN
PMN
Hypothalamus

Figure 4. Outputs of the AOB. The AOB receives direct input from the vomeronasal organ (VNO). The axons of AOB mitral cells in turn project to several central brain regions, including the bed nucleus of the stria-terminalis (BNST), and the nucleus of the accessory olfactory tract (NAOT). Mitral cell axons also project to the so-called "vomeronasal amygdala", which includes the medial cortical amygdala (m-CoA), and the posteromedial cortical amygdala (pm-CoA). Amygdalar outputs terminate in several hypothalamic nuclei, including the supraoptic nucleus (SON), the medial preoptic (MPO) nucleus, the ventromedial nucleus (VMN), and the premammilary nucleus (PMN).

1.3 DENDRITIC NEUROTRANSMITTER RELEASE

1.3.1 The phenomenon and mechanisms of dendritic neurotransmitter release

Under the classical view, neuronal output is thought to occur exclusively from axons. The precursors of this doctrine were insights by James and Sherrington, who observed that signal propagation in sensory-motor circuits was unidirectional (James, 1890;Sherrington, 1906;Shepherd, 1991). Both physiological and anatomical substrates of this phenomenon were investigated, with Sherrington emphasizing the role of a 'valve-like action' at sites of 'synapsis' between neurons, and Van Gehuchten and Cajal proposing that "axipetal polarization of the protoplasma" of single cells could define an oriented axis for signal propagation. Ultimately, these ideas led Cajal to decree that 'a functional synapse… can only be formed between the collateral or terminal axon ramifications of one neuron and the dendrites or cell body of another.' (quoted in Cajal, 1995)

In light of this influential proposal, early observations of certain axon-less neurons - including amacrine cells in the retina and granule cells in the olfactory bulb - raised obvious questions about their output properties. It has since been established that these cells, as well as many others in the CNS, release transmitter from their dendrites – a fact that has considerable implications for understanding how neurons integrate their synaptic inputs, how neuronal activity is coupled to output, and how neurons communicate with one another in small functional networks (Ludwig and Pittman, 2003;Shepherd, 1978).

Work by Shepherd, Rall and colleagues led to the first proposal of dendrites acting as presynaptic elements in the olfactory bulb (Rall et al., 1966;Rall and Shepherd, 1968). In early *in vivo* recordings from rabbit, Phillips et al (1963) observed that antidromic activation of the MOB by lateral olfactory tract stimulation evoked lamina-specific extracellular potentials with stereotyped waveforms. Mitral cell activity, in particular, was reliably observed as 'giant' spikes followed by an AHP-like negativity that reversed polarity when the recording electrode was advanced beyond the mitral cell layer. Conditioning prepulses delivered to the lateral olfactory tract suppressed subsequent mitral cell activity, which, based on later recordings from putative

granule cells, was attributed to activation of postsynaptic interneurons impinging on mitral cells in a reciprocal manner (Shepherd, 1963).

The early thinking of these investigators was that *axon collaterals* from mitral cells activated granule cells to implement "a feedback system by which naturally discharging mitral cells could limit their frequency of discharge." However, later modeling studies suggested that the observed synaptic excitation of granule cells occurred within the external plexiform layer (consisting mostly of mitral and granule cell dendrites), rather than in the deeper granule cell layer where collaterals were thought to terminate.

To account for these results, Shepherd and Rall hypothesized that dendro-dendritic synaptic interactions occur between mitral and granule cells (Rall et al., 1966;Rall and Shepherd, 1968). This proposal was soon bolstered by EM data from Reese (in Rall et al., 1966) showing bidirectional synaptic contacts between mitral and granule cell dendrites. Further verification of this general mechanism came in the early 1980s with direct intracellular recordings from mitral cells performed by Jahr and Nicoll (1980;1982a;Nicoll and Jahr, 1982). In recordings from turtle olfactory bulb, these researchers showed that a long-lasting IPSC observed in mitral cells could be elicited by direct somatic depolarization or antidromic stimulation of the lateral olfactory tract, which persisted in the presence of TTX and TEA. Presumably these pharmacological manipulations blocked regenerative axonal conduction while leaving dendritic Ca^{2+} spikes intact.

Roughly in parallel with this pioneering work in the bulb, investigators were also exploring the possibility of dendritic release of dopamine from neurons of the substantia nigra(Besson et al., 1969). In contrast to the work of Shepherd and colleagues, which inferred dendritic release from cellular recordings and simulations, the proposal for dendritic release by nigral neurons grew out of neurochemical and histological work. In 1975, Bjorklund and Lindvall demonstrated catecholamine-induced fluorescence in the soma and long apical dendrite of SN neurons. Shortly after this, Geffen and others (1976) began investigating the uptake and release of tritiated dopamine in SN dendrites in response to pulses of high molarity KCl. This work, and related studies by Korf et. al (1976), showed that depolarization of SN neurons by antidromic stimuli evoked a calcium dependent release of dopamine similar to that seen in axonal terminals.

In the decades following this early work, dendritic neurotransmitter release has been observed in close to a dozen brain regions. There is now evidence for dendritic release of various neuromodulators, including nitric oxide (Schuman and Madison, 1991) and cannabinoids from pyramidal (Wilson and Nicoll, 2001) and Purkinje cells (Kreitzer and Regehr, 2001), as well as release of various neuropeptides, such as vasopressin and oxytocin from magnocellular neurons of the hypothalamus (Pow and Morris, 1989). More recently, dendrites of pyramidal cells have been shown to release both glutamate and GABA onto presynaptic neurons(Zilberter et al., 1999;Zilberter, 2000). These observations of fast transmitter release from dendrites are among the most intriguing recent developments, providing counterexamples to the notion that dendritic release typically occurs in a slow, pericrine-like manner to modulate synaptic processing only over long time scales.

Unlike axonal transmitter release, in which highly stereotyped electrochemical and molecular events evoke quantal transmitter release, dendritic release can occur by a wide variety of mechanisms. One of the more exotic and controversial of these is the proposed activity-dependent reversal of dopamine transporters in substantia nigra neurons (Falkenburger et al., 2001). In some cases, dendritic signaling via molecules such as arachidonic acid (Williams et al., 1989), endocannabanoids (Wilson and Nicoll, 2001), and Nitric Oxide (Schuman and Madison, 1991) relies on activity dependent, *de novo* synthesis of retrograde messengers via second messenger cascades. Release of such molecules into the synaptic cleft is generally believed to be non-vesicular, and is thought to occur only for particular types of patterned activity or during regimes of intense firing. In other cases, dendritic release appears to be vesicular and calcium dependent, but is triggered by "atypical" calcium sources, including calcium permeable AMPA receptors (Chavez et al., 2006), NMDA receptors (Schoppa et al., 1998;Chen et al., 2000;Halabisky et al., 2000), or LVA calcium channels (Pan et al., 2001). Finally, a number of studies in the olfactory bulb have described transmitter release from mitral and granule cell dendrites evoked by backpropagating spikes that appear to rely on classical, axon-like release mechanisms (Isaacson and Strowbridge, 1998;Isaacson, 2001;Egger et al., 2003;Murphy et al., 2005).

1.3.2 Dendritic Excitability and neurotransmitter release

1.3.2.1 Dendritic release evoked by action potentials

In some of the early work investigating transmitter release from dendrites, a tacit assumption was that mechanisms mediating dendritic transmitter release were likely comparable to those observed in axonal release, and hence required active dendritic conductances (Bhalla and Bower, 1993)[1]. Under this view, one may expect that release competent dendrites exhibit regenerative electrical behavior similar to axonal electrogenesis. Direct verification of this proposal had to wait for the advent of dendritic patch-clamping techniques. Following Stuart and Sakmann's discovery (Stuart and Sakmann, 1994) that axo-somatically initiated action potentials could backpropagate into the dendritic tree, a number of investigators studied backpropagation by direct dendritic recording in cells known to release transmitters. The appeal of these model systems was that dendritic conduction of action potentials could be clearly linked to a specific function – fast release of transmitter by "traditional" large and rapidly repolarizing action potentials. Intriguing early results of such studies indicated that in contrast to the decremental AP conduction observed in pyramidal cell apical dendrites (Stuart and Sakmann, 1994;Stuart et al., 1997), APs propagated non-decrementally in both mitral cell (Bischofberger and Jonas, 1997;Chen et al., 1997;Chen et al., 2002) and substantia nigra neuron apical dendrites (Hausser et al., 1995), suggesting that these dendrites are in some sense tailored to function in an axon-like manner. Indeed, Na+ and K+ conductance densities in mitral cell dendrites are approximately twofold higher than those in pyramidal cells (Bischofberger and Jonas, 1997;Migliore and Shepherd, 2002), and under conditions where the somatic membrane is inhibited, full-blown action potentials can even be initiated close to the tuft(Chen et al., 1997;Chen et al., 2002). These basic results have been confirmed in AOB mitral cells, with recent studies showing uniform invasion of somatic action potentials even into the most distal tuft branches (Ma and Lowe, 2004). Similar robust propagation of dendritic action potentials has also been observed in mitral cell lateral dendrites (Xiong and Chen, 2002), though conduction may in some cases may be

[1] Interestingly however, the early simulations of Rall and Shepherd (1968) showed that passive properties of mitral cell lateral dendrites were sufficient to account for MOB field potentials observed in extracellular recordings. This prompted these investigators to consider the possibility of graded release from these dendrites.

decremental (Margrie et al., 2001) and modulated by dendritic A-type potassium currents (Christie and Westbrook, 2003) or local synaptic inhibition (Lowe, 2002;Xiong and Chen, 2002).

There is some evidence to support the idea that mitral cells are suited to release glutamate only for suprathreshold stimuli. Studies by Isaacson and Strowbridge (1998) showed that dendrodendritic inhibition observed in mitral cells was relatively unaffected by the LVA and L-type calcium channel blockers Nickel and Nifedipine, but fully blocked by the P/Q calcium channel antagonist ω-conotoxin MVIIC. Later work by Isaacson (2001) underscored this same basic point, and suggested that GABA release from granule cells was also required HVA (N and/or P/Q) calcium channels. These studies are consistent with the basic hypothesis that release-competent dendrites have the requisite calcium channels and readout machinery for coupling action potentials to transmitter release. It should be emphasized, though, that they do not exclude the possibility that other forms of dendritic activity (including subthreshold activity) can evoke release (see next section).

1.3.3 Subthreshold release from dendrites

1.3.3.1 Local spikes and dendritic release

In addition to supporting full-blown action potentials, dendrites exhibit regenerative activity that is spatially localized and independent of somatic spiking (Hausser et al., 2000;Hausser and Mel, 2003). Although direct demonstrations of such localized dendritic activity again had to wait for advances in recording methods – including dendritic patch clamping and calcium imaging techniques- prescient work by Spencer and Kandel (1968) hinted that dendrites were not merely passive "receivers," but rather active contributors to synaptic integration. Specifically, these investigators described fast "pre-potentials" in hippocampal cells evoked by synaptic input that they took as evidence of local dendritic spikes. More direct evidence of local dendritic excitability was obtained by Llinas et al (1968), via intracellular recordings from Purkinje cell dendrites. Subsequent work described dendritic spikes in a number of cell types, including cortical and hippocampal pyramidal cells, Purkinje cells, retinal ganglion cells, and mitral cells (reviewed in Hausser and Mel, 2003). Although mechanisms of

electrogenesis in these cells can vary considerably as a function of input source and local membrane potential, most dendritic spikes are mediated by a combination of sodium and calcium conductances. Purkinje cells, which lack dendritic sodium channels, are a notable exception to this generalization (Stuart and Hausser, 1994).

Many functions of dendritic spikes have been proposed. In pyramidal cells, they may be critical for amplifying coincident synaptic inputs (Urban et al., 1998;Urban and Barrionuevo, 1998), and also seem to be sufficient triggers of synaptic plasticity (Golding et al., 2002). In addition, local spikes can contribute to regenerative boosting of synaptic inputs on common dendritic branches(Schiller et al., 2000;Schiller and Schiller, 2001;Wei et al., 2001), allowing single neurons to perform complex operations such as nonlinear addition and multiplication (Mel, 1993). One repeated observation in studies of local spikes is that they tend to be relatively poorly propagating – an attribute that may be desirable for functionally isolating distal dendritic processing from somatic spiking. From the perspective of one studying dendritic transmitter release, local dendritic excitability provides a mechanism by which neuronal output can be strongly and locally coupled to synaptic input. With dendrites excitable over small spatial scales, release can occur over comparably small spatial scales independently of other dendritic and even axonal release sites.

In olfactory bulb circuits, local dendritic excitability was first suggested by the studies of Mori et al (1981;1982b), who showed TTX insensitive regenerative events in mitral cells evoked by ON volleys. These events were believed to correspond to potentials generated at the distal dendritic tuft of the apical dendrite. One possible function of these regenerative potentials is to influence integrative events by activating local, glomerulus-specific circuits prior to initiation of somatic spikes. More recent work studying synaptically evoked, regenerative events localized to tufts has shown that stimulation of the ON (in MOB) or VN (in AOB) can elicit “hot spots” of activity in tuft branches (Yuan and Knopfel, 2006b). Although no studies to date have simultaneously monitored activity in juxtaglomerular interneurons and tuft branches, one intriguing proposal is that fine, branch-specific control of spiking in tufts may allow a single mitral cell to communicate with select populations of interneurons. Such observations of spatial heterogeneity and branch-independence of spiking are perhaps more physiologically relevant in multi-tufted AOB mitral cells, where local “tuft-spikes” may contribute to independent integration across distinct tufts.

1.3.3.2 Other mechanisms of subthreshold dendritic release

Both local spikes and backpropagating action potentials have been shown to occur in vivo (Waters et al., 2003;Waters and Helmchen, 2004), and hence it is likely that these events can mediate dendritic neurotransmitter release under physiological conditions. However, these results do not close the door on dendritic release mechanisms that operate independently of regenerative, "stereotyped" activity.

For low levels of input, synapses provide an essentially passive source of current flow to dendrites which results in subthreshold fluctuations of membrane voltage. The dynamics of these subthreshold voltage changes are governed by the membrane time constant, and hence are an integrated "running average" of synaptic input fundamentally different from the signal conveyed by regenerative responses. One intriguing question is whether this running average of dendritic activity can be coupled to neuronal output. Specifically, can dendrites produce graded (analog) outputs for graded inputs as well as for stereotyped regenerative responses?

This question is certainly still an open one, but several lines of work suggest that dendrites can produce bona-fide subthreshold outputs. Most recently, calcium influx through calcium permeable AMPA receptors has been shown to be coupled to glutamate release in retinal amacrine cells (Chavez et al., 2006). In F2 terminals, made by the dendrites of thalamic interneurons onto relay cells, direct pharmacological activation of ligand-gated receptors was found to alter rates of asynchronous IPSCs observed in relay cells (Cox et al., 1998;Cox and Sherman, 2000). In particular, mGluR agonists enhanced these events, while activation of muscarinic receptors diminished them. Intriguingly, these effects persisted in the presence of TTX (which blocks all forms of interneuron spiking), suggesting a relatively direct coupling of receptor activation to transmitter release.

Similarly, olfactory bulb granule cells may also produce graded outputs via activation of NMDA receptors (though, given the inherent voltage dependence of NMDAR currents and the existence of regenerative NMDAR spikes, this should be interpreted with care). Following up on experiments showing that NMDAR activation is an absolute requirement for recurrent inhibition of mitral cells (Isaacson and Strowbridge, 1998), several groups set about investigating mechanisms controlling GABA exocytosis from granule cells. In experiments in which NMDA was focally applied to mitral/granule synapses, Halabisky et al (2000) found that inhibition observed in mitral cells persisted even during blockade of voltage gated calcium channels with

cadmium. Related work by Chen et al (2000) used uncaging methods to directly evoke transmitter release from mitral cell dendrites and found that feedback inhibition was only minimally affected by a cocktail of Cadmium and Nickel. In contrast, APV abolished uncaging-evoked feeback IPSPs. Given these results, GABA release from granule cells may occur in a graded manner, in which continuous glutamatergic input evokes prolonged subthreshold GABA release.

1.3.4 (Is) Dendritic release evoked by subthreshold membrane voltage (?)

Although many of the kinds of dendritic release described above occur in the absence of somatic spikes, it is still a matter of debate (and definition) whether they qualify as graded. At least two conditions must be met for transmitter release to be called graded: 1) transmitter output must occur for subthreshold, non-stereotyped electrical activity, and 2) the rate or magnitude of transmitter output must vary as a function of stimulus amplitude. Typically, graded (analog) signaling and action-potential coupled (digital) signaling are thought to be mutually exclusive, as each serves a distinct computational or physiological end. Spike-coupled release is usually described as an adaptation for reliable and high fidelity long distance signaling, while graded release is thought to enhance the bandwidth of local synaptic processing when signal propagation is not a constraint. Based on theoretical arguments, it is estimated that graded information transfer from photoreceptors to large monopolar cells (in the blowfly retina) may be up to five times higher than that between typical spiking neurons (Juusola et al., 1996).

The best studied examples of graded synapses are from cells near the sensory periphery – bipolar cells in the retina, and inner hair cells of the cochlea. In both of these nonspiking cell types, transmitter release occurs at specialized ribbon synapses which can support vesicle exocytosis rates of up to 2,000 vessicles/second(reviewed in Prescott and Zenisek, 2005;Sterling and Matthews, 2005). These synapses have conspicuous ultrastructural features, most notably a large electron dense presynaptic element with a halo of vesicles tethered to it. In addition, calcium influx – and hence transmitter release - at such synapses appears to be mediated mostly by L type calcium channels (Lewis and Hudspeth, 1983;Hayashi and Stuart, 1993;Barnes, 1994) which have generally rapid activation (~ 1ms at 0 mV) and weak inactivation (Lipscombe et al.,

2004;Helton et al., 2005). These two properties of ribbon synapses– a conspicuously large pool of vesicles and a calcium conductance that can rapidly "track" subthreshold membrane voltage appear to support the notion that graded release requires specialized machinery for producing subthreshold calcium signals and transducing these signals into neural output. How specialized is this subthreshold machinery though? Is it absent from synapses of spiking neurons? Alternatively, could subthreshold calcium currents and release processes mediate graded release in spiking neurons? Although it is typically assumed that graded transmitter release occurs at specialized synapses, even the earliest investigations of neurotransmitter release suggested this may not strictly be the case. Working in the frog neuromuscular junction, Castillo and Katz (1954) observed that even slight (presumably subthreshold) nerve polarization enhanced rates of miniature EPPs. Below, I further argue that based on considerations of electrical compartmentalization, the complement of calcium channels expressed in dendrites, and what is known about asynchronous, prolonged transmitter release, dendrites may support graded neurotransmitter release.

Classical work done by Llinas and others in the squid giant synapse uncovered a set of stereotyped calcium-mediated events that initiate and trigger action potential evoked neurotransmitter release (Llinas et al., 1981;Augustine et al., 1985). Numerous studies since have supported the essential idea that transmitter release is exquisitely tuned to the rapid dynamics of the action potential by coupling exocytosis to a two-step process of calcium influx. In the first step, the depolarizing phase of the action potential activates high-voltage activated (HVA) calcium channels (typically of the N and P/Q type) in approximately 100 μs. The majority of calcium influx typically occurs during the repolarizing phase of the action potential when calcium driving force is elevated (a process requiring about 300 μs). At the molecular level, release of a synaptic vesicle is proposed to depend on the formation of transient calcium microdomains in the vicinity of one or a handful of HVA calcium channels. Such microdomains are postulated to occur only within nanometers of the channel mouth, and presynaptic imaging of the calcium indicator n-aequorin-J, together with biophysical modeling suggested that the penultimate step in release of a single vesicle was the rapid (~300 μs) elevation of intracellular calcium to ~250 μM in spatially restricted domains (Llinas et al., 1992;Llinas et al., 1994;Serulle et al., 2007).

This basic sequence of events suggests a fail-safe mechanism in which the machinery controlling transmitter release is unaffected by subthreshold activity. However, recent work has reinvestigated this claim, finding evidence of so-called "hybrid" forms of release in which subthreshold membrane potential can affect the quantity of transmitter released per action potential (Alle and Geiger, 2006;Clark and Hausser, 2006;Shu et al., 2006). Although steady state changes in membrane potential can certainly influence transmitter release by changing the action potential waveform, Alle and Geiger (2006) and Awatramani et al. (2005) found that when the slow calcium buffer EGTA was introduced presynaptically, the grading of release by subthreshold voltage was diminished without marked changes in AP amplitude or duration. This indicates that at least part of the observed grading effect depended on levels of resting calcium.

Thus, the effects of subthreshold voltage on neural output may have been underappreciated due to the longstanding assumption that the axon length constant is prohibitively short. The work described above has led to newer estimates of cortical axon length constants that are on the order of 400 µm. In concrete terms, this means that for such an axon, a 15 mV EPSP observed at the soma will depolarize a bouton 200 µm distal by ~ 9 mV (15 mV/exp (200/400). A 9 mV depolarization from a resting potential of -60 mV could produce appreciable LVA calcium current and possibly a small window current mediated by HVA channels. These rough electrotonic calculations are compelling when applied to dendrites, which have generally longer length constants due to their greater diameter. The length constant of a mitral cell apical dendrite, for example, may be on the order of 1 mm (Djurisic et al., 2004;Shepherd, Shepherd, 2004), which would predict little somatofugal voltage attenuation.

One intriguing hypothesis given this work is that such relatively long length constants (compared to axons) may allow release-competent dendrites to function in a graded release mode *in addition to* a spike-evoked release mode. Consistent with this line of reasoning, large invertebrate neurons with short neurites can release transmitter for both sub and suprathreshold stimuli (Graubard et al., 1980). Similar dual-mode release was also observed in leech heart-interneurons by Ivanov et al (2006a;2006c), who used paired recordings to show occlusion of phasic 'high threshold' release by long conditioning prepulses that induced sustained graded release. This occlusion was diminished by Nickel and low external [Ca^{2+}], which argues that its physiological basis is the depletion of vesicles "visible" to both the sub and suprathreshold release machinery.

One interpretation of these results is that phasic and tonic release of transmitter are not mutually exclusive phenomena, but rather different operating regimes of a multi-purpose release apparatus responsive to large, phasic calcium transients, as well as smaller sustained transients. At least two lines of evidence are consistent with such a view. First, recent uncaging experiments in which presynaptic calcium was rapidly and directly elevated to fixed concentrations have shown that calcium levels relevant for release are substantially lower than previously thought (Bollmann et al., 2000;Schneggenburger and Neher, 2000). In particular, transmitter release was observed for uniform calcium elevations as low as 1 μM - an order of magnitude smaller than classical estimates. This argues that bulk calcium concentrations may contribute to release, and could explain some ectopic forms synaptic output from sites lacking ultrastructurally obvious active zones (Matsui and Jahr, 2003;Matsui and Jahr, 2004). Second, studies of asynchronous release in a number of systems suggest that presynaptic terminals have "readout" mechanisms that support prolonged release. In CCK expressing hippocampal interneurons, for example, trains of action potentials evoke compound postsynaptic potentials in granule cells that consist of a rapid component as well as a second slowly accumulating, calcium dependent component (Hefft and Jonas, 2005). Although it is unclear if this slow release is due to a prolonged program of vesicle fusion following transient calcium influxes, molecular work indicates that some isoforms of synaptotagmin – the presumed calcium sensor for release – operate at high affinity and/or low cooperativity, and are suited for "sniffing out" small and slow fluctuations of calcium (Sun et al., 2007).

These results may have particular relevance for the possibility of graded release from dendrites, as presynaptic sites on dendrites (in cells where they occur), can experience substantial voltage dependent changes in basal calcium concentration that occur independently of action potentials or local spikes. In hippocampal CA1 pyramidal neurons, for example, Magee et al (1996) described sustained dendritic calcium currents that were graded for changes in command voltage near rest. This current was evidently activated at low voltages, yet blocked by dihydropyridines, which was thought to be a curious pharmacology at the time. A current with similar activation and pharmacology was also described recently for the GABA releasing dendrites of periglomerular cells in the MOB, and was found to mediate a component of dendritic release (Murphy et al., 2005). One possibility is that this low threshold current is carried by the Cav1.3 channel described by Lipscombe (2004), which activates rapidly at low

voltages (>-60mV) and experiences relatively little inactivation. Such properties could be well suited for transducing instantaneous fluctuations in membrane voltage into a graded calcium signal that could be "read out" by release machinery. Consistent with this, L-type currents have been observed in mitral cells dendrites (Schild et al., 1995), and may mediate the striking sniff-coupled subthreshold oscillations of dendritic calcium observed *in vivo*(Charpak et al., 2001).

1.3.5 Role of dendritic excitability and dendritic transmitter release in neural computation

What does it mean when a neuron spikes? An obvious answer is that it has received enough input to reach spike threshold. On another level though, a spike may indicate that rather more specific conditions - such as a particular spatial arrangement of active synaptic inputs- have been met. This latter view is suggested by recent models and experiments investigating the computational properties of dendrites. In particular, these studies show that dendrites integrate their inputs nonlinearly with different summation rules for different spatial and temporal input patterns (Polsky et al., 2004;Chapter 1 in Shepherd, Shepherd, 2004). An important corollary of this result is that by implementing these different rules, neurons will tend to be driven best by certain preferred or "special" input patterns. Under this view, spiking activity can be seen as an ongoing assessment of *relationships among inputs* in addition to simply being a correlate total input (Konig et al., 1996).

Regardless of whether this view is exactly correct, it highlights the point that activity within the dendritic tree at any given moment- even if this activity fails to evoke axosomatic spikes- can carry important information about a neuron's "instantaneous" state. Although not all states will lead to spiking, the distribution of activity across the dendritic tree reflects the "results" of numerous local computations. A plateau potential in one dendrite may have been elicited by the synchronous activity of few synapses in close proximity; a rapid calcium spike in different branch may indicate that many synapses were activated diffusely; even a silent dendrite may signify that a tonically active input was inhibited.

The major advantage of having transmitter release occur from excitable dendrites is that the results of such local computations are potentially available to postsynaptic cells. Moreover,

in cases where these postsynaptic targets feed-back locally onto their presynaptic dendrites, as occurs at reciprocal synapses in the AOB, this feedback can affect subsequent integration of inputs. Under this view, periglomerular or granule cells could monitor the local computational states of mitral cell dendrites, while the axonal spike generator is sensitive to the overall "state of states."

The stereotypy and compartmentalization of inputs to AOB mitral cells, together with these cells' excitable presynaptic dendrites, make them a superb model system for investigating such basic aspects of dendritic computation. The convergence of phenotypically identical VRNs onto common tufts, for example, takes much of the guesswork out of assigning roles to specific sets of active afferents: input to a given tuft indicates that a specific ligand is present at the periphery. In addition, certain characteristics of mitral cell responsiveness observed *in-vivo* suggest that spikes are regulated by a selective pattern recognition mechanism, and that considerable subthreshold computation occurs prior to spike initiation. First, recordings from AOB mitral cells in behaving mice show that mitral cells have low basal firing rates, and respond selectively for only particular combinations of strain and gender. Given that the cues conveying precise strain, gender, or individual identity are likely to be represented by multi-component pheromone blends, this task requires integration of information about these components, possibly across tufts. Second, AOB mitral cells fire only many seconds after stimulus presentation, suggesting that local processing mechanisms exist to promote selectivity of responses and accuracy of pheromone identification.

1.4 GOALS OF DISSERTATION RESEARCH AND SUMMARY OF FINDINGS

Dendrites support events with diverse dynamics and mechanisms (e.g. subthreshold EPSPs, calcium spikes, plateau potentials). Thus, dendrites that release neurotransmitters may produce many types of outputs. The goals of this thesis are to better understand 1) the functional relationship(s) between dendritic activity and dendritic output, and 2) the ways that dendritic

output from a neuron affects its activity state via direct and disynaptic feedback. I have pursued these goals by studying dendrodendritic processing in accessory olfactory bulb circuits.

The research described in **chapter 2** characterizes basic excitable properties of AOB mitral cell principal dendrites using *in-vitro* whole cell recording and calcium imaging. These results set the stage for subsequent experiments investigating how local excitability contributes to the integrative and output properties of these dendrites. The work of **chapter 2** culminates in a demonstration that synaptically–evoked, local regenerative events in mitral cell dendrites (dendritic spikes) are triggers of glutamate release and subsequent recurrent inhibition. This is, to our knowledge, one of the first direct demonstrations of such an output role for dendritic spikes.

The ability of a single neuron's dendrites to support multiple potential output signals suggests that each such signal may be useful for a particular kind of computation. One interesting question is whether the relative efficacies of these signals can be modified. If they can be, then dendrites may be able to alternate between multiple computational "modes" to differentially engage their post-synaptic targets.

In **chapter 3,** I study the modulation of dendritic signaling by investigating how reciprocal, dendrodendritic inhibition of AOB mitral cells is regulated by group I metabotropic glutamate receptors. This is a topic of considerable interest since modulation of this inhibition is postulated to play a key role in well-described pheromonally-mediated behaviors. Interestingly, I discovered that recurrent inhibition of mitral cells requires the activation of group I metabotropic glutamate receptors. Moreover, endogenous application of group I mGluR agonists alone was sufficient to elicit enhanced rates of IPSCs. A striking aspect of this observed enhancement of IPSCs was its persistence even under complete blockade of action potentials with TTX, suggesting that transmitter release may occur locally in the absence of propagating dendritic spikes. Perhaps most intriguing was the observation that the IPSC rate observed in mitral cells depended strongly on mitral cell voltage. This suggested that transmitter release may occur via a mode of continuous, subthreshold neurotransmitter release.

This latter observation prompted me to more carefully investigate the types of subthreshold activity that are coupled to dendritic transmitter release. The experiments done to study this phenomenon form the backbone of **chapter 4**, in which I characterize a novel form of continuous, graded release from mitral cells that is enhanced by activation of metabotropic

glutamate receptors. Taken in total, these results show that mitral cell dendrites support multiple types of output signals, and that the relative efficacies of these signals can be modulated.

2.0 DENDRITIC SPIKES IN ACCESSORY OLFACTORY BULB MITRAL CELLS

2.1 ABSTRACT

AOB mitral cells are highly selective, spiking only in response to particular pheromones that convey strain and gender-specific cues. In this chapter we describe synaptically-evoked, regenerative dendritic spikes in mitral cell tufts that may contribute to this selectivity. These events, which we termed “tuft spikes”, were found to amplify synaptic inputs and trigger dendritic glutamate release and subsequent feedback inhibition via local interneurons. These results establish that localized activity in mitral cell dendrites can produce local transmitter output, and that this output is visible to post-synaptic cells. In our discussion, we speculate on how the interplay between dendritic excitability and dendritic output at tufts may allow for highly selective integration of pheromonal information.

2.2 INTRODUCTION

The dendritic branches of many neuron types support synaptically evoked, regenerative events that occur in the absence of somatic spiking (dendritic spikes) (Llinas et al., 1968;Spencer and Kandel, 1968;Regehr et al., 1989;Markram and Sakmann, 1994;Schiller et al., 1997;Schiller et al., 2000). These spatially restricted events underlie various nonlinear aspects of synaptic integration, and are likely to be important determinants of the selectivity and computational capacity of single neurons (Larkum et al., 1999;Euler et al., 2002;Poirazi et al., 2003). Mel and colleagues, in particular, emphasize that local spiking enhances the relative independence of nonlinear operations performed on subsets of the dendritic tree (Polsky et al., 2004). Under this view, the dendritic tree is parsed into independent processing networks, each of which reports the "results" of a local computation to the soma.

The phenomenon of dendritic neurotransmitter release, though less well studied, may provide an additional and complementary means by which dendrites perform subthreshold computations on a fine-grained spatial scale (Govindaiah and Cox, 2004). In release-competent dendrites, activity is coupled to transmitter release, allowing a dendrite to influence the activity of local cell populations (Rall and Shepherd, 1968). Moreover, in cases where transmitter release occurs at reciprocal dendrodendritic synapses, as in the olfactory bulb, dendrites can also regulate their own activity by serving as both input and output structures (Schoppa and Westbrook, 2001;Schoppa and Westbrook, 2002;Urban and Sakmann, 2002;Schoppa and Urban, 2003). An intriguing extension of this idea is that local spikes may be sufficient to evoke transmitter release and recurrent inhibition via interneurons. Such a mechanism could allow for highly compartmentalized input processing, as inhibition would be "directed" only to active subsets of the dendritic tree. In effect, local dendritic compartments and their associated interneurons would function as fine grained neural networks working independently of one another.

Here we examined compartmentalized dendritic integration in mitral cells of the mouse accessory olfactory bulb (AOB) - a CNS structure involved in processing pheromonal information (Holy et al., 2000;Leinders-Zufall et al., 2000;Leypold et al., 2002;Stowers et al., 2002). AOB mitral cells extend multiple smooth primary dendrites, each of which terminates in a highly branched tuft up to several hundred microns from the soma. (Takami and Graziadei,

1991;Belluscio et al., 1999;Rodriguez et al., 1999). The excitatory inputs to a given mitral cell occur only at its tufts, and inputs to a given tuft derive from sensory neurons expressing the same receptor type (Del Punta et al., 2002b). In addition, mitral cells form reciprocal dendrodendritic synapses with local interneurons in the vicinity of their tufts. These anatomical features motivate the view that tufts are self-regulating integrative compartments that may function independently of one another.

In the present study, we describe several aspects of mitral cell dendritic excitability that may contribute to the functional independence of tufts. Specifically, we show that 1) excitatory input to mitral cells can evoke regenerative spikes localized to tufts, and 2) these spikes are robust triggers of dendritic glutamate release and concomitant recurrent inhibition. Finally, we speculate on how the highly local regulation of integration and output at tufts may contribute to the selectivity of pheromone detection.

2.3 MATERIALS AND METHODS

2.3.1 Slice Preparation

Methods are as described previously (Urban and Castro, 2005). Briefly, peri-saggital olfactory bulb slices (300-350 μm thick) were prepared from young mice [postnatal day 14 (P14 to P28)]. At these ages, the olfactory bulb is fully developed, with mitral cell dendritic morphology at P7 being indistinguishable from adult (Lin et al., 2000). Mice were anesthetized (0.1% ketamine/0.1% xylaxine; ~ 3mg/kg, i.p.) and decapitated. Olfactory bulbs were sectioned on a vibratome while submerged in ice-cold oxygenated Ringer's solution containing the following (in mM): 125 NaCl, 2.5 KCl, 25 $NaHCO_3$, 1.25 NaH_2PO_4, 1$MgCl_2$, 25 glucose, 2 $CaCl_2$. In some experiments, 0.5 mM ascorbate, 1mM pyruvate, and 2mM *myo*-inositol were added to the slicing medium.

For imaging of population calcium responses, slices were incubated in a well-plate chamber for 90 minutes at 37ºC in a solution containing 500 μL of the Ringer's solution described above, in addition to 3μL of 0.01% Pluronic (Molecular Probes), and 5 μL of a 1mM solution of Fura2 acetoxymethyl (AM) ester (Molecular Probes) in 100% DMSO solution.

Humidified air (95% O_2/5% CO_2) was passed above the surface of the liquid in the chamber to keep the solution oxygenated.

2.3.2 Electrophysiology

Whole cell voltage recordings were obtained from the somata of identified AOB mitral cells (Stuart and Spruston, 1995). Slices were superfused with oxygenated Ringer's solution containing the following (in mM): 125 NaCl, 2.5 KCl, 25 $NaHCO_3$, 1.25 NaH_2PO_4, 1$MgCl_2$, 25 glucose, 2 $CaCl_2$, warmed to 34-36º C. Whole-cell recordings were established using pipettes (resistances of 2-8 MΩ) filled with a solution containing the following (in mM): 120 postassium gluconate, 2 KCl, 10 HEPES, 10 sodium phosphocreatine, 4 MgATP, and 0.3 Na_3GTP, adjusted to pH 7.3 with KOH. In the indicated experiments, 1mM BAPTA was included in the internal solution. Single cell calcium imaging was performed on cells filled with calcium orange (100-200μM); Molecular Probes, Eugene, OR). Biocytin (2mg/ml; Sigma, St. Louis, MO) was included routinely in the intracellular solution to allow the morphology of neurons to be analyzed. Reconstructions of mitral cell morphology were performed using Neurolucida (MicroBrightField, Williston, VT). Voltage and current were measured in current clamp and voltage clamp, respectively, with a MultiClamp 700B amplifier (Molecular Devices, Union City, CA). Data were filtered (4 kHz low pass) and digitized at 10 kHz using an ITC-18 (Instrutech, Mineola, NY) controlled by custom software written in Igor Pro (Wavemetrics, Lake Oswego, OR). Fluorescence imaging in single cells (Margrie et al., 2001) was performed using a 16 bit back illuminated frame transfer camera with 10 MHz digitization and 16 μm /pixel (Roper Scientific, Trenton, NJ) on an Olympus Optical (Melville, NY) BX51WI microscope fitted with a 20X .95 NA objective at 20-50 Hz. Calcium orange was excited using a monochromator (TILL Photonics, Munich, Germany) using a standard CY3 filter set (excitation filter removed). For fluorescence imaging of Fura2-AM bulk-loaded slices, a 16 bit back illuminated frame transfer camera with 1 or 10 MHz digitization and 13 μm pixels was used. This was mounted to an Olympus optical BX51WI microscope fitted with 20X and 60X objectives, and images were collected at 20-50 Hz. Excitation was delivered via a Xenon lamp (Opti Quip, Highland Mills, NY) and a standard Fura filter set. In all imaging experiments (single cell and bulk loading), calcium transients were measured along lines of interest.

Extracellular stimulation was delivered using constant current pulses (100-200 μs, up to 1mA) delived via theta glass electrodes with ~ 1μm tip size. Movement of the electrode by > 10 μm eliminated tuft transients and EPSPs in all experiments in which this was tested, indicating that stimulation was highly localized.

2.3.3 Electron Microscopy

Tissue was prepared from the glomerular layer of a fixed P14 mouse brain. The specimen was post-fixed for 2 hours in 1% osmium tetroxide and washed in 3 changes of dH_2O followed by a series of 4 rinses in ethanol (50%, 70%,95%, and 100%). Proylene oxide was used as a transitional solvent. The specimen was then infiltrated overnight in a 1:1 mixture of Epon-Araldite and propylene oxide. The following day, the mixture was removed and replaced with 100% Epon-Araldite resin, infiltrated with Epon Araldite an additional 8 hours, placed in embedding capsules, and polymerized for 48 hours at 60ºC. Finally, the specimen was sectioned (100 nm thick) using a Reichert-Jung Ultracut E and a DDK Diamond Knife. Thin sections were stained with 1% uranyl acetate and Reynold's lead citrate, and viewed on a Hitachi 7100 transmission electron microscope. Digital images were obtained using an AMT Advantage 10 CCD Camera System and NIH Image software.

All data below are reported at mean ±SEM. Significance was assessed by paired or unpaired Student's t-tests, as appropriate. All animal care was performed in accordance with the guidelines of Institutional Animal Care and Use Committee of Carnegie Mellon University.

2.4 RESULTS

2.4.1 Backpropagating action potentials in mitral cell dendrites

Before assessing the possible role of active dendritic conductances in mitral cell synaptic integration, we first tested whether mitral cell dendrites contain voltage-dependent channels by observing dendritic calcium transients following APs evoked by somatic current injection. Single

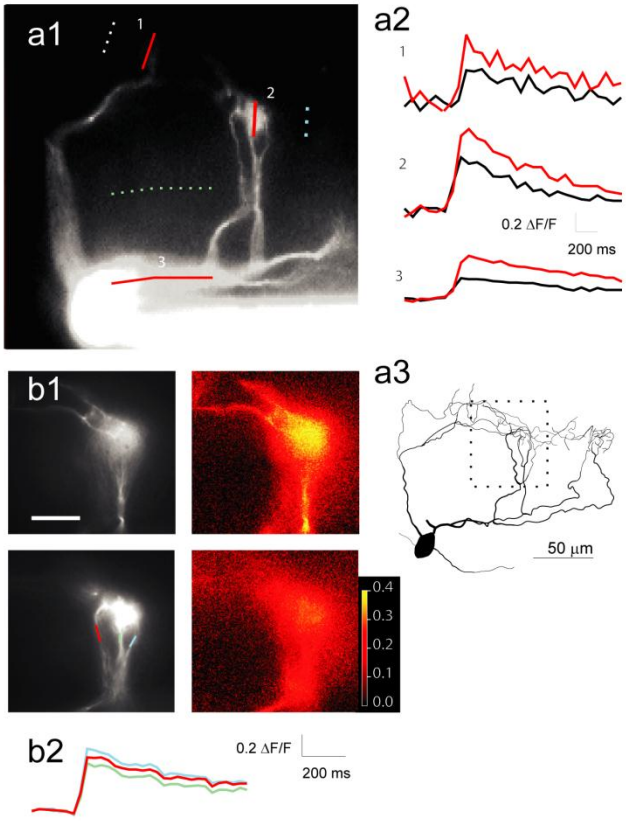
a1
1
2
3
a2
1
2
0.2 ΔF/F
200 ms
3
b1
a3
50 μm
0.4
0.3
0.2
0.1
0.0
b2
0.2 ΔF/F
200 ms

Figure 5. Backpropagation of APs to AOB mitral cell tufts. (a1) Fluorescence image of an AOB mitral cell showing multiple dendrites converging onto two glomeruli. Solid and dotted lines (1-3) show locations from which calcium transients and background fluorescence were measured in **a2**. **(a2)** Calcium transients evoked at the locations indicated in **a1** by single APs (black) or pairs of APs at 40 Hz (red). **(a3)** Reconstruction of the cell in **a1** including additional tufts (on the right) that were not visible in the fluorescence image. The area imaged in **b1** is indicated by the dotted square. **(b1)** Images of the subregion of the dendrite shown in **a3**. Two planes of focus are shown (top and bottom rows). Grayscale images show morphology and color images plot peak ΔF/F for each pixel in the same focal plane shown on the left. **(b2)** ΔF/F plotted (in corresponding colors) vs. time for the three dendrites seen in the bottom row of **b1**. Scale bar (shown in **b1**): 100μm (**a1**); 50 μm (**b1**). The color bar shows values of ΔF/F for the images in the right column of **b1**.

action potentials evoked uniform calcium elevations throughout mitral cell principal dendrites (Fig. 5). Calcium elevations in the tuft were generally larger than those observed in the soma (156 ± 14%; $p<0.05$; paired t test; n=20), and were uniform across the fine dendritic branches of a single tuft (average fractional difference between transients in different branches: 10 ± 5%; n=8 pairs of branches in 6 cells; Fig. 5b2). Thus, the principal dendrites of AOB mitral cells contain calcium channels and faithfully propagate APs from the soma to all branches in all tufts. The presence of voltage gated channels in these dendrites suggests that inputs to mitral cell tufts may be boosted en route to the soma, allowing for amplification of incoming excitatory inputs.

2.4.2 Responses of mitral cell dendrites to synaptic input

We next investigated spread of synaptic inputs from the tuft to the soma. After cells were filled with the fluorescent calcium indicator Calcium Orange (100-200μM) via a somatic patch pipette, a glass stimulating electrode was placed in the glomerular layer, in the vicinity of a visible tuft. The position of the electrode tip was adjusted until a low-amplitude stimulus elicited an EPSP in the mitral cell being recorded. The voltage responses and calcium transients observed in most mitral cells varied with the intensity of the stimulus current used. At low stimulation intensities, small EPSPs but no calcium transients were observed. Increasing the stimulation intensity resulted in larger EPSPs and calcium transients that were restricted to the tuft closest to the stimulating electrode (Fig. 6a3). Further increasing the stimulation intensity elicited a somatic AP and calcium elevation in all visible compartments of the cell (Fig. 6a4). These AP-evoked transients were comparable in amplitude and time course to those evoked by somatic current injection (Fig. 6b).

Local synaptic stimulation was effective at evoking calcium transients in 15 AOB mitral cells. Twelve of these cells showed synaptically evoked calcium transients (mean peak $\Delta F/F$ = 0.32 ± 0.05; n = 12) in the tuft that were accompanied by subthreshold EPSPs recorded at the soma. In these cases, calcium transients were not observed in proximal dendrites [ratio of proximal (>100 μm from the tuft) to tuft calcium transients, 7 ± 6%; n=9 cells in which tuft and proximal dendritic transients were measured simultaneously; $p<0.02$; paired t test]. We refer to these events as tuft calcium spikes, or “tuft spikes.”

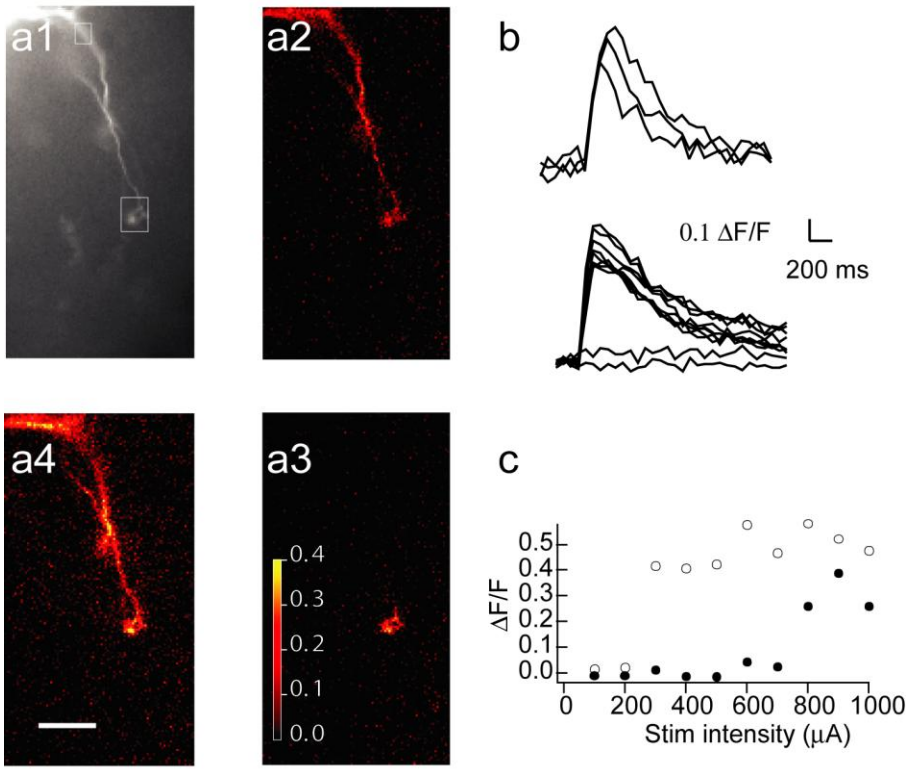
a1
a2
b
0.1 ΔF/F
200 ms
a4
a3
0.4
0.3
0.2
0.1
0.0
c
ΔF/F
0.5
0.4
0.3
0.2
0.1
0.0
0
200
400
600
800
1000
Stim intensity (μA)

Figure 6. Synaptically evoked calcium transients in mitral cell tufts. (a1) Fluorescence image of the dendritic tree of an AOB mitral cell. The boxes show regions of interest from which data in **b** and **c** are taken. **(a2-a4)** ΔF/F maps of calcium transients evoked in this cell by a single backpropagating AP evoked by somatic current injection **(a2)** and by low **(a3)** or high **(a4)** intensity extracellular stimulation of synaptic input to one tuft. **(b)** The traces show calcium transients evoked by three consecutive backpropagating APs (top traces) or by extracellular stimulation of varying intensities (as in **c**, bottom traces). **(c)** Plot of peak ΔF/F at the tuft (open circles) and at the proximal dendrite (filled circles) as a function of stimulation (Stim) intensity. Low intensity stimulation evoked no response. Higher-intensity stimulation (corresponding to **a3**, above) evoked a transient in the tuft (open circles), whereas the highest intensity stimulation (corresponding to **a4,** above) evoked a somatic AP and both tuft and somatic (closed circles) calcium transients. Scale bar (shown in **a4**), 50 μm.

2.4.3 Local excitability and local transmitter release from mitral cell tufts

A number of studies indicate that action potentials in MOB mitral cells can trigger dendritic glutamate release from tufts, mediating either self excitation or "spillover" excitation of tufts in a common glomerulus (Nicoll and Jahr, 1982;Isaacson, 1999;Schoppa and Westbrook, 2002). Because we observed that synaptically evoked tuft calcium spikes were comparable in amplitude to calcium transients elicited by single backpropagating spikes (compare Fig. 6a2 & a3; Fig. 6b), we speculated that tuft spikes may trigger glutamate release and activate local interneurons. Since relatively little is known about the presynaptic function of tufts in AOB mitral cells, we first assessed their competence for glutamate release by studying their ultrastructure.

In tissue prepared for EM from the glomerular layer of mouse AOB, we found that most mitral cell tuft dendritic branches contained clear, spherical vesicles localized in clusters near the dendritic membrane (Figs. 7a1 & a2). In several sections we also identified reciprocal, asymmetric synapses between tufts and apposed dendrites (Figs. 7a1 & a2) similar to those seen in the MOB (Pinching and Powell, 1971b;Pinching and Powell, 1972), confirming that AOB mitral cell tufts make dendrodendritic contacts with PG cells.

To verify that mitral cell activity can evoke transmitter release from tufts onto PG cells, we bulk loaded peri-saggital sections of AOB with the membrane permeable calcium indicator Fura2-AM and recorded PG cell calcium transients in response to current injection in single mitral cells. Mitral cells were filled with Alexa 594 so that tufts were easily visualized and we could confirm that PG cells were being activated in the vicinity of a tuft. In 5/5 cells tested in this manner (n = 5 animals), we found that a sequence of 5-10 backpropagating action potentials at 100 Hz in mitral cells was sufficient to elicit somatic calcium transients in 4.0 ± .54 PG cells/tuft (mean $\Delta F/F$=.04 ±.005) (Figs. 7b1-b3). These transients were eliminated by the glutamate antagonists CNQX and APV, indicating that they required glutamate release from mitral cell tufts (Fig. 7b3).

We next assessed the efficacy of local, synaptically-evoked tuft spikes as triggers of glutamate release. In several experiments in which we stimulated tufts extracellularly and recorded somatic voltage and tuft calcium transients, we observed that the largest tuft calcium spikes were correlated with rapid EPSP decay phases and the presence of negative-going, IPSP-like events (Fig. 8d). These negative deflections are likely to be the result of asynchronous

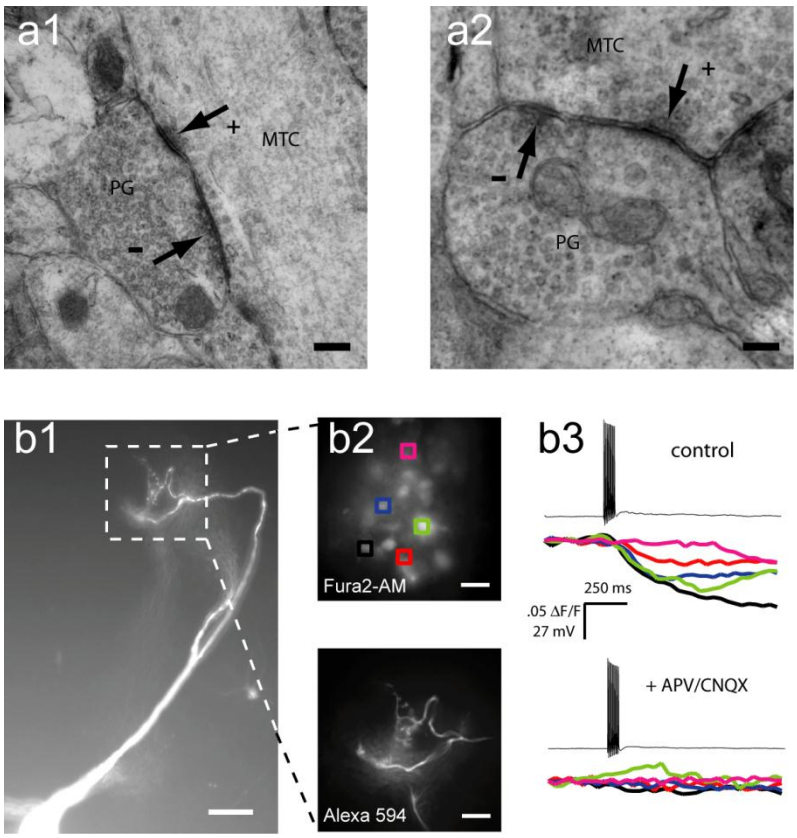

Figure 7. Release competence of AOB mitral cell tufts. (**a1 and a2)** Electron micrographs of tissue prepared from the glomerular layer of mouse AOB showing asymmetric, reciprocal synapses between a mitral-tufted cell dendrite and a periglomerular cell dendrite. Arrows indicate polarity of synapses from pre to post-synaptic. MTC, mitral tufted cell; PG, periglomerular cell; +, excitatory synapse; -, inhibitory synapse. Scale bars: 0.23 µm, **a1**; 0.14 µm, **a2**. (**b1)** 20 X image of an AOB mitral cell filled with the fluorescent indicator Alexa 594. The soma is at the bottom left, and the dendritic tuft is within the dashed box. Scale bar 50 µm. (**b2)** 60 X magnifications of the area indicated in the square region of **b1**. The top image shows periglomerular (PG) cells stained with Fura2-AM. Colored squares are regions of interest (ROI) used to calculate the PG cell calcium transients shown in **b3**. The bottom image shows the branched tuft of the recorded mitral cell, filled with Alexa 594 (same region as **b2**, top). (**b3)** *Top:* PG cell calcium transients evoked by a sequence of 10 backpropagating spikes at 100 Hz. Colors of traces correspond to colors of the ROIs shown in **b2,** top. *Bottom*: Calcium transients from the same PG cells were blocked, after addition of APV (50 µM) and CNQX (20 µM).

inhibition, since they were blocked by 10μM bicuculline (Fig. 8a-c). In similar experiments in which the mitral cell soma was voltage clamped, tuft stimulation evoked a large EPSC with smaller barrages of discrete outward currents superimposed on the EPSC. These barrages were also eliminated by 10μM bicuculline (n=6) (Figs 8b1 & b2). Quantifying the amount of inhibition received by the mitral cell in response to tuft stimulation proved somewhat difficult, as individual events were not always separable due to their high frequency. Thus we used an approach in which we quantified the rapid fluctuations during EPSC decay by calculating the power spectrum of the detrended decay phase of the EPSC. The kinetics of the compound inhibitory events were variable, with rise times ranging between 10-20 ms. Thus, as a measure of the intensity/frequency of these events, we calculated the integral of the power spectrum between 50-110Hz after eliminating any 60 Hz component which may be due to line noise (Fig. 8b2). This approach allowed us to isolate the fast fluctuations putatively due to inhibition without regard to the slow changes in the EPSC.

The above experiments (shown in Fig. 8) demonstrate that local glomerular stimulation results in EPSPs or EPSCs in mitral cells in tandem with fast GABA-A mediated inhibitory events, and that large calcium-transients predict larger amounts of inhibition. However, this does not establish a causal link between local calcium transients in a single mitral cell and recruitment of local interneurons. This observation could potentially be explained by two alternative mechanisms. First, the positive correlation between tuft spike amplitude and inhibitory events might reflect direct activation of PG cells via the stimulating electrode, assuming that greater feedforward inhibition of the mitral cell would be correlated with greater direct excitation of the tuft via vomeronasal nerve axons. Second, tuft stimulation that is subthreshold for the recorded mitral cell may be evoking spikes in mitral cells associated with the same glomerulus. In this case, spiking in neighboring mitral cells may evoke lateral inhibition of the recorded mitral cell. Given these potential confounds, we designed two further experiments to determine whether stimulus evoked inhibition recorded in mitral cells depends on mechanisms specific to the cell being recorded.

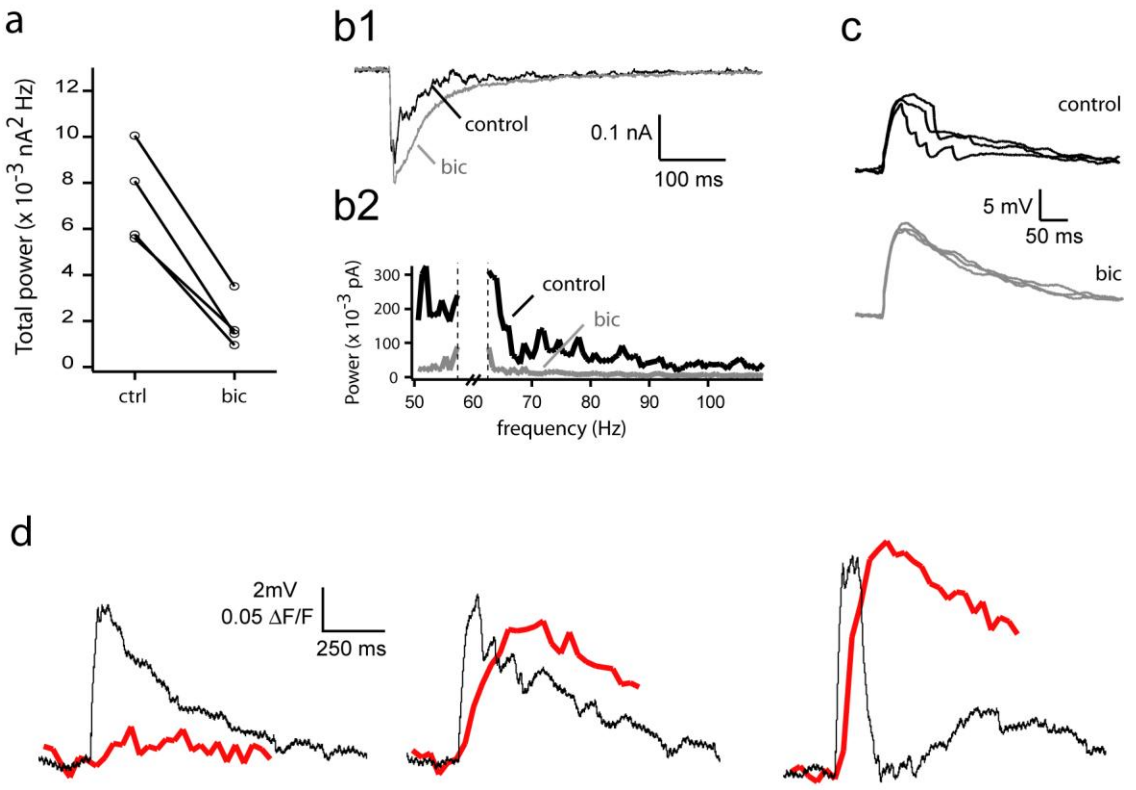

Figure 8. Asynchronous inhibitory events evoked by stimulation of tufts. (a) Total power of fast fluctuating currents evoked by synaptic stimulation of tufts for control and bicuculline (10 µM) cases. As described in the text, power was measured in the 50-110 Hz band after removing the slow EPSC component by detrending. Two sample traces from which these data were generated are shown in figure **b1**. The residual power observed in the bicuculline case is presumably from non-synaptic sources. (**b1)** Sample traces of somatically recorded currents evoked by tuft stimulation under control conditions and following addition of bicuculline. Note the barrage of asynchronous outward currents in the control sweep, which are absent in the bicuculline sweep. (**b2)** Power spectra of the two traces shown in **b1**, after the slow EPSC was removed by detrending. (**c)** Sample traces of somatically recorded EPSPs recorded in current clamp evoked by stimulation of tufts. Note the large, negative-going deflections of membrane voltage in the control case (top), which are eliminated by addition of bicuculline (bottom). **(d)** Simultaneously recorded somatic EPSPs (black) and tuft calcium transients (red) elicited by synaptic stimulation of a tuft. Note that larger calcium transients are associated with rapid, IPSP-like events.

2.4.4 Mitral cell hyperpolarization blocks inhibition associated with tuft spikes

If local, stimulus-evoked calcium transients in tufts are responsible for a substantial portion of somatically recorded inhibition, then manipulations that affect tuft spike amplitude should cause corresponding changes in reciprocal inhibition. More specifically, favoring larger tuft spikes by manipulation of mitral cell voltage should result in enhanced inhibition, while favoring smaller tuft spikes should decrease reciprocal inhibition. Moreover, if release competence is compromised in the recorded cell – by including calcium chelators in the internal patch solution – then reciprocal inhibition should no longer be coupled to tuft calcium influx and thus reduced. In the remainder of the Results section, we describe experiments confirming these two predictions.

Figure 9 summarizes experiments in which mitral cells were voltage clamped at various potentials and tuft spikes evoked via extracellular stimulation as described above. Our first observation was that tuft spikes persist even under voltage clamp – this is unsurprising given that tufts are thin, distal structures electronically isolated from the soma (~2.5 space constants from the soma, meaning that voltage escape will allow regenerative tuft events to occur (see Urban and Castro (2005)). Despite this electronic isolation, we were still able to control tuft spike amplitude via changes in command voltage while recording barrages of inhibitory currents. We observed a strong relationship between holding potential and tuft spike amplitude, such that more hyperpolarized potentials resulted in smaller tuft spikes (Figs 9a & b). It is worth noting that this change in tuft spike amplitude is in the opposite direction predicted by a simple change in calcium driving force, and implies that our voltage manipulations altered the opening of voltage gated conductances responsible for tuft spikes. Figure 9a shows data from an example experiment in which mitral cells were held at progressively more negative potentials and tuft spikes and somatic inhibition were recorded. In this cell, we observed that both tuft calcium influx and the frequency of IPSCs decreased at more negative holding potentials. The voltage dependence of the observed inhibitory events was extraordinarily sensitive (Figs. 9a & b) and is inconsistent with an explanation in which a small decrease in chloride reversal accounts for the several fold change in the amplitude/frequency of inhibitory events. For the example shown in figure 9a, a 5 mV change in holding potential resulted in a 3.7 fold change in inhibition (as calculated by our power spectrum estimate described above). Even with the conservative

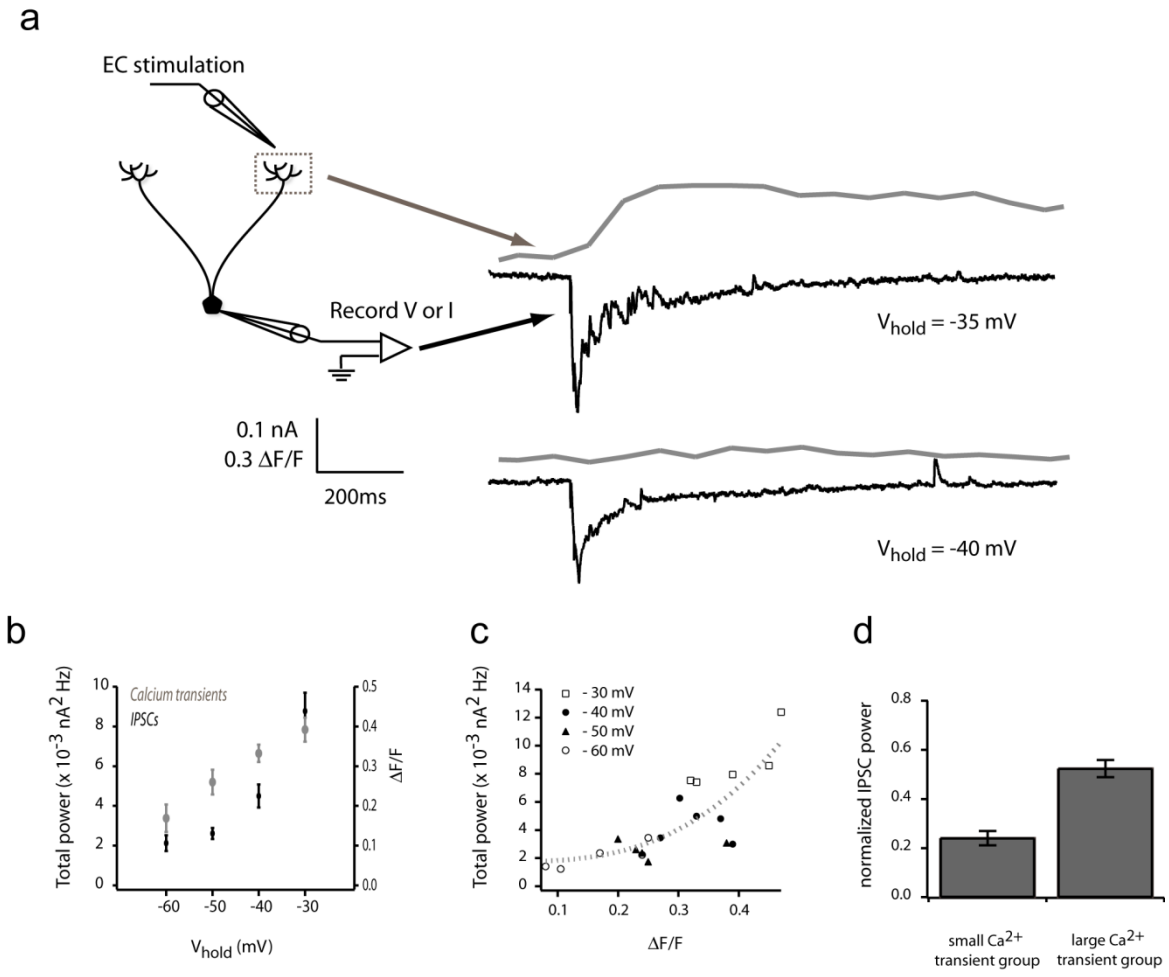
a
EC stimulation
Record V or I
0.1 nA
0.3 ΔF/F
200ms
Vhold = -35 mV
Vhold = -40 mV
b
Calcium transients
IPSCs
Total power (x 10-3 nA2 Hz)
ΔF/F
Vhold (mV)
c
- 30 mV
- 40 mV
- 50 mV
- 60 mV
Total power (x 10-3 nA2 Hz)
ΔF/F
d
normalized IPSC power
small Ca2+ transient group
large Ca2+ transient group

Figure 9. Covariation of tuft spike amplitude and IPSC frequency. (a) The schematic on the left shows the basic stimulation and recording arrangement. Mitral cell somata were current or voltage clamped and filled with Calcium Orange (200 μM); extracellular stimulation was delivered via a theta-glass electrode placed in the immediate vicinity of the tuft. Traces on the right show the sensitive dependence of both tuft calcium transients (grey) and fast inhibitory currents (black) on membrane voltage. At -35 mV (top traces) a large calcium transient and pronounced inhibitory events are clearly visible. With a 5 mV hyperpolarization (bottom traces), both the calcium transient and inhibitory events were substantially reduced. **(b)** Plot of IPSC associated power and peak amplitude of tuft calcium transients vs. holding potential for a different cell. Stimulation intensity was the same for all data points shown. At progressively more negative potentials, tuft calcium transients and IPSC power drop off rapidly. Error bars show ± SEM. **(c)** Same data as in **b**, showing covariation between IPSC associated power and tuft transient amplitude for all traces for several holding potentials. The relationship between ΔF/F at the tuft and IPSC power is fit by an exponential of order 2.91. (**d)** Average, normalized IPSC power evoked by tuft stimulation for cases in which corresponding calcium transients were either large or small (n=5 cells). For each cell, power and ΔF/F were normalized to their respective maxima. These data were then pooled and divided into the two groups shown. The small Ca^{2+} transient group shows the IPSC power for sweeps in which tuft ΔF/F was < 0.5 the maximum, and the large Ca2+ transient group shows IPSC power for sweeps in which tuft ΔF/F was ≥ 0.5 the maximum. Error bars are ± SEM ($p<.05$, unpaired t test, n=33 (small transient), n=44 (large transient)).

estimate of -70mV for chloride reversal (Calculated Nernst potential given our internal and Ringer's is -113mV, though we typically see GABA-A events reverse in the -80 mV to -90 mV range), the change from -35mV to -40 mV would represent a change of only 15% in the amplitude of inhibitory events. In addition, a simple change in reversal potential would predict that the amplitude of individual events should change, but not their number, which is clearly not the case.

This experiment was performed on a total of 5 cells, and all showed the same dependence of IPSC power on tuft calcium transient amplitude. Since absolute values of ΔF/F are generally difficult to compare across tufts (due differences dye loading and tuft volume), we analyzed group data by normalizing tuft ΔF/F and IPSC power by their respective maxima for each cell. These data were then pooled, and divided into two groups: one in which tuft spikes were < 0.5 maximum amplitude, and one in which tuft spikes were > 0.5 maximum amplitude. We found that the IPSC power associated with large calcium transients was significantly higher than IPSC power associated with small calcium transients (Fig. 9d, $p<.05$, t-test).

2.4.5 Inhibition evoked by VN stimulation requires mitral cell calcium elevations

In a final set of experiments, we directly tested whether the inhibition evoked by extracellular stimulation of VN inputs depends on calcium elevation in mitral cells. Mitral cells were patched with a normal internal solution (see methods) and Alexa 594 to visualize tufts. An extracellular stimulating electrode was placed near a visible tuft, and stimuli were delivered to evoke EPSCs and putative reciprocal inhibitory events. Before proceeding with the experiment, several sweeps were collected at various holding potentials to confirm that the observed IPSCs were sensitively dependent on holding voltage (as described above). Cells were then voltage clamped at relatively depolarized potentials (-40 to -30 mV), or maintained at rest in current clamp (to allow physiological tuft spikes), and 10-20 baseline sweeps were collected. Following this, the patch pipette was carefully withdrawn and cells were repatched with an internal solution containing 1mM of the calcium chelator BAPTA, and the stimulation protocol was continued. Series resistance was monitored throughout, and varied less than 15% in all experiments described.

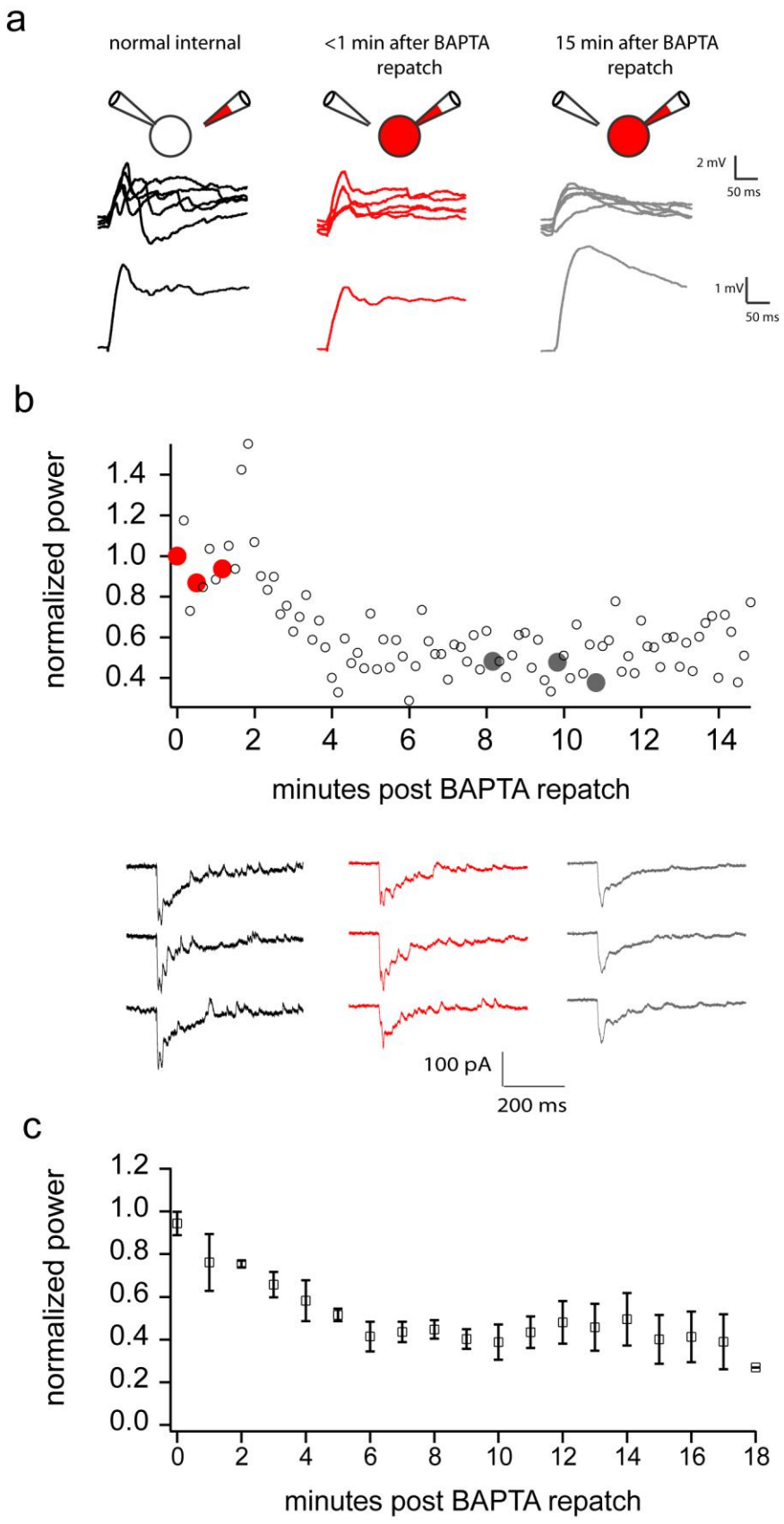
a
normal internal
<1 min after BAPTA repatch
15 min after BAPTA repatch
2 mV
50 ms
1 mV
50 ms
b
normalized power
1.4
1.2
1.0
0.8
0.6
0.4
0
2
4
6
8
10
12
14
minutes post BAPTA repatch
100 pA
200 ms
c
normalized power
1.2
1.0
0.8
0.6
0.4
0.2
0.0
0
2
4
6
8
10
12
14
16
18
minutes post BAPTA repatch

Figure 10. Intracellular BAPTA reduces IPSCs evoked by tuft stimulation. (a) Schematic on the top row illustrates the general experiment design: a mitral cell was patched with normal internal + Alexa 594 to allow visualization of tufts and placement of the stimulating electrode (top row, left). Several sweeps were collected to verify that extracellular stimulation evoked concomitant IPSPs/IPSCs (middle row, left). Following this, the recording electrode was removed from the cell, and the cell was repatched with an electrode containing 1 mM BAPTA (top row, middle). EPSPs/EPSCs were recorded immediately after whole cell break-in and inhibitory events were still evident in these traces (middle row, middle traces). Following dialysis of BAPTA (<15 minutes), inhibitory events were eliminated (middle row, right). Sets of superimposed traces in the middle row are 5 example sweeps from each of the recording conditions schematized in the corresponding figures above. The single traces in the bottom row are averages of 15 sweeps from the recording conditions schematized in the corresponding figures above. (**b)** A second example experiment identical to the one described in **a**, except that the soma was held in voltage clamp to allow quantification of discrete inhibitory events. *Top graph*: time course of reduction of normalized IPSC associated power following BAPTA repatch. *Bottom traces*: sets of three sweeps for the three recording configurations schematized in **a**. Black traces are from the normal internal condition. Red traces are < 2 minutes post BAPTA repatch, and gray traces are between 8 and 12 minutes post BAPTA repatch. Data points corresponding to the red and gray sweeps are indicated on the figure above. (**c)** Group data (n=5) for experiments identical to the one described in **b**. Error bars show ± SEM

One such experiment is shown in figure 10a. Less than one minute after repatching this mitral cell with BAPTA containing internal, EPSPs were qualitatively similar to those evoked with the normal internal – they were characterized by having a number of inhibitory events that occurred shortly after the EPSP peak (Fig. 10a, left column). However, within 15 minutes of repatching this cell, these events were eliminated, leaving a smooth EPSP with a peak 52% greater than the EPSPs collected < 1minute after repatching. This indicates that calcium influx in mitral cells is required for producing the inhibitory deflections observed in response to tuft stimulation. Since these inhibitory deflections were shown above (Fig. 8 a-c) to be the result of GABA-mediated inhibition, and the stimulation intensity used was subthreshold for mitral cell spiking, we conclude that the inhibitory events must be the result of subthreshold release via a calcium dependent mechanism.

In the remaining experiments, this same protocol was followed, the only difference being that mitral cells were voltage clamped at depolarized potentials (-40 to -30 mV) to allow us to quantify inhibitory events as described earlier. An example of this experiment is shown in figure 10b and demonstrates that the power associated with fast inhibition rapidly declines within 2 minutes of repatching a mitral cell with a BAPTA internal. Group data (n=5) is shown for this experiment in figure 10c. As described above, series resistance was monitored during these experiments, and never drifted by more than 15 % throughout. To make sure that the reduced inhibition is not due to some unexpected reduction in afferent drive to mitral cells, we measured the slope of the EPSC and found no significant differences between early and late sweeps ($p>0.5$, t-test). Finally, to ensure that the reduced inhibition is not due to GABA rundown in PG cells or short-term plasticity at VN-PG or PG-mitral synapses, we performed several control experiments in which mitral cells were not repatched with the BAPTA containing internal. Under these conditions, inhibitory responses in mitral cells persisted for over one hour (n=5). In summary, these experiments indicate that the occurrence of stimulus evoked IPSCs require calcium influx in mitral cells. Taken together with earlier evidence showing the covariation between tuft spike amplitude and the magnitude of inhibition recieved, we conclude that stimulation of tufts evokes neurotransmitter release, and recruitment of reciprocal inhibition via periglomerular cells.

2.5 DISCUSSION

2.5.1 Summary of findings

We have studied several aspects of mitral cell dendritic excitability that may allow for highly compartmentalized dendritic input processing and signaling. In particular, we show: 1) mitral cell principal dendrites support full-blown, backpropagating action potentials (BAPs) that invade distal tufts non-decrementally, 2) synaptic inputs to tufts can elicit regenerative calcium spikes restricted to tufts, and 3) these tuft spikes can serve as potent triggers of transmitter release and concomitant feedback inhibition. Taken together, these data argue for a model of AOB mitral cell integration in which tufts serve as independent processing stations capable of amplifying inputs and interacting with local cell populations.

BAPs have been observed in the dendrites of many cell types, and there is considerable heterogeneity in how effectively somatically initiated spikes invade distal dendrites. In cortical pyramidal cell apical dendrites, for example, BAPs are attenuated by ~40% within 400μm of the soma, while Purkinje cells fail to support BAPs altogether (Llinas and Sugimori, 1980;Stuart and Hausser, 1994). Interestingly, BAP conduction in many neurons that release transmitter from their dendrites – including substantia nigra dopaminergic neurons, and main olfactory bulb mitral cells - is non-decremental (Hausser et al., 1995;Bischofberger and Jonas, 1997;Chen et al., 1997;Chen et al., 2002;Debarbieux et al., 2003). Consistent with this general trend, we found no attenuation of BAP evoked calcium transients between the soma and distal dendrites of AOB mitral cells. Although calcium transients in distal dendrites may be biased toward larger values due to geometric factors (i.e. elevated dye concentrations in lower-volume distal compartments), we also observed little attenuation of BAPs when membrane voltage was recorded directly from principal neuron dendrites (100-200μm from the soma). The nondecremental conduction BAPs in mitral cell principal dendrites, and their uniformity across dendritic branches suggests that mitral cells may support an “axon-like” dendritic output mode. Under conditions of sufficient input when mitral cell spikes are elicited, this may allow for uniform activation of tufts, and concomitant self-inhibition (via activation of PG cells) or self-excitation (via glutamate spillover) of all tufts in parallel.

In addition to supporting robust somatofugal signaling, the active properties of mitral cell dendrites may contribute to the boosting of synaptic inputs to tufts (Yuan and Knopfel, 2006b;Zhou et al., 2006b). Indeed, when we stimulated mitral cells with brief shocks to presynaptic vomeronasal nerve axons, we observed calcium spikes confined to tufts. These spikes were regenerative, all-or-none events with amplitudes comparable to transients evoked by single BAPs (Fig. 6). Similar, isolated spikes have also been observed in tufts of main olfactory bulb mitral cells, but only when somatic spikes were prevented by somatic hyperpolarization, either by direct current injection or activation of inhibitory inputs (Chen et al., 1997). This difference in the relative ease with which local spikes are evoked may be due to geometric factors, including the considerable electrotonic isolation of AOB mitral cell tufts from the soma .

Although many cell and context-specific functions of dendritic spikes have been investigated, two general themes have emerged: 1) local spikes allow inputs to distal, electrotonically "disadvantaged" regions of the dendritic tree to contribute to neural output (Golding and Spruston, 1998; Urban et al., 1998), and 2) local spikes enhance the compartmentalization of dendritic function (Schiller et al., 1995;Schiller et al., 1997;Euler et al., 2002;Polsky et al., 2004). In some sense these seem to be mutually exclusive roles for dendritic spikes. For dendrites that produce outputs though, these roles may be fully compatible: the electrogenic events underlying dendritic spikes allow for boosting of synaptic inputs en route to the soma, while the confinement of spikes may allow neurons to produce local output. This reconciliation requires, of course, that local spikes are viable triggers of dendritic output.

We have demonstrated that synaptic stimulation of tufts of accessory olfactory bulb mitral cells evokes somatic responses comprised of a slow EPSP/EPSC in tandem with an asynchronous barrage of GABA-A mediated inhibitory events. In addition, the presence and frequency of these inhibitory events was strongly correlated with occurrence and magnitude of calcium transients in the tuft. To determine whether the release events underlying the observed inhibition were the result of feedforward inhibition, or required conditions favorable for transmitter release in mitral cells, we performed several manipulations on the recorded cells. The stimulus evoked inhibitory barrages were found to be steeply dependent on postsynaptic voltage (under both current and voltage clamp), with reductions in holding potential by as little as 5 mV capable of abolishing both tuft calcium transients and inhibitory events. When mitral cell release competence was compromised by intracellular dialysis with 1mM BAPTA,

inhibitory events were also diminished, indicating that the source of inhibition depended on calcium influx in mitral cells. The most parsimonious explanation consistent with these findings is that subthreshold activation of mitral cell tufts evokes local calcium transients that are sufficient triggers for transmitter release.

2.5.2 Significance for AOB function

As in the main olfactory bulb, AOB mitral cell tufts receive convergent input from the axons of receptor neurons expressing the same receptor phenotype (Del Punta et al., 2002b). Given that vomeronasal receptor neurons exhibit extraordinary specificity for single ligands (Leinders-Zufall et al., 2000), and that this specificity is largely concentration invariant (unlike in the MOB)(Holy et al., 2000), AOB tufts can be regarded as "labeled" processing modules that report the presence of single (or very few) specific ligands. Moreover, since AOB mitral cells are multi-tufted, a single cell can draw multiple samples from each of its independent, labeled modules (Luo et al., 2003). Our present results put forward a view in which AOB tufts are independent, self regulating structures: active conductances in the tuft amplify synaptic inputs, and these same regenerative events engage local inhibitory circuitry that may oppose this amplification. What is the benefit of coupling local amplification with local inhibition? We propose that this mechanism allows mitral cells to maintain sensitivity without compromising selectivity in the following manner. Due to regenerative conductances in the tuft, only small numbers synaptic inputs are necessary to induce appreciable subthreshold responses in the soma. However, with increasing input, local feedback inhibition will be engaged, and synaptic amplification at the tuft will be opposed. In effect, an individual tuft is "clamped" to operate only within a small dynamic range: small inputs result in robust responses, but larger inputs evoke an inhibitory feedback response that limits the maximum level of tuft depolarization. In the extreme, the tuft would function to generate a response to synaptic inputs that is all-or-none, but *still subthreshold* for somatic or axonal spiking. Thus, a single mitral cell could only spike when several of its tufts are activated, and mitral cell spiking would be a function of the number of tufts activated, with no single activated tuft being sufficient to produce spiking output. Two benefits may accrue from such a strict requirement for tuft cooperativity. Under the assumption that all tufts of a mitral cell receive input from phenotypically identical receptor neuron populations (homotypic connectivity

(Del Punta et al., 2002b)), a mitral cell's output would become more highly selective for its single ligand. Rather than depending on a single, potentially noisy report on the presence of ligand from a single tuft, several such "votes" would be necessary and would reduce the number of false positive responses. A second interesting scenario is that in which different tufts of a mitral cell receive inputs from different receptor phenotypes (heterotypic connectivity) – a view for which there is accumulating evidence (Dulac and Torello, 2003;Wagner et al., 2006a). In this case, a mitral cell would only generate responses to a unique conjunction of compounds in a multi-component pheromone mixture, since single active tufts would be unlikely to induce axosomatic spiking. This model implies that AOB mitral cells may be the site of integration of pheromonal signals that consists of multiple components, and have local control mechanisms to ensure that this process is robust and reliable.

3.0 RECIPROCAL INHIBITION OF AOB MITRAL CELLS REQUIRES MGLUR1

3.1 ABSTRACT

The selectivity of AOB function depends on both mitral cell excitability, and the degree to which mitral cell activity recruits reciprocal inhibitory circuits. Reciprocal inhibition (RI) acts on mitral cells close to their sites of excitatory input and axonal output, and hence allows for local, cell-specific feedback control of integration and discharge. Consequently, changes in the efficacy of this feedback inhibition could have pronounced effects on mitral cell selectivity. A number of behavioral studies are consistent with this notion, and allude to the important role of metabotropic glutamate receptors (mGluRs) in regulating reciprocal inhibition. In this chapter we describe a previously unknown, obligatory role of mGluR1 in mitral cell reciprocal inhibition, and identify granule cells as one of mGluR1s sites of action.

3.2 INTRODUCTION

Accessory olfactory bulb mitral cells are exquisitely selective for particular pheromones, and are few synapses removed from brain structures believed to induce pheromonal effects. Because these effects include behavioral or endocrine responses that could be maladaptive in inappropriate contexts, mechanisms that promote mitral cell selectivity (or limit mitral cell discharge) are likely critical for pheromone processing. To a large degree, the throughput of information from the AOB to downstream structures is controlled by recurrent inhibition (RI) of mitral cells by periglomerular and granule cells – populations of GABA-ergic interneurons that inhibit mitral cells via reciprocal dendrodendritic synapses (Rall et al., 1966;Rall and Shepherd, 1968;Isaacson and Strowbridge, 1998;Schoppa et al., 1998;Taniguchi and Kaba, 2001;Urban, 2002). These cells provide the only sources of inhibition intrinsic to the AOB, and act on mitral cell dendrites close to sites of integration and output. Thus, regulation of recurrent inhibition is a potentially potent means of controlling mitral cell selectivity and discharge.

Consistent with this, a number of studies have shown that the selectivity of pheromone recognition during certain olfactory behaviors is eliminated when the AOB is infused with either lignocaine (Kaba and Keverne, 1988), or antagonists that diminish GABA release from granule cells (Kaba et al., 1994). In addition, these and related studies described a critical role for metabotropic glutamate receptors (mGluRs) in certain forms of olfactory learning believed to result from changes in recurrent inhibition. mGluRs are G-protein coupled receptors expressed throughout the CNS and couple glutamate binding to a host of changes in the intrinsic and synaptic properties of neurons. These changes include spatially localized increases in intracellular calcium via activation of ryanodine receptors (Chavis et al., 1996;Finch and Augustine, 1998b;Takechi et al., 1998;del et al., 1999), up or down-regulation of potassium and calcium conductances (Charpak et al., 1990;Schoppa and Westbrook, 1997;Chavis et al., 1998;Fagni et al., 2000;Heinbockel et al., 2006), and reduction in the strength of electrical synapses (Landisman and Connors, 2005). Given these diverse effects, mGluRs could conceivably influence many aspects of dendritic excitability and/or output.

Although expression levels of mGluRs in the AOB are among the highest in the brain, there have been surprisingly few physiological investigations of mechanisms by which mGluRs modulate AOB mitral cell recurrent inhibition. Thus, in this chapter, we examined the role of

mGluRs in mediating recurrent inhibition. Surprisingly, we found that RI of AOB mitral cells requires activation of the group I metabotropic glutamate receptor mGluR1. This requirement for mGluR1 was dramatically reduced when extracellular magnesium concentration was lowered, suggesting that mGluR1 activation may enhance the coupling of NMDA receptors to inhibition. Inhibition was also induced by direct application of the group I mGluR agonist DHPG, and partially persisted following blockade of ionotropic glutamatergic synaptic transmission and sodium spikes. In addition, DHPG depolarized granule cells via a mechanism dependent on mGluR1. These results demonstrate that mGluR1 regulates granule cell excitability, and, concomitantly, recurrent inhibition of mitral cells.

3.3 MATERIALS AND METHODS

3.3.1 Slice Preparation

Methods are as described previously in Urban and Castro (2005). Briefly, peri-saggital olfactory bulb slices (300-350 μm thick) were prepared from young mice [postnatal day 14 (P14 to P28)]. Mice were anesthetized (0.1% ketamine/0.1% xylaxine; ~ 3mg/kg, i.p.) and decapitated. Olfactory bulbs were removed and sectioned on a vibratome while submerged in ice-cold oxygenated Ringer's solution containing the following (in mM): 125 NaCl, 2.5 KCl, 25 $NaHCO_3$, 1.25 NaH_2PO_4, 1$MgCl_2$, 25 glucose, 2 $CaCl_2$. In some experiments, 0.5 mM ascorbate, 1mM pyruvate, and 2mM *myo*-inositol were added to the slicing medium. All animal care was in accordance with the guidelines of Institutional Animal Care and Use Committee of Carnegie Mellon University.

3.3.2 Electrophysiology

Whole cell voltage recordings were obtained from the somata of identified AOB mitral cells (Stuart and Spruston, 1995). Slices were superfused with the oxygenated Ringer's solution

described above, warmed to 34-36º C. Whole-cell recordings were established using pipettes (resistances of 2-8 MΩ) filled with a solution containing the following (in mM): 120 postassium gluconate, 2 KCl, 10 HEPES, 10 sodium phosphocreatine, 4 MgATP, and 0.3 Na_3GTP, adjusted to pH 7.3 with KOH. Voltage and current clamp recordings were preformed using a MultiClamp 700B amplifier (Molecular Devices, Union City, CA). Data were filtered (4 kHz low pass) and digitized at 10 kHz using an ITC-18 (Instrutech, Mineola, NY) controlled by custom software written in Igor Pro (Wavemetrics, Lake Oswego, OR). In all experiments in which membrane current was recorded, mitral cells were held at -40 mV to facilitate the recording of $GABA_A$-mediated IPSCs.

3.3.3 Data Analysis

Miniature IPSCs were detected using custom written functions in IGOR pro (Wavemetrics, Lake Oswego, OR), which implemented the algorithm described by (Kudoh and Taguchi, 2002b). Event rates for control conditions were calculated in a 1 minute window prior to the addition of drug. For drug conditions, a window three minutes after drug addition was used to calculate event rate. For analysis of the onset kinetics of the enhanced rate of IPSCs, sigmoids were fit to plots of IPSC rate (calculated in 500 ms bins) vs. time. These sigmoids were normalized by their maxima and aligned to the first point where the derivative of a given fitted sigmoid was non-zero. From these aligned curves, a mean sigmoid was generated according to $y=1/(\exp(t_{half}-t)/rate)$, where the parameters t_{half} and *rate* were averages of these same parameters from the individual sigmoids. For more standard measures of time-to-peak of these same IPSC rate data (the values reported in the text) an alternative procedure was used. The standard deviation of IPSC event rate (also calculated in 500 ms bins) was calculated for a one minute period prior to DHPG addition, and onset was defined as first time point when IPSC event rate exceeded the mean of the baseline period by two standard deviations. The mean event rate and standard deviation were then calculated for a period of two minutes following the onset (defined as above), and peak time was defined as the first point following onset when this mean event rate was achieved and maintained within one standard deviation of this value for at least 10 seconds

(20 samplings of the rate). Data are reported as mean ± SEM unless otherwise indicated. Statistical significance was assessed using paired or unpaired t-tests as appropriate.

3.3.4 Drugs

APV, CNQX, bicuculline, and Cyclopiazonic acid (CPA) all were obtained from Sigma – Aldrich (St. Louis, MO) and used at concentrations of 50, 20, 10, and 30 µM, respectively. Gabazine, DHPG and LY367385 were obtained from Tocris (Ellisville, MO), and used at final concentrations of 10, 20 and 100 µM, respectively. 3-((2-Methyl-1,3-thiazol-4-yl)ethynyl)pyridine (MTEP) (Calbiochem, La Jolla, CA) was used at 2µM and prepared from a 25 mM stock in 100% DMSO. CPA and LY367585 were prepared in stocks of 18 and 100mM respectively, both in 100% DMSO. The DHPG stock was prepared in dH_20 at 100 mM. The voltage gated channel blockers TTX, Nickel, and Cadmium were used at concentrations of 1µM, 100µM, and 30µM respectively.

3.4 RESULTS

3.4.1 Recurrent inhibition of AOB mitral cells requires mGluR1 activation

In mitral cells of the MOB and AOB, action potentials or large membrane depolarizations evoke long-lasting inhibition mediated by $GABA_A$ receptors (Isaacson and Strowbridge, 1998;Schoppa et al., 1998;Margrie et al., 2001;Taniguchi and Kaba, 2001). This form of inhibition, in which activity in an excitatory neuron results in self inhibition dependent on dendrodendritic synapses with inhibitory interneurons, is typically termed recurrent inhibition (RI). We adhere to this nomenclature in the remainder of this chapter to differentiate RI from inhibition that is evoked pharmacologically and not strictly by spiking in a presynaptic excitatory neuron. In an initial set of experiments, we characterized RI in AOB mitral cells. In voltage clamp, a 100 ms depolarization of mitral cells from -40mV to +20 mV evoked a slow outward current (Fig. 11)

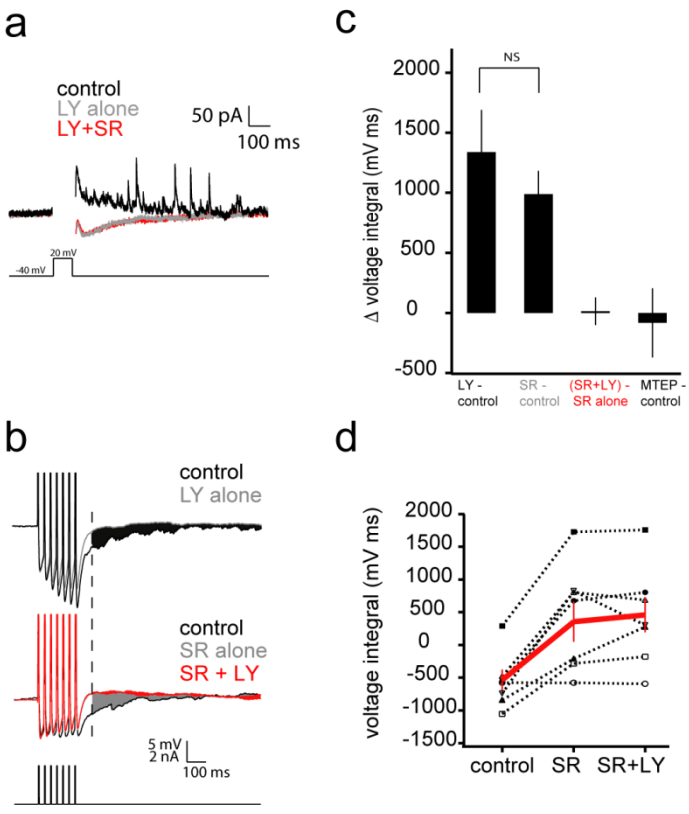
a
control
LY alone
LY+SR
50 pA
100 ms
20 mV
-40 mV
b
control
LY alone
control
SR alone
SR + LY
5 mV
2 nA
100 ms
c
NS
2000
1500
1000
500
0
-500
Δ voltage integral (mV ms)
LY - control
SR - control
(SR+LY) - SR alone
MTEP - control
d
2000
1500
1000
500
0
-500
-1000
-1500
voltage integral (mV ms)
control
SR
SR+LY

Figure 11. The mGluR antagonist LY367385 eliminates recurrent inhibition in AOB mitral cells. (a) Single sweeps showing currents evoked by depolarization of a mitral cell from -40 mV to 20 mV. Action currents during the depolarization are blanked for better visibility. *Black*: control sweep showing slow outward component and discrete outward events. *Gray*: sweep showing blockade of the slow and discrete outward currents with addition of LY (100µM). *Red*: sweep showing lack of effect of SR95531 (gabazine,10µM) added after LY. **(b)** Single sweeps from current clamp experiments in which recurrent inhibition was elicited by current pulses (3ms x 40 Hz). *Top:* traces showing the effect of LY on recurrent inhibition. Note the discrete events evident in the control case that are eliminated by LY addition. The black shaded area corresponds to the difference in voltage integrals used to measure changes in recurrent inhibition between the control and LY cases. *Middle:* occlusion-type experiments in which recurrent inhibition was first completely blocked by SR and LY subsequently added. The gray shaded area corresponds to the difference between voltage integrals for the control and SR cases. The red shaded area corresponds to the difference between voltage integrals for the SR and *SR + LY* cases. **(c)** Summary data for experiments similar to those shown in B. The colors of the group labels correspond to the colors of the shaded regions shown in B (n=8 for LY-control and n=7 for ((*SR+LY*) – *SR alone*) group), except for the (*MTEP-control*), group (n=7), which has no corresponding trace in **b**. (**d)** Summary of individual experiments showing the occlusion effect of SR on LY. Red lines and markers indicate mean ± SEM for all experiments. (Control: -536.36 ± 160.52 mV ms, SR: 355.90 ± 306.67 mV ms, SR+LY: 459.14 ± 264.49 mV ms, n=7).

consisting of many discrete outward synaptic events superimposed on the slower current (Fig. 11a). This current was eliminated by addition of the $GABA_A$ specific antagonist gabazine (SR95531, 10μM), indicating that these voltage steps evoke recurrent inhibition. In similar experiments, trains of seven action potentials at 40Hz were evoked in mitral cells by current injection, and recurrent inhibition was observed as a slow, gabazine-sensitive hyperpolarization (Fig. 11b). Recurrent inhibition in this case was quantified as the voltage integral following the final spike in the series of action potentials (from 70 ms following the final injected current step to 1130 ms following this step; this latter number corresponded to the end of the sweep). We typically saw asynchronous IPSP-like events lasting most or all of this period (see, for example, both control cases in Fig. 11b). These results demonstrate that both action potentials and membrane depolarization evoke long-lasting recurrent inhibition in AOB mitral cells, consistent with previous results (Taniguchi and Kaba, 2001).

We next tested whether recurrent inhibition was modulated by activation of mGluRs in AOB slices. Adding the mGluR1 antagonist LY367385 (LY, 100μM) to the bathing medium resulted in a decrease in RI that was comparable to the decrease seen with the addition of gabazine (Δ voltage integral = 1338.48 ± 351.74 mV·ms (LY, n=7), 988.63 ± 193.79 mV·ms (gabazine, n=8), p=0.40), suggesting that a large fraction of recurrent inhibition required activation of mGluR1 (Figs. 11c & d). By contrast, the selective mGluR5 antagonist MTEP (2 μM) had no effect recurrent inhibition (Fig 11c).

It is possible, though unlikely, that blockade of mGluR1 upregulates a depolarization-evoked inward current that masks recurrent inhibition. To test whether the mGluR1-dependent component of RI is the same as the GABA-A dependent component, we first blocked inhibition with gabazine, and then added LY (an example is shown in the bottom of Fig. 11b). Under these conditions, addition of gabazine completely occluded the subsequent effect of LY (Fig. 11d). Taken together, these data demonstrate that mGluR1 activation is necessary for recurrent inhibition in AOB mitral cells in control conditions.

3.4.2 Activation of mGluRs evokes spontaneous IPSCs in mitral cells

Given the strong dependence of recurrent inhibition on mGluR1, we next determined whether direct activation of group I mGluRs is sufficient to evoke IPSCs in mitral cells. Mitral cells were voltage clamped at -40 mV during addition of the broad-spectrum group I mGluR agonist DHPG (20 μM). DHPG elicited a more than a ten-fold increase in the rate of spontaneous outward events, with the event rate increasing from an average of 0.41 ±0.20 Hz to 5.86 ±1.26 Hz (n = 6, $p<0.01$, t-test) (Fig. 12a & b). These events were completely blocked by 10 μM bicuculline (Figs. 13b & c) indicating they are mediated by $GABA_A$ receptors. In addition, the kinetics and amplitudes of these events were nearly identical for the baseline and DHPG cases (see cumulative amplitude distribution in figure 12c and corresponding traces in the inset), suggesting that DHPG is causing release of GABA at reciprocal synapses onto mitral cells. Amplitude, rise time, and decay time histograms of observed events were unimodal (data not shown), consistent with a single presynaptic source. The effect of DHPG persisted in the presence of the glutamate receptor blockers APV (50μM) and CNQX (20μM) (Fig. 13a), indicating that the effect was at least partially independent of glutamate release from mitral cells. However, the rate of DHPG-evoked IPSCs was substantially lower when ionotropic glutamate receptors were blocked than in the control case (control + DHPG: 5.89 ± 1.26; APV+CNQX+DHPG: 2.40 ± 0.72 Hz, n=6, $p<0.03$).

It is worth noting that the ~15 pA slow inward current observed in figure 12a was not observed in all mitral cells. Changes in steady state current evoked by DHPG were heterogeneous: in some cells DHPG evoked slow inward currents, and in others slow outward currents. The mean change in mitral cell holding current was -9.4 ± 10.6 pA (n=8), which is a smaller and less reliable effect than observed in MOB mitral cells (Ennis et al., 2004). In addition, we failed to find a strong relationship between the magnitude of DHPG-evoked current and the DHPG evoked increase in IPSC rate within cells ($R^2 = 0.16$ for event rate vs. holding current). By contrast, the very rapid onset of enhanced IPSCs was seen in all mitral cells tested. The mean time to peak event rate from onset across all cells was 24.3 ± 6.3 s (n=6) (see **Materials and Methods (3.3.3)** for definitions of onset and peak).

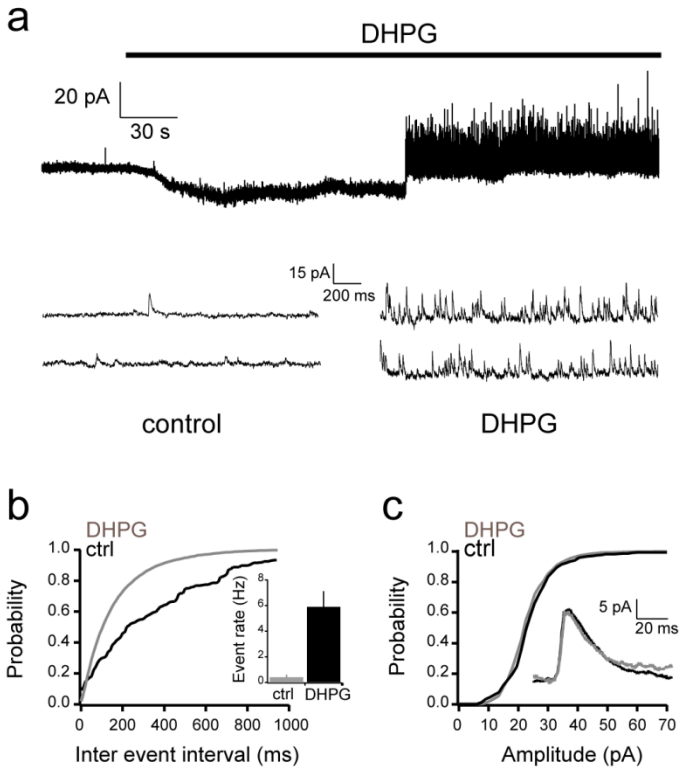

Figure 12. DHPG enhances the rate of spontaneous IPSCs in mitral cells. (a) Bath application of DHPG (20 μM) greatly increases the occurrence of spontaneous IPSCs in mitral cells. Addition of DHPG in general evoked a slow inward or outward current followed by a rapid transition to a high rate of IPSCs. Traces on the bottom of **a** show expanded versions of the control and DHPG conditions. **(b)** Cumulative probability plot of inter-event intervals for control and DHPG conditions (n=6). Inset shows mean event rate for the two conditions (control: 0.41±0.2 Hz, DHPG: 5.86 ± 1.26 Hz, n=6, $p<0.01$). **(c)** Cumulative probability plot of event amplitudes for control and DHPG conditions indicating no significant differences. (Inset shows average IPSC waveforms for each of the conditions.

3.4.3 mGluR1 is responsible for increases in IPSC rate

DHPG is a broad spectrum group I mgluR agonist (Ito et al., 1992), and therefore activates both receptors in this class – mGluR1, and mGluR5 (Conn and Pin, 1997). To determine which of these mGluRs contributes to the increase in mitral cell IPSCs, we performed experiments in which DHPG was added in the presence of LY367385 (LY), or 3-((2-Methyl-1,3-thiazol-4-yl) ethynyl) pyridine (MTEP), specific blockers of mGluR1 and mGluR5, respectively. When DHPG (20 μM) was added to the bathing medium in the presence of 100 μM LY, the rate of mitral cell IPSCs did not increase (LY alone: 0.35 ± .23 Hz, LY+DHPG: .19 ± .08 Hz, n=5, p=.53) (Figs. 14a & d). By contrast, the rate of IPSCs was enhanced when DHPG was added in the presence of 2 μM MTEP (MTEP alone: 0.27 ± .10 Hz, MTEP + DHPG: 2.88 ± .46 Hz,n=4, p=.0009) (Figs. 14 & d). These results indicate that DHPG-evoked IPSCs are due to the effect of DHPG on mGluR1.

3.4.4 DHPG evoked IPSCs require calcium influx, but not sodium spikes

As noted above, and similar to what others have seen in MOB (Heinbockel et al., 2004), we sometimes observed a slow DHPG-evoked inward current in mitral cells that accompanied the increase in IPSCs (see, for example, figure 12a). Hence, a potential mechanism for the increased barrage of spontaneous IPSCs is direct depolarization of mitral cells, with concomitant elevated mitral cell firing rates. Thus, we next tested whether action potentials are required for the increase in IPSC rate by mGluR agonists by including 1μM TTX in the bath solution prior to addition of DHPG. Under these conditions the rate of mitral cell IPSCs was still increased (baseline: .04 ± .02 Hz, DHPG: 1.99 ± .76 Hz, $p<.05$, n=4) (Figs. 15a & c), indicating that sodium spikes are not required for mGluR activation to evoke IPSCs. Since the IPSC rate was lower in TTX than control conditions, sodium channels and spontaneous spiking by granule or PG cells are likely to play a role in setting the rate of IPSCs. By contrast, when the calcium channel blockers cadmium (30 μM) and nickel (100 μM) were included in the bath, DHPG did not cause a significant increase in IPSC rate (baseline: 0.34 ± 0.09Hz, DHPG: 0.33 ± 0.17 Hz, $p>0.05$, n=5) (Figs. 15b & c).

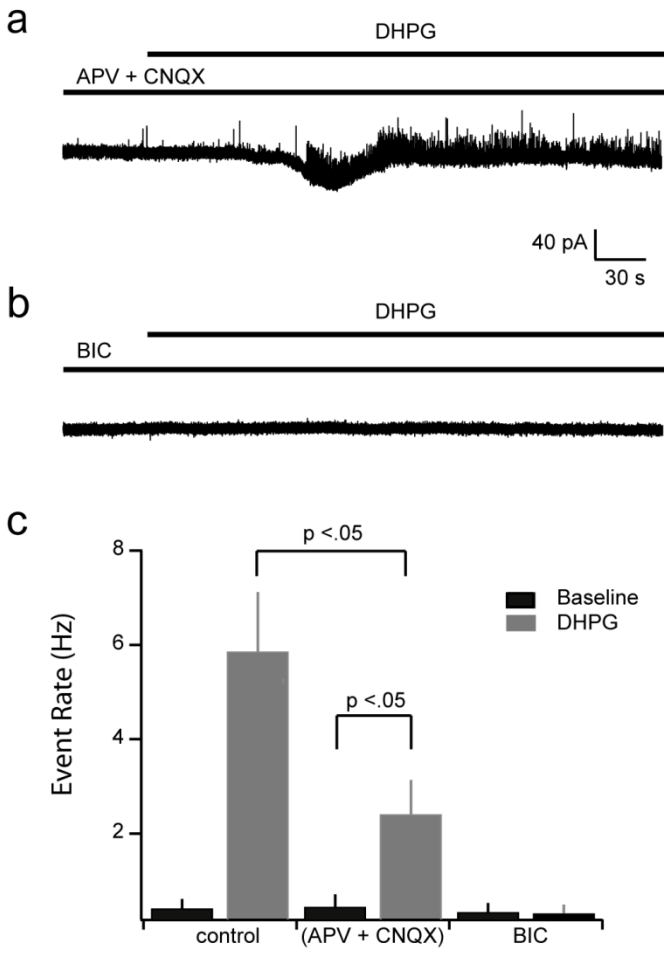

Figure 13. The increase in IPSC rate with DHPG addition can occur via a mechanism presynaptic to mitral cells. (a) Sample sweep in which APV (50 µM) and CNQX (20 µM) were bath applied for 10 minutes prior to addition of 20 µM DHPG (baseline period is truncated). **(b)** Sample sweep showing complete absence of spontaneous and DHPG-evoked IPSCs in 10 µM bicuculline. As above, bicuculline addition preceded DHPG addition by 10 minutes (baseline is truncated). **(c)** Summary data of effects of synaptic blockers on DHPG-induced IPSCs.

3.4.5 Release from internal stores is not required for DHPG-evoked inhibition

In a number of cell types, activation of mGluRs is coupled to release of calcium from internal stores either via second messengers or calcium influx through voltage gated calcium channels (Chavis et al., 1996;Finch and Augustine, 1998a;Takechi et al., 1998;del et al., 1999). The experiments above indicate that calcium influx through voltage gated calcium channels is necessary to evoke recurrent IPSCs, but does not address the question of whether GABA release also depends on release of calcium from internal stores. To test this possibility, we bath applied the sarcoplasmic reticulum calcium pump inhibitor CPA (30 μM) to deplete internal calcium stores prior to adding DHPG. Enhanced rates of IPSCs were still observed under these conditions, with a mean DHPG-evoked rate (8.23 ± 2.27 Hz, n = 5) (Fig. 16) comparable to that observed under control conditions (5.86 ±.1.26 Hz, n=6). This indicates that DHPG likely acts by causing a direct, calcium-dependent depolarization in granule cells – possibly activation of a calcium conductance, or closure of a potassium channel (see (Schoppa and Westbrook, 1997) and that GABA release is then triggered by voltage-gated calcium current in granule cells.

3.4.6 Mechanisms of mGluR1 action in granule cells

In the main and accessory olfactory bulbs, recurrent inhibition evoked by mitral cell spiking is mediated predominantly by granule cells, the major interneuron population (Price and Powell, 1970a;Price and Powell, 1970b;Isaacson and Strowbridge, 1998;Schoppa et al., 1998;Isaacson, 2001). Given that we saw complete elimination of recurrent inhibition in AOB mitral cells with blockade of mGluR1 (Fig. 11) and that DHPG-evoked IPSCs in mitral cells persisted when ionotropic glutamateric transmission was blocked (Fig. 13), we reasoned that granule cells are likely to be the major cell type contributing to the large increase in miniature IPSCs observed in our experiments. In addition, the persistence of DHPG-evoked spontaneous IPSCs in the presence of TTX, but their elimination by blockers of VGCCs is consistent with studies in granule cells demonstrating that local or global calcium spikes are potential triggers of transmitter release (Egger et al., 2003;Pinato and Midtgaard, 2003;Egger et al., 2005;Pinato and Midtgaard, 2005;Zelles et al., 2006). Thus, one possible mechanism for the action of DHPG is

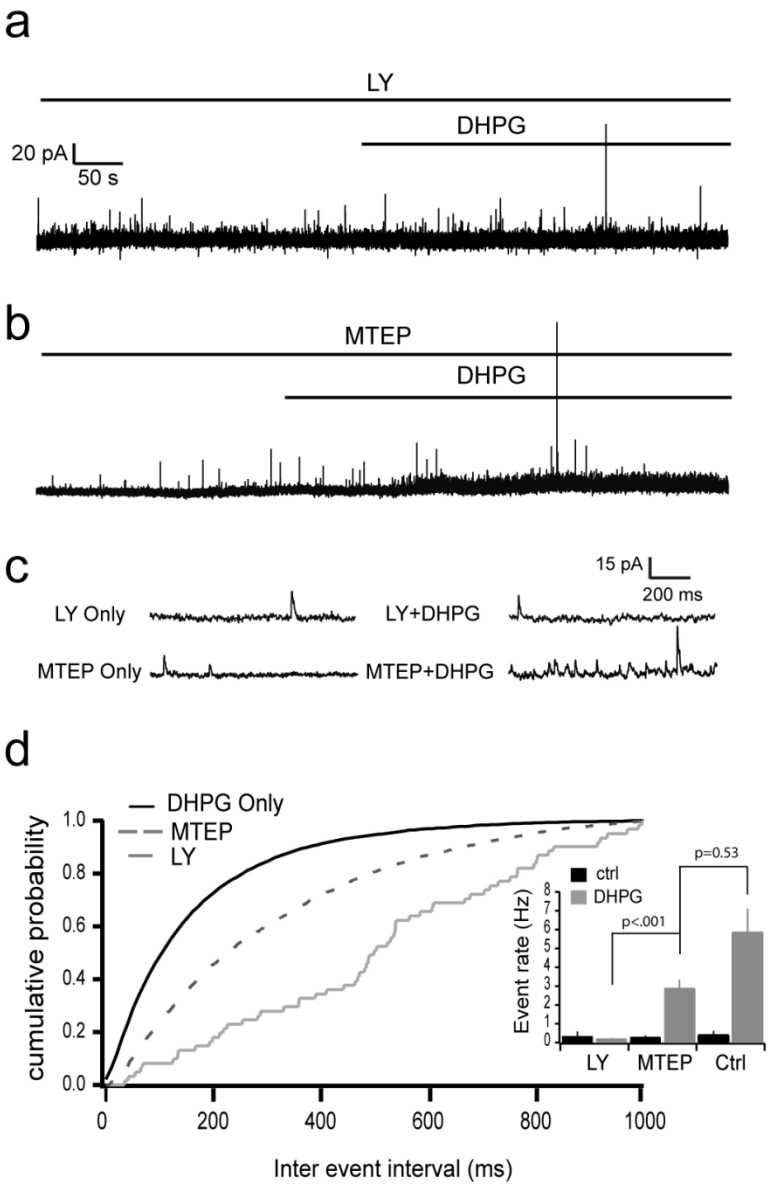
a
LY
DHPG
20 pA
50 s
b
MTEP
DHPG
c
15 pA
200 ms
LY Only
LY+DHPG
MTEP Only
MTEP+DHPG
d
DHPG Only
MTEP
LY
cumulative probability
1.0
0.8
0.6
0.4
0.2
0.0
0
200
400
600
800
1000
Inter event interval (ms)
ctrl
DHPG
p=0.53
p<.001
Event rate (Hz)
LY
MTEP
Ctrl

Figure 14. The effect of the mGluR evoked increase in IPSC rate is mediated primarily by mGluR1. **(a)** Bath application of DHPG (20 μM) in the presence of mGluR1 antagonist LY (100 μM) eliminated the increase of spontaneous IPSCs in mitral cells. **(b)** Bath application of DHPG in the presence of mGluR5 antagonist MTEP (2 μM) still showed a significant increase in the occurrence of IPSCs in mitral cells. In both cases, slices were bathed in the individual antagonist for 15 minutes before addition of the antagonist plus DHPG. **(c)** Expanded version of traces showing individual events in two conditions: IPSCs in the presence of the individual antagonist alone (left) and with addition of DHPG along with the antagonist (right). **(d)** Cumulative probability plot of inter-events intervals for control DHPG conditions (black line), DHPG in the presence of MTEP (dashed line), and DHPG in the presence of LY (gray line). Inset shows mean event rates for all conditions (LY baseline: 0.35 ± 0.23 Hz, LY + DHPG: 0.19 ± 0.08 Hz (n=5), MTEP baseline: 0.27 ± 0.10 Hz, MTEP + DHPG: 2.88 ± 0.46 Hz (n = 4).

via direct depolarization of granule cells. In this scenario, glutamate released from mitral cells would bind to metabotropic receptors on granule cells, and cause a local or global calcium elevation sufficient to evoke GABA release from granule cells. To test this possibility, we recorded from granule cell somata in the presence of blockers of fast glutamatergic transmission (50 μM APV, 20 μM CNQX) and added DHPG (20 μM). In 4 granule cells tested, we observed a depolarization of 6.79 ± 0.79 mV by the third minute after DHPG addition – an effect which persisted for the duration of drug addition (Fig. 17a). Granule cells were also depolarized by 5.15 ± 0.42 mV (n=5) by DHPG when MTEP (2μM) was included in the bath solution (Fig. 17b), indicating that activation of mGluR1 is sufficient for the effect. By contrast, no significant depolarization was observed when mGluR1 was blocked by LY367385 prior to DHPG addition (n=5) (Fig. 17b). It is worth noting granule cell spines are electrotonically isolated from the granule cell soma (Rall and Shepherd, 1968;Woolf et al., 1991;Egger and Urban, 2006), and that depolarization observed at the soma may be an underestimate of voltage changes more local to spines and associated release machinery.

Studies in both the main and accessory olfactory bulb have demonstrated that NMDA receptors (NMDARs) – likely those present on granule cell spines - are important for recurrent inhibition of mitral cells (Chen et al., 2000). In control conditions, blockade of NMDARs results in near-complete elimination of action potential evoked recurrent inhibition; some of these findings also suggest that calcium influx through NMDARs can be directly coupled to transmitter release (Chen et al., 2000;Halabisky et al., 2000). Given that NMDAR activation is required for recurrent inhibition in control conditions, our results suggest that activation of mGluR1 may play a modulatory, but still critical role in evoking transmitter release from granule cells.

One possibility we considered was that due to its depolarizing effect on granule cells, mGluR1 may facilitate voltage dependent calcium influx that is directly coupled to GABA release. Specifically, mGluR1 may depolarize granule cells by an amount sufficient to relieve magnesium blockade of NMDARs and facilitate reciprocal communication via the "classical" ionotropic pathway. One possible mechanism, which we did not investigate further, is that activation of mGluR1 activates a non-specific cation conductance to elicit calcium and sodium spikes. In Purkinje cells, for example, a long-lasting mGluR ESPC elicited by parallel fiber

stimulation is known to depend on a transient receptor potential (TRP) channel. Regardless of the actual molecular players in this model, one prediion is that under conditions permissive for NMDA receptor activation, mGluR1 antagonists should be relatively less effective at eliminating spike- evoked recurrent inhibition. To test this, we evoked action potentials (7 spikes at 40 Hz) in mitral cells under low magnesium (0.2 mM) conditions and measured the magnitude of recurrent inhibition before and after addition of LY367385. In agreement with our proposed mechanism, LY did not cause a significant change in recurrent inhibition in 0.2 mM magnesium (Figs. 17c & d; 76 ± 24% of control post LY) compared to the change observed in 1.0 mM magnesium (Figs. 17c & d; 28 ± 17% of control post LY, p=0.012, n=6).

3.5 DISCUSSION

3.5.1 Summary of findings

We describe two main findings in this chapter. First, under control, physiological conditions, mGluR1 is required for recurrent inhibition of AOB mitral cells. Second, direct activation of group I mGluRs can evoke a robust GABA-ergic inhibition of mitral cells via a presynaptic mechanism that depends on voltage gated calcium channels.

Much of the interest in metabotropic glutamate receptors in the olfactory bulb stems from their dense expression in this structure, and from reports of their role in regulation of AOB-dependent behaviors. Mitral cells express at least four mGluRs including mGluR1, 2, 7, and 8 (Masu et al., 1991; Martin et al., 1992;Shigemoto et al., 1992). mGluR2 has been localized to granule cells and its activation is reported to underlie suppression of granule cell inhibition of mitral cells that is linked to forms of olfactory memory (Kaba et al., 1994). Despite the considerable attention that has been given to the role of specific activation of mGluR2 in this form of olfactory memory (Hayashi et al., 1993;Kaba et al., 1994) synaptic release of glutamate from mitral cells is likely to activate both class 1 and class 2 mGluRs are thus understanding the role that both these receptor types play in regulation of olfactory bulb neurons is critical. In this regard, our observation that activation of mGluR1 results in effects on granule cell activity and

inhibition at reciprocal synapses that oppose the effects reported for mGluR2 activation raises interesting questions about how these receptors influence mitral cell activity.

mGluR1 immunoreactivity in the AOB is concentrated largely in the mitral-tufted cell layer, with less robust staining observed in the granule cell layer (Sahara et al., 2001). Given that we observed granule cell depolarization in response to DHPG (Fig. 17), and that recurrent inhibition was eliminated by an antagonist of mGluR1 but not mGluR5 (Fig. 14),our results are consistent with expression pattern in which mGluR1 is highly localized to granule cell spines contacting mitral cell dendrites.

Our observations that mGluR activation is required for recurrent inhibition is particularly surprising, since experiments in both MOB and AOB have demonstrated that reciprocal inhibition of mitral cells is eliminated by blockade of AMPA and NMDA receptors (NMDARs). Our interpretation of this finding is that activation of mGluR1, by glutamate released from mitral/tufted cells, is necessary to create conditions favorable for dendrodendritic inhibition via the "classical" reciprocal ionotropic pathway – a result supported by the low magnesium experiments of figure 17. This may result from direct, mGluR dependent depolarization of granule cells, similar to what we observed in figure 17. With typical magnesium concentrations (our bath solution contained 1 mM Mg^{2+}), NMDA receptors in granule cells will be blocked by Mg^{2+}, especially at the hyperpolarized resting potentials (~-80 mV) typical of these cells. The depolarization of granule cells by mGluR activation may thus be required to relieve this Mg^{2+} block, which is in turn required to elicit GABA release from granule cells.

It is interesting that the direct effects of DHPG (depolarization of granule cells, inconsistent changes in mitral cell holding current) occur on the timescale of minutes, while the synaptic effects of DHPG (increase in mitral cell IPSC rate) occur with considerable delay but rapid onset (~20 seconds). Although we did not test directly how these two effects are inter-related, we offer two speculations on how the timescales can be reconciled. First, assuming that granule cell voltage gates recurrent inhibition by the NMDAR dependent mechanism described in the *Results* above (Fig. 17), DHPG evoked IPSCs will not begin until relatively depolarized potentials are reached. However, given the negative slope conductance of the NMDAR occurring at ~-65mV, when these potentials are reached, a large fraction of NMDARs may become available very rapidly – resulting in rapid onset of the increase in spontaneous IPSCs.

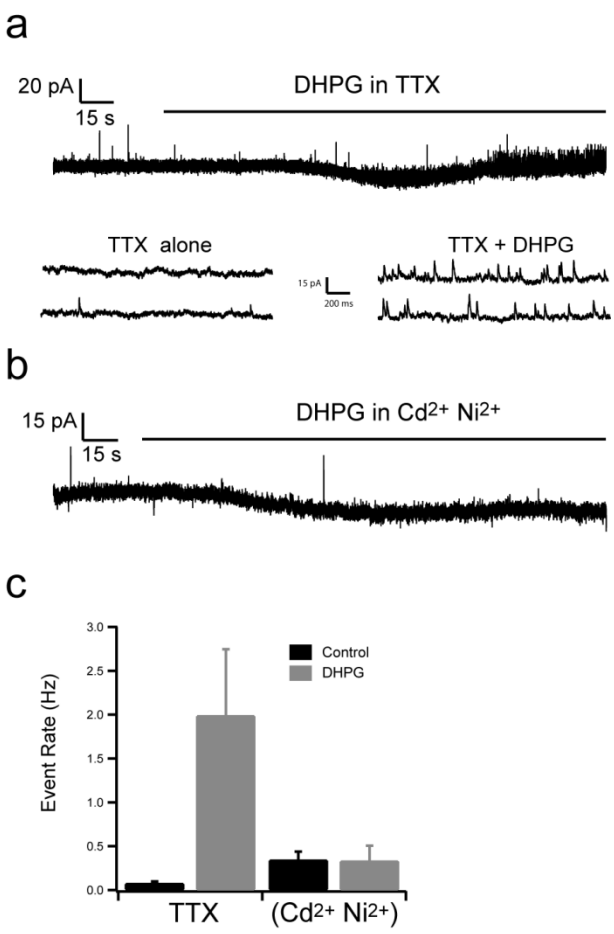

Figure 15. The increase in spontaneous IPSCs is dependent on voltage gated calcium channels, but not sodium channels. (a) Sample sweep in which DHPG was bath applied following addition of TTX. Bottom shows expanded sections from the baseline period and TTX addition period. **(b)** Sample sweep in which DHPG was bath applied following addition of cadmium and nickel. **(c)** Summary data for the effects of voltage gated channel blockers on DHPG-induced IPSCs.

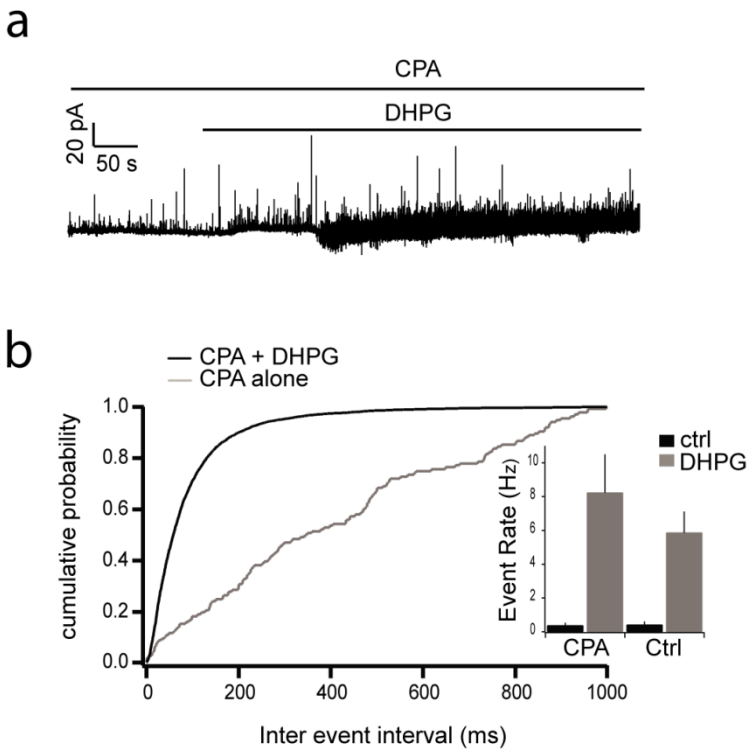

Figure 16. DHPG evoked IPSCs do not depend on internal calcium stores. (a) Application of DHPG in the presence of CPA (100 μM) still induced a large increase in the occurrence of IPSCs in mitral cells. The slice was bathed in CPA for 20 minutes before the application of CPA plus DHPG. (**b)** Cumulative probability plot of inter-event intervals for CPG + DHPG (black line) and control CPA (gray line). Inset shows events rates for both conditions, (CPA only: 0.37 ± 0.17 Hz, CPA + DHPG: 8.23 ± 2.27 Hz, n=5).

mGluR1 immunoreactivity in the AOB is concentrated largely in the mitral-tufted cell layer, with less robust staining observed in the granule cell layer (Sahara et al., 2001). Given that we observed granule cell depolarization in response to DHPG (Fig. 17), and that recurrent inhibition was eliminated by an antagonist of mGluR1 but not mGluR5 (Fig. 14),our results are consistent with expression pattern in which mGluR1 is highly localized to granule cell spines contacting mitral cell dendrites.

Our observations that mGluR activation is required for recurrent inhibition is particularly surprising, since experiments in both MOB and AOB have demonstrated that reciprocal inhibition of mitral cells is eliminated by blockade of AMPA and NMDA receptors (NMDARs). Our interpretation of this finding is that activation of mGluR1, by glutamate released from mitral/tufted cells, is necessary to create conditions favorable for dendrodendritic inhibition via the "classical" reciprocal ionotropic pathway – a result supported by the low magnesium experiments of figure 17. This may result from direct, mGluR dependent depolarization of granule cells, similar to what we observed in figure 17. With typical magnesium concentrations (our bath solution contained 1 mM Mg^{2+}), NMDA receptors in granule cells will be blocked by Mg^{2+}, especially at the hyperpolarized resting potentials (~-80 mV) typical of these cells. The depolarization of granule cells by mGluR activation may thus be required to relieve this Mg^{2+} block, which is in turn required to elicit GABA release from granule cells.

It is interesting that the direct effects of DHPG (depolarization of granule cells, inconsistent changes in mitral cell holding current) occur on the timescale of minutes, while the synaptic effects of DHPG (increase in mitral cell IPSC rate) occur with considerable delay but rapid onset (~20 seconds). Although we did not test directly how these two effects are inter-related, we offer two speculations on how the timescales can be reconciled. First, assuming that granule cell voltage gates recurrent inhibition by the NMDAR dependent mechanism described in the *Results* above (Fig. 17), DHPG evoked IPSCs will not begin until relatively depolarized potentials are reached. However, given the negative slope conductance of the NMDAR occurring at ~-65mV, when these potentials are reached, a large fraction of NMDARs may become available very rapidly – resulting in rapid onset of the increase in spontaneous IPSCs. Another possibility is that the rapid onset of IPSCs may reflect a population-level phenomenon, such as the onset of synchrony among granule cells.

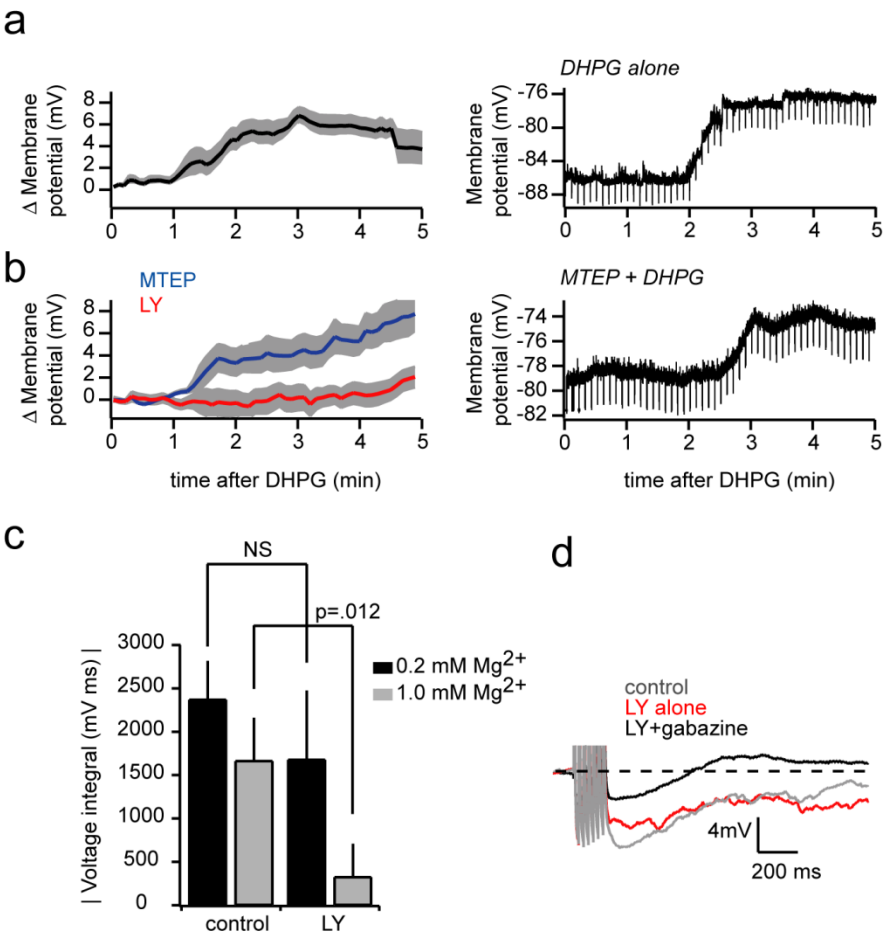
a
Δ Membrane potential (mV)
DHPG alone
Membrane potential (mV)
b
MTEP
LY
MTEP + DHPG
time after DHPG (min)
time after DHPG (min)
c
NS
p=.012
| Voltage integral (mV ms) |
0.2 mM Mg2+
1.0 mM Mg2+
control
LY
d
control
LY alone
LY+gabazine
4mV
200 ms

Figure 17. DHPG depolarizes granule cells. (a) Left: group data showing granule cell depolarization with addition of DHPG (20 μM) starting at t=0 (n=4, mean depolarization = 6.79 ± 0.79; shaded areas correspond to ± SEM). Right: example experiment. Negative-going deflections are hyperpolarizing pulses used to monitor input resistance. **(b)** Same layout and experiment design as in **a**, only with 2 μM MTEP (n=5) or 100 μM LY367385 (n=5) included in the bath to block mGluR5 or mGluR1, respectively. Right: example experiment showing persistence of DHPG - evoked granule cell depolarization when mGluR5 is antagonized. **(c)** Effectiveness of LY367385 in blocking recurrent inhibition at normal (1.0 mM, n=7) and low (0.2mM, n=6) magnesium concentrations. **(d)** Single sample sweeps showing recurrent inhibition following 7 evoked spikes at 40 Hz in 0.2 Mg2+. Gray, control; Red, following LY alone; Black, LY+gabazine.

We also observed that direct application of DHPG evoked IPSCs in mitral cells even when excitatory synaptic transmission was blocked (Figs. 13a & c). This observation indicates that activation of mGluR1 by synaptically-released glutamate may result directly in GABA release without requiring activation of AMPA and NMDA receptors. However, bath application of an mGluR agonist is likely to cause stronger mGluR1 activity than glutamate supplied by physiological release from mitral cells. Nevertheless, the results from these agonist experiments are important for understanding the cellular consequences of activating mGluR1. In particular, the results of the experiments shown in figures 15 and 16 indicate that activation of group I mGluRs evokes release in a manner that is dependent on voltage gated calcium channels, but does not require sodium spikes and internal calcium stores. These observations suggest that mGluRs are likely to elicit the kind of large depolarization required to open voltage gated calcium channels coupled to release. However, since we observe only ~7 mV depolarization in granule cell somatic recordings, it is possible that granule cell dendrites are substantially more depolarized by mGluR activation than are granule cell somata. Alternatively, mGluRs may facilitate activation of calcium channels by voltage independent mechanisms. Several studies have shown that granule cells exhibit low threshold calcium spikes that can be localized to granule cell spines, or can propagate along the granule cell apical dendrite (Egger et al., 2003;Egger et al., 2005). In summary, we propose that mGluR1 activation in granule cells may act in two capacities: first, it may play a facilitating role in recurrent inhibition by partially relieving magnesium block of NMDA receptors, and second, under conditions of high network activity, it may be capable of evoking release in a manner that is independent of activation of ionotropic glutamate receptors.

3.5.2 Significance for AOB function

A number of studies have examined the extent to which metabotropic glutamate receptors control information throughput in sensory systems – a function sometimes referred to as “gating”. In the thalamus, for example, mGluRs are coupled to presynaptic release from GABA-containing interneurons, and strongly modulate feedforward information flow to higher cortical areas (Cox and Sherman, 2000;Govindaiah and Cox, 2004). Similarly, in the main

olfactory system, a presynaptic group II mGluR has been shown to be critical for habituation of the odor-induced heart-rate orienting response (Best et al., 2005). The AOB provides perhaps the most tractable example of a feedforward system in which information flow is controlled by mGluRs. Classically, work has addressed how activation of mGluR2 in granule cell spines results in diminished recurrent inhibition of mitral cells. This reduction in inhibition is believed to be a neural substrate of the Bruce effect – the failure of embryo implantation following exposure of a female rodent to pheromones of non-stud males (Brennan and Keverne, 1997;Hayashi et al., 1993;Kaba et al., 1994). Regardless of the precise mechanisms underlying this behavior, the Bruce effect highlights the importance of controlling the propagation of activity in the AOB, since presumably small subsets of active mitral cells can communicate signals that result in terminated pregnancy. The requirement for mGluR1 in recurrent inhibition observed in the present study suggests that this receptor plays a powerful role in controlling how pheromone detection is coupled to behavioral and endocrine responses.

4.0 MGLUR ACTIVATION PROMOTES GRADED SUBTHRESHOLD RELEASE FROM MITRAL CELL DENDRITES

4.1 ABSTRACT

The previous chapter described the obligatory role played by mGluR1 in mitral cell recurrent inhibition. Although a component of mitral cell inhibition was elicited by the direct actions of mGluR1 on interneuron output, this effect was generally much smaller than that observed when ionotropic glutamatergic transmission was left in-tact. This prompted us to investigate whether mitral cell dendritic *output* is also affected by mGluRs. In the experiments of this chapter, we observed that activation of group I mGluRs greatly enhanced a previously undescribed capacity for graded, continuous, subthreshold release from mitral cell dendrites. This suggests that not only does transmitter output occur in mitral cell dendrites for 'subthreshold' activation (as described in **Chapter 2**), but that the qualitative nature of this output (phasic vs. graded) can be modulated. The ability to switch from phasic to graded release modes may allow for sustained recurrent inhibition during pheromone integration. This may in turn enhance the selectivity of mitral cells by requiring them to integrate VN inputs for long epochs before spike threshold is reached.

4.2 INTRODUCTION

The study of dendritic excitability has led to fundamental changes in our understanding of synaptic integration and plasticity. Excitable dendrites exhibit a wide range of activity types that vary in their spatiotemporal extent and their biophysical mechanisms (Hausser and Mel, 2003), and may thus function as highly versatile or specialized input processing devices. Dendritic responses to synaptic input range from highly focal calcium influxes sequestered at single spines (Sabatini and Svoboda, 2000), to regenerative, branch-specific spikes (Zelles et al., 2006), to full blown action potentials that are initiated in or propagate to distal dendrites (Stuart and Sakmann, 1994;Chen et al., 1997). This diversity of dendritic activity is especially interesting for neurons whose dendrites also function as presynaptic structures that release transmitters. For such cells, each class of dendritic responses is also a distinct candidate output signal. In principle, transmitter release from dendrites could be mediated by both sub- and suprathreshold activity to allow for multiple forms of output from a single cell.

The efficacy of a particular type of dendritic electrical event as an output trigger will depend critically on dendritic "readout" properties – that is, the mechanisms available for coupling membrane voltage to transmitter release. If a dendritic tree richly expresses HVA but not LVA calcium channels, for example, backpropagating spikes will likely be required to trigger dendritic transmitter release. Conversely, if a dendritic tree has calcium conductances activated at low voltages, and for sustained periods, release could conceivably occur for subthreshold and sustained activity.

Here, we describe work in which we studied the readout of dendritic activity in AOB mitral cells. The AOB is an excellent model system for studying excitation-secretion coupling in dendrites since the majority of its cell to cell coupling is via dendrodendritic synapses, and specific alterations of dendritic output in this structure have known behavioral consequences (Kaba et al., 1994). We were particularly interested in exploring the possibility of graded subthreshold release from mitral cells given our earlier work on independent integration of synaptic inputs across mitral cell tufts (**Chapter 2**). These earlier studies pointed to a model of pheromone/odor processing in which each tuft communicates with local interneuron populations via "tuft spikes" – local regenerative events that occur in the absence of somatic spiking.

Sustained subthreshold release from these same tufts could allow glomerular processing to persist even when VRN input is weak, thus extending the dynamic range of AOB processing.

In the work described below, we demonstrate that both sub- and suprathreshold activity in mitral cell dendrites are coupled to glutamate release. Specifically, we observed responses in postsynaptic interneurons during subthreshold depolarizations in mitral cells, as well as backpropagating spikes. Moreover, dendritic output was graded and persistent; larger depolarizations evoked higher rates of release, which could be sustained for seconds. The rate of graded release was typically low under control conditions, but was enhanced several fold following either exogenous or endogenous activation of group I mGluRs. This suggests that not only are there multiple modes of dendritic readout in mitral cells, but that these neurons can readily switch their dominant mode of output from digital (action-potential coupled) to analog (graded).

4.3 MATERIALS AND METHODS

4.3.1 Slice Preparation

Basic procedures for slice preparation were identical to those described in section **2.3.1**. For experiments in which population calcium responses were imaged (**section 4.4.1**) slices were incubated in a well-plate chamber for 90 minutes at 37°C in a solution containing 500 µL of the Ringer's solution described in (**2.3.1**), with 3 µL of 0.01% Pluronic (Molecular Probes), and a 5 µL of a 1mM solution of Fura-2 acetoxymethyl (AM) ester (Molecular Probes) in 100% DMSO solution. Humidified air (95%O_2/5% CO_2) was passed above the surface of the liquid in the chamber to keep the solution oxygenated. All animal care was performed in accordance with the guidelines of the Institutional Animal Care and Use Committee of Carnegie Mellon University.

4.3.2 Electrophysiology and Imaging

Basic electrophysiological and imaging procedures were identical to those described in section **2.3.** In the indicated experiments, 5mM BAPTA was included in the internal solution described earlier **2.3.2**. For experiments in which we evoked a fixed number of mitral cell spikes followed recordings of subthreshold, voltage dependent currents, we made use of the multiclamp 700B's mode switching function. MK801, APV, CNQX, and bicuculline were obtained from Sigma-Aldrich (St. Louis, MO) and used at final concentrations of 100, 50, 20, and 10 µM, respectively. Gabazine, DHPG, and LY367385 were obtained from Tocris (Ellisville, MO), and used at final concentrations of 10, 20, and 100 µM, respectively. 3-((2-Methyl-1,3-thiazol-4-yl)ethynyl) pyridine (MTEP) (Calbiochem, La Jolla, CA) was used at 2 µM and prepared in a stock of 100 mM in 100% DMSO. DHPG stocks were prepared in dH_2O at 100 mM.

For comparing spatiotemporal maps of dendritic calcium influx across different cells (as in Figure 22b), the following procedure was used. First, spatiotemporal $\Delta F/F$ profiles along single lines of interest (LOIs) were calculated using IGOR pro. These maps were resampled to be 100 points in length (along the spatial dimension), and the 13 distal-most points of the map were reserved for the tuft. In previous analysese, we had observed that tufts occupy ~13% of principal dendrite length. For all such obtained maps, the timing of stimulation was identical, so that maps were properly normalized in both space and time and could be averaged (as in Fig. 22b)

4.3.3 Data analysis and statistical tests

All data are reported as mean ± SEM. Significance was assessed by paired or unpaired Student's *t*-tests, and nonparametrical statistical tests for smaller sample sizes, as appropriate. IPSCs were detected using custom-written functions in IGOR pro (Wavemetrics, Lake Oswego, OR), which implemented the algorithm described by (Kudoh and Taguchi, 2002a). In certain indicated experiments in which we compared pre- and post- drug levels of spontaneous synaptic activity, data were analyzed in the frequency domain. Our reasons for this were twofold. First, in experiments in which inhibition was blocked and subthreshold, spike-independent recurrent excitation was studied, it was difficult to resolve discrete inward currents that could be detected automatically. This is likely due to the fact that glutamate release was tonic and asynchronous,

resulting in noisy fluctuations in current records. Glutamate is also likely to activate predominantly NMDARs, generating relatively slow synaptic currents which are difficult to detect by standard methods. Such phenomena have also been described for other CNS synapses (see for example (Neher and Sakaba, 2001)). Second, we wanted to be certain that counts of synaptic events at various holding potentials were independent of driving force. By calculating power spectra of current records, we were able to more confidently report ratios of pre- and post-drug conditions.

For experiments in which spontaneous and spike-evoked rates of IPSCs were compared, IPSCs were detected using the above-described mini-detection algorithm. IPSC rasters were then constructed in which the peak event times were counted as single events. These rasters (10-20 trials per cell) were pooled across cells in two groups for spontaneous and evoked activity, and plots of instantaneous IPSC rate (10 ms bins) vs. time were calculated. Grand-average plots of IPSC rate vs. time were fit using Bayesian Adaptive Regression Splines (BARS), which performs spline based generalized nonparametric regression(Behseta and Kass, 2005;Behseta et al., 2007). A likelihood ratio (LR) test was used to compare the two fitted curves pointwise, and significance was assessed for the time dependent quantity – log (LR), which has a χ^2 distribution with 1 degree of freedom for details.

4.3.4 Simulations

A simulation was performed in IGOR pro (Wavemetrics, Lake Oswego, OR) to confirm that changes in IPSC rate could be reliably detected as changes in the power spectra of current records. Briefly, a poisson process was simulated to construct binary vectors of IPSC times. These vectors were convolved with an alpha function (τ=45 ms) to simulate IPSCs. IPSC amplitudes were chosen from a Gaussian distribution with $\bar{X}$= 1 and σ=0.2. A 200 s simulated IPSC record (10 kH sampling) with λ = 20 Hz was chosen as a baseline case, and IPSC records with λ = 2 Hz λ = 5 Hz λ = 10 Hz were compared to the 20 Hz record. Power spectra were taken across all records and normalized to the 20 Hz spectrum to observe the approximate frequency band over which differences in IPSC rate were seen.

4.4 RESULTS

4.4.1 Sub and suprathreshold depolarization of mitral cells activates postsynaptic interneurons

The principal dendrites of mitral cells are "axon-like" in that they can initiate and conduct action potentials in a non-decremental fashion (Bischofberger and Jonas, 1997;Chen et al., 1997). This suggests that these dendrites may make use of classical, axon-like readout mechanisms. Thus, we first examined glutamate release from AOB mitral cells evoked by backpropagating action potentials. Action potentials (APs) were elicited by whole cell current injection (10 pulses x 3ms at 40 Hz), while calcium transients were monitored in periglomerular and granule cells in slices loaded with the membrane permeable calcium indicator Fura2-AM. Only PG cells in the vicinity of the tuft of the stimulated mitral cell were activated (Fig. 18; 4 ± 0.54 PG cells/tuft, avg $\Delta F/F$ of 4.0 ± 0.5%, n = 5 mitral cells from 5 animals). Similar activation of local PG cells has been observed in the main olfactory bulb following mitral/tufted cell spiking (Murphy et al., 2005). AP evoked calcium transients in PG cells were blocked by addition of APV and CNQX, indicating that PG cell activity was caused by spike-evoked glutamate release from mitral cells (Fig. 18).

Surprisingly, PG cell calcium transients also could be elicited by subthreshold voltage or current steps in mitral cells (Fig. 18b), suggesting that mitral cells release glutamate during subthreshold depolarization, and that this release is sufficient to activate some local interneurons (median of 2.5 PG cells activated/tuft, avg $\Delta F/F$ of 0.8% ± 0.2%, n=4 mitral cells from 3 animals). Subthreshold depolarization of AOB mitral cells in whole cell current clamp recordings also resulted in an increase in IPSP-like membrane potential fluctuations (Fig. 19a). These fluctuations were blocked by 10 µM gabazine (Fig. 19a, n=3) indicating that they were due to activation of recurrent inhibition by subthreshold release of glutamate from the recorded mitral cell. To more fully study these events, mitral cells were voltage clamped at -55 mV and stepped to command potentials between -45 and -25 mV for 1.5 seconds (Figs. 19b & c). Spontaneous synaptic events were rarely observed at -55 mV, but elevated IPSC rates were seen at more depolarized command potentials (7.31 ± 3.18 Hz (n=6) for steps to -25 mV, which was 6.6 fold higher than the rate observed at -55 mV ($p<.03$, Wilcoxon rank sum test) (Fig. 19c).

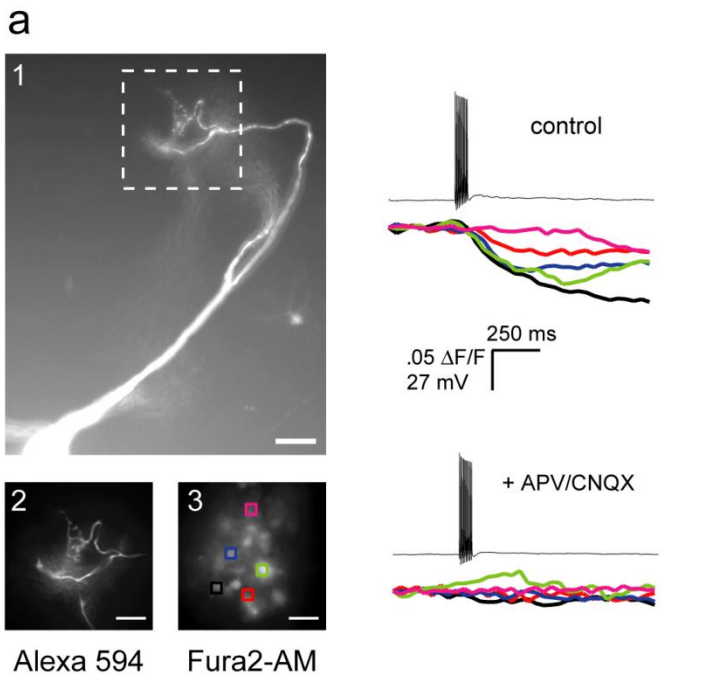
a
1
2
3
Alexa 594
Fura2-AM
control
250 ms
.05 ΔF/F
27 mV
+ APV/CNQX
b
Δ voltage
1% ΔF/F
500 ms
-15 mV
-55 mV

Figure 18. Activation of postsynaptic interneurons by sub and suprathreshold depolarization of mitral cells. (a) 1) 20 X image of an Alexa 594 filled mitral cell. Scale bar, 50 μm. Images beneath the main panel are 3X magnifications of the area demarcated by the white dashed box (60X total). **2)** Close up of the mitral cell tuft shown in a1. **3)** PG cells bulk-loaded with Fura2-AM. Colored squares are regions of interest (ROI) used to calculate the calcium transients shown on the right. Scale bars (**a2** & **a3**), 30 μm. ***Top right:*** PG cell calcium transients evoked by a sequence of 10 backpropagating spikes at 100 Hz. Trace colors correspond to ROI colors in a3. ***Bottom right***: Spike-evoked calcium transients from the same PG cells after addition of APV (50 μM) and CNQX (20 μM). **(b)** ***Left:*** Mitral cell filled with Alexa 594 in a slice incubated in Fura2-AM, as in **a**. Colored squares are ROIs corresponding to PG cells activated during subthreshold voltage or current steps; Fura image is not shown. ***Right:*** PG cell calcium transients evoked by a subthreshold voltage step from -55mV to -15 mV. Trace colors correspond to ROI colors in the left panel.

IPSCs were observed for the duration of the depolarizing step, and terminated rapidly upon repolarization to -55 mV (Fig. 19b). Although the voltage steps we used to elicit transmitter release appear rather depolarized in comparison to other cell types (i.e. Pyramidal cells), they are in fact within the range of potentials that mitral cells visit during subthreshold input. In some cases, we have elicited EPSPs of >25 mV from resting potentials of ~-50 mV. For all experiments in which we investigated subthreshold release, we were sure to reject sweeps in which obvious action currents were present.

One possible confound in interpreting these results is that depolarization is accompanied by increased inhibitory driving force, which would make spontaneous events more discernable at elevated potentials. Alternatively, mitral cells could be influencing postsynaptic targets directly via gap junction coupling. We thus performed another set of experiments in which we blocked inhibition with 10 µM gabazine, and monitored mitral cell self-excitation self-excitation in Ringer's with 0 Mg^{2+}. These conditions allow for a conservative measure of increased glutamate release with depolarization, since depolarization will tend to decrease driving force on glutamatergic currents. In these experiments, self-excitation was markedly diminished by APV or MK801 (Fig.20).

4.4.2 Subthreshold release of transmitter from mitral cells is enhanced by mGluR activation

Together with the previous results (Fig. 18), these data show that mitral cells support readout of both backpropagating action potentials (digital signals) and subthreshold (analog or graded) signals. Transmitter release by both subthreshold and suprathreshold activity has been described in leech peripheral interneurons (Ivanov and Calabrese, 2006b;Ivanov and Calabrese, 2006c) and the stomatogastric ganglion of lobsters (Graubard et al., 1980). Early work by Rall and Shepherd raised the possibility that graded release could occur from mitral cell lateral dendrites, but this is, to our knowledge, the first demonstration of a CNS neuron capable of such a combination of analog and digital signaling.

Observing these two modes of dendritic release raises the question of whether the relative strength of these modes can be modulated, for example by changes in the input to these cells or by neuromodulators; such switching of release mode has some precedent in invertebrate neurons

(Ayali et al., 1998). We were especially interested in knowing whether subthreshold release could be enhanced. Previously, we had observed that activation of mGluR1 causes depolarization and GABA release from AOB granule cells (**Chapter 3**, (Castro et al., 2007). This observation, along with the high level of mGluR expression in the main and accessory olfactory bulbs (Martin et al., 1992;Sahara et al., 2001;Shigemoto et al., 1992), prompted us to investigate how transmitter release is influenced by activation of mGluRs. Addition of the group I mGLuR agonist DHPG (20 μM) caused a large and significant increase in the rate of IPSCs or IPSPs observed in mitral cells (Fig. 19). This enhancement of IPSC frequency was dependent on mitral cell voltage and partially blocked when 5 mM BAPTA was included in the recording internal

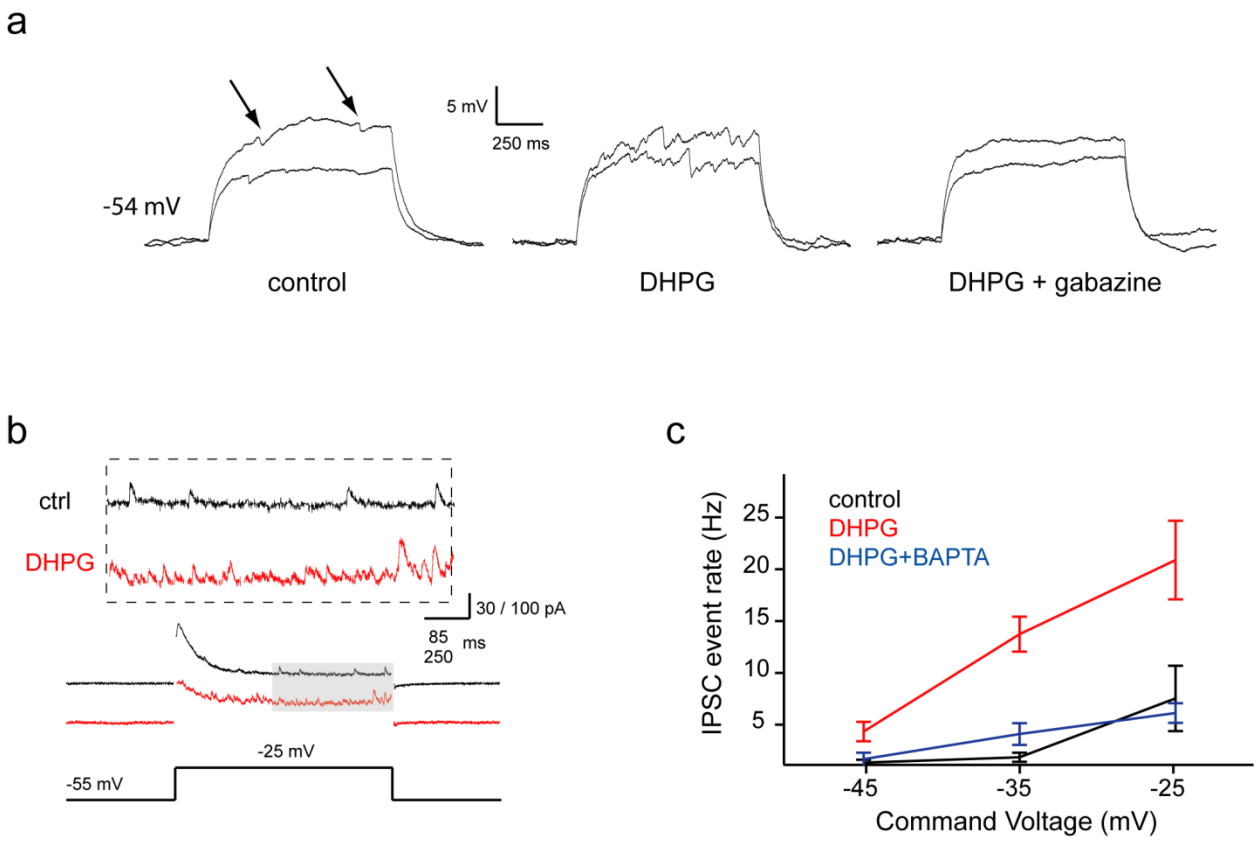
a
5 mV
250 ms
-54 mV
control
DHPG
DHPG + gabazine
b
ctrl
DHPG
30 / 100 pA
85
250
ms
-25 mV
-55 mV
c
IPSC event rate (Hz)
control
DHPG
DHPG+BAPTA
25
20
15
10
5
-45
-35
-25
Command Voltage (mV)

Figure 19. Recurrent inhibition in mitral cells is elicited by subthreshold depolarizations. **(a)** ***Left:*** Mitral cell voltage traces in response to two depolarizing current steps (220 and 290 pA). Arrows indicate presumed IPSPs. ***Middle:*** Responses from same cell after addition of 20 µM DHPG to the bath. ***Right:*** Responses from same cell after addition of 10 µM gabazine. This cell was maintained at ~-54 mV for all shown conditions by steady current injection. **(b)** Sample traces showing recurrent IPSCs evoked by a 30 mV voltage step (subthreshold for spiking) under control conditions (black) and following bath application of 20 µM DHPG (red). **(c)** Summary data for experiments similar to **b** showing IPSC event rate as a function of command voltage (control, DHPG: n=10; BAPTA internal (5 mM): n=6).

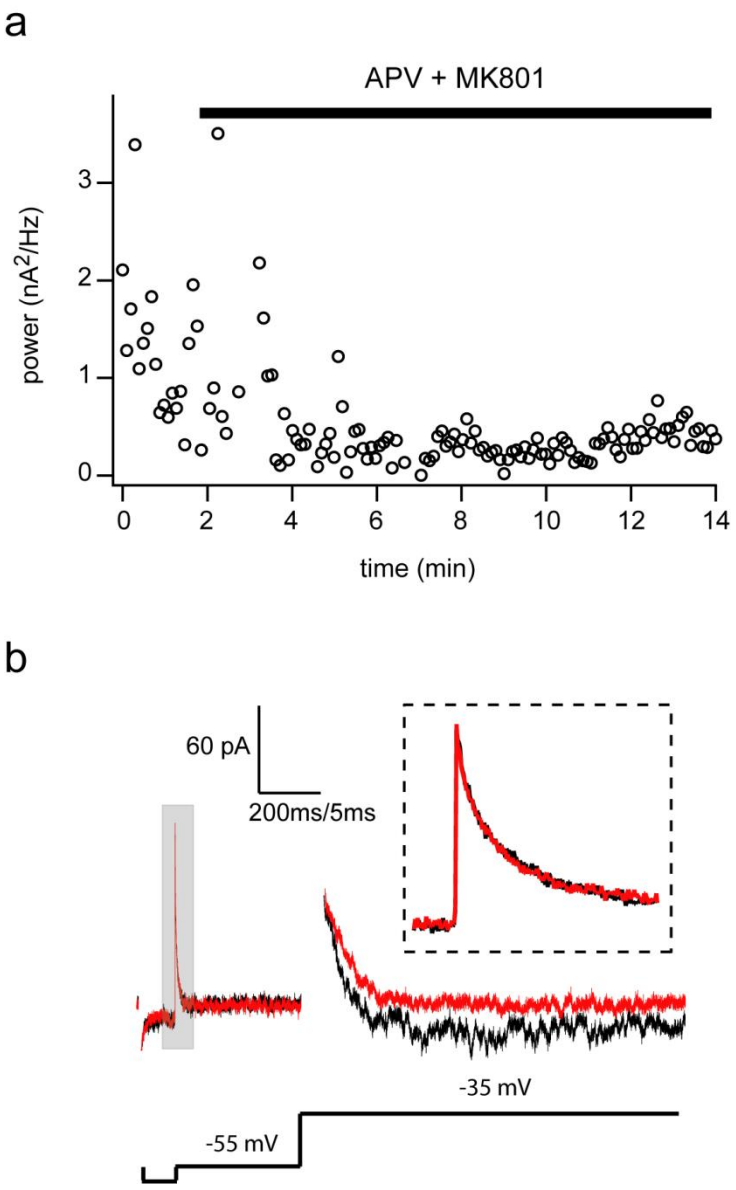
a
APV + MK801
power (nA²/Hz)
0
1
2
3
0
2
4
6
8
10
12
14
time (min)
b
60 pA
200ms/5ms
-35 mV
-55 mV

Figure 20. Measurement of subthreshold glutamate release from mitral cells by self-excitatory currents. (a) Example experiment in which a mitral cell was stepped from a command potential of -55 mV to -35 mV, and power monitored during the period of depolarization (1.5s). APV (50 μM) and MK801 (100 μM) were added following 2 minutes of baseline recording. **(b)** Sample sweeps from the experiment shown above. Black trace, control; Red trace, after APV + MK801. Inset shows magnification of capacitive currents shown in the gray box, indicating no significant change in series resistance. Inward capacitive current is trimmed for clarity, and the sweep is truncated to emphasize inward currents during the period of depolarization.

solution (Fig. 19c). IPSC rates recorded at hyperpolarized potentials were only weakly affected by DHPG, but were enhanced dramatically at depolarized potentials (Fig. 19), with a 30 mV depolarization from -55 mV resulting in an IPSC rate of 20.69 ± 3.80 Hz.

The above data are consistent with the hypothesis that subthreshold glutamate release is enhanced by group I mGluRs. However, they do not exclude the possibility that the mGluR-mediated changes in the voltage dependence of IPSC frequency are due to effects of mGluRs on presynaptic interneurons. Specifically, subthreshold glutamate release from mitral cells could be unaltered, but enhanced PG or granule cell excitability would lead these cells to respond to glutamate more than in control conditions. To test this possibility, we again made use of the fact that mitral cells detect the glutamate released from their own dendrites, which mediates a form of self-excitation (Nicoll and Jahr, 1982;Isaacson, 1999;Margrie et al., 2001;Urban and Sakmann, 2002). We examined self excitation evoked by subthreshold depolarizations of mitral cells following blockade of inhibition by 10 μM gabazine (in 0 Mg^{2+} Ringers). This allowed us to assess glutamate release directly from the recorded mitral cell since the excitatory synaptic currents caused by depolarization result exclusively from glutamate released by the stimulated mitral cell. In mitral cells clamped at -55 mV and stepped to depolarized potentials, DHPG caused enhanced rates of EPSCs and glutamate receptor dependent fluctuations in synaptic current at depolarized potentials (Figs. 20 & 21). Thus, activation of group I mGluRs enhances subthreshold release of glutamate by AOB mitral cells.

4.4.3 Dendritic calcium influxes evoked by sub and suprathreshold activity

We next asked what cellular mechanisms might underlie subthreshold glutamate release in mitral cells and its enhancement by mGluR activation. Given the steep exponential relationship between calcium influx and transmitter release described at most synapses (Dodge, Jr. and Rahamimoff, 1967;Bollmann et al., 2000;Schneggenburger and Neher, 2000), the most likely candidate mechanisms involve changes in voltage-dependent calcium influx. We therefore compared dendritic calcium transients due to single backpropagating spikes and subthreshold current injection. Both of these manipulations evoked relatively uniform calcium elevations along mitral cell primary dendrites (Fig. 22a). Interestingly, subthreshold transients were visible even in the most distal tufts in response to current injection or command depolarizations (Fig. 22

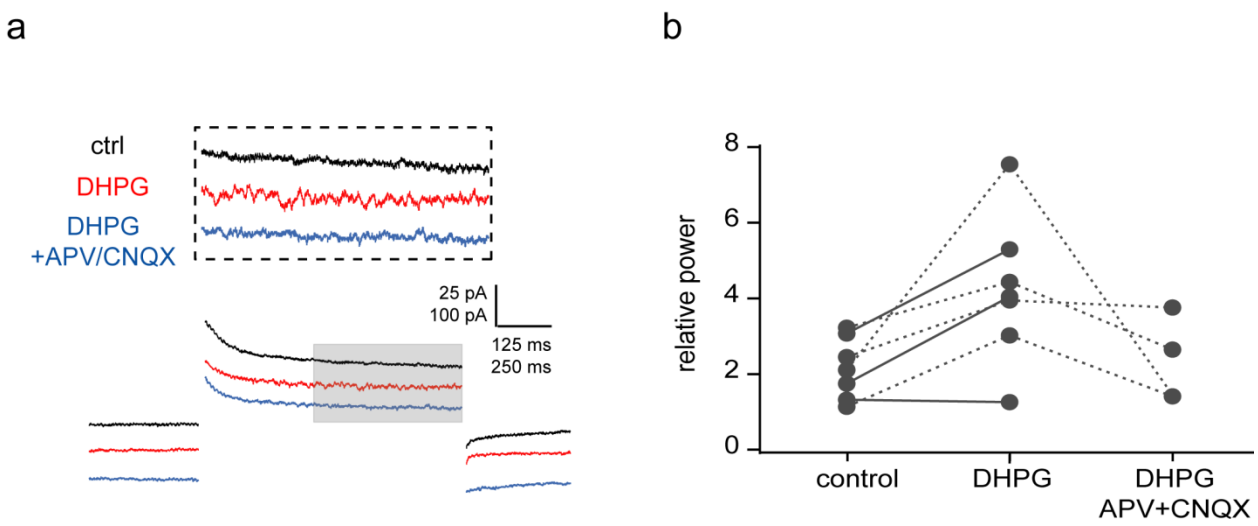

Figure 21. Activation of group I mGluRs enhances subthreshold glutamate release from mitral cells. (a) Sample traces showing mitral cell recurrent self-excitation evoked by voltage steps from -55 mV to -25 mV in control (black), DHPG (red), and DHPG +APV/CNQX (blue) conditions. All recordings (including control) were made in 10 µM gabazine and 0.2 mM Mg^{2+} to enhance detectability of self-excitation, a component of which will be NMDAR mediated. **(b)** Group data showing relative power in the 0-110 Hz band (power during Vc_{md}/power during V_{hold}) during voltage steps from -55mV to -25 mV for the same three conditions in (**a**).

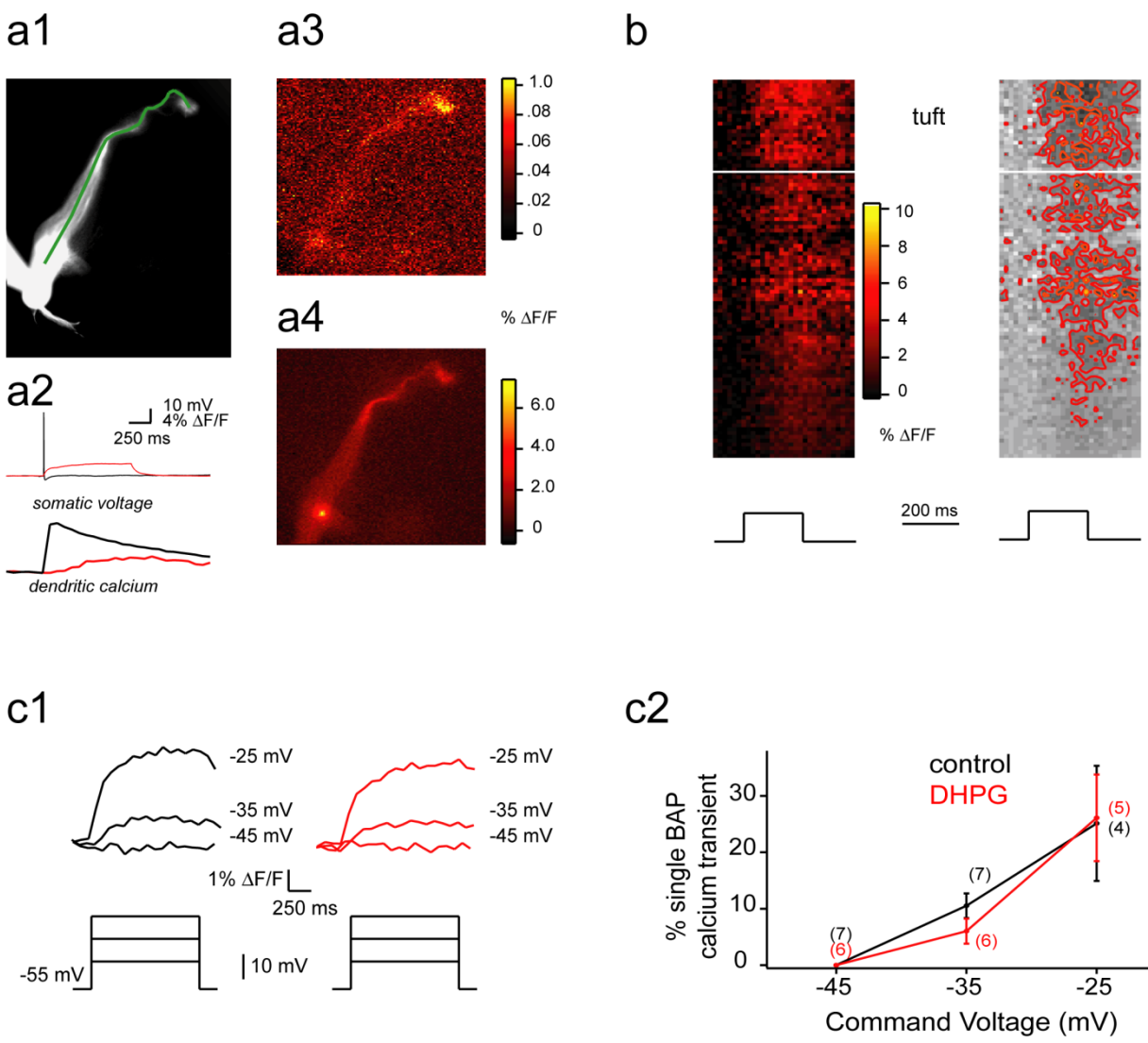
a1
a2
10 mV
4% ΔF/F
250 ms
somatic voltage
dendritic calcium
a3
1.0
.08
.06
.04
.02
0
a4
% ΔF/F
6.0
4.0
2.0
0
b
tuft
10
8
6
4
2
0
% ΔF/F
200 ms
c1
-25 mV
-35 mV
-45 mV
-25 mV
-35 mV
-45 mV
1% ΔF/F
250 ms
-55 mV
10 mV
c2
control
DHPG
% single BAP calcium transient
30
20
10
0
(7)
(6)
(7)
(6)
(5)
(4)
-45
-35
-25
Command Voltage (mV)

Figure 22. Sub- and supratheshold calcium dynamics in mitral cell principal dendrites following depolarizing stimuli. (**a),** *1* – fluorescence image of a mitral cell (tuft is toward the top right) with line of interest (LOI) shown along the principal dendrite. *2* – somatic voltage and dendritic calcium (calculated along indicated LOI) in response to a single backpropagating spike (black) and a 1s subthreshold current step (red). *3* – peak fluorescence (% ΔF/F) observed in the principal dendrite following the subthreshold current step shown in **a2** (red). Note that calcium influx is observed even in the distal dendrite and tuft. 4 – peak fluorescence (% ΔF/F) in response to the single backpropagating spike shown in **a2** (black). (**b),** spatiotemporal map of mean % ΔF/F in 5 principal dendrites from 5 cells following subthreshold current steps. LOIs used for analysis were scaled to 100D vectors; 13 dimensions of these "normalized" LOIs were reserved for the tuft (see *methods*). (**c)** *1*- sample sweeps showing dendritic calcium influx for a representative experiment from **c1**. *2*- dendritic calcium transients in response to subthreshold voltage steps from -55mV to the indicated command potentials for control (black) and DHPG (red) conditions.

a3 & b). This capacity for long-distance subthreshold calcium signaling along the dendrite is likely to support subthreshold release from these cells, especially given the calcium dependence of this release (Fig. 19c). These subthreshold transients were uniformly smaller than single-AP associated transients (Fig. 22a) and showed delayed onsets and slow kinetics. Dendritic calcium transients evoked by subthreshold somatic current or voltage steps were unchanged by DHPG (Fig. 22c). For depolarizations to -25 mV, for example, control transients were 25.1 ± 10.2% the amplitude of single BAP-evoked transients, while transients following DHPG addition were 26.1 ± 7.7% the amplitude of BAP-evoked transients ($p=0.33$, Wilcoxon rank sum test, $n=4$); calcium influx in response to single BAPs was not altered appreciably by DHPG. This suggests that activation of group I mGluRs enhances the coupling between calcium influx and transmitter release but does not directly alter properties of dendritic calcium channels.

4.4.4 Endogenous activation of mGluRs is sufficient to enhance subthreshold dendritic transmitter release

A crucial question is whether mGluR-dependent enhancement of subthreshold release occurs under physiological circumstances, or only during pharmacological application of mGluR agonists. Thus, we asked whether the endogenous glutamate released by a single mitral cell is sufficient to enhance subthreshold release in this same cell. To test this, we evoked action potentials (7 x 3ms x 40Hz) in mitral cells in current clamp and rapidly switched to voltage clamp at potentials of either -45 or -35 mV in interleaved trials (Fig. 23, see also *Methods*). This allowed us to control the number of mitral cell APs, and thus the amount of glutamate release and mGluR activation, and then examine the voltage dependent, subthreshold component of recurrent inhibition. Since the number of spikes was identical across trials, the rate of action potential evoked recurrent IPSCs should be identical for the two command potentials. Thus, differences observed in IPSC rate observed at the two potentials will be a function of voltage command potential following the spikes (see Fig. 25). To ensure that the IPSCs studied were not spike-evoked, we only examined IPSC rates starting 500 ms after the final spike. This allowed us to eliminate any contribution of spike evoked inhibition to the rate of IPSCs (Fig. 24). Under control conditions, IPSC rate was approximately 3 fold greater at -35 mV than at -45 mV (Fig. 23), similar to the fold difference we observe between these two potentials following addition of

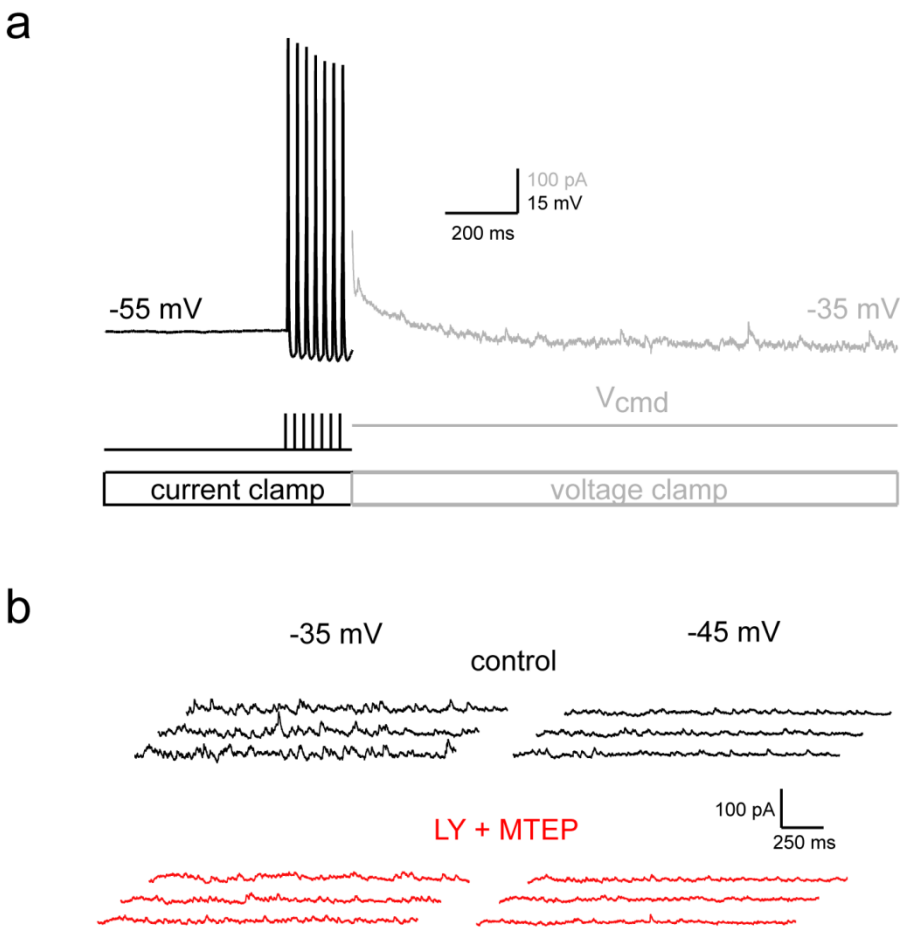
a
100 pA
15 mV
200 ms
-55 mV
-35 mV
Vcmd
current clamp
voltage clamp
b
-35 mV
-45 mV
control
100 pA
250 ms
LY + MTEP
c
*
power (nA2/ Hz)
3.5
3.0
2.5
2.0
1.5
1.0
0.5
0.0
control
LY+MTEP
-35 mV
-45 mV

Figure 23. Endogenous glutamate is sufficient to enhance mGluR-dependent subthreshold release. (a) Stimulation protocol. Mitral cells were maintained at -55mV in current clamp and stimulated with brief current pulses (7 x 3ms at 40 Hz) to evoke the same number of spikes across trials and conditions. Immediately following the last spike, the amplifier was rapidly switched from current clamp to voltage clamp mode to more easily resolve IPSCS and test the subthreshold voltage dependence of IPSC rate. IPSCs observed later than 500 ms after the last spike are due exclusively to subthreshold release (see Fig. 24) **(b)** Example of strong subthreshold voltage dependence of IPSC rate. Traces shown correspond to the gray region of **a** (detrended for clarity). More IPSCs are observed when the mitral cell is clamped to -35 mV (top left, black), than when it is clamped to -45 mV (top right, black). This subthreshold voltage dependence is eliminated by blockade of group I mGluRs by the antagonists LY367385 and MTEP (bottom, red). **(c)** Summary data for experiments described above (n=13). Power in the 0-300 Hz band (for detrended, mean-subtraced current traces) for conditions in which cells were voltage clamped to either -35 mV or -45 mV. LY + MTEP selectively reduces power for the more depolarized condition. (* $p < 0.05$, paired t-test)

DHPG (Fig. 19). Addition of the mGluR1 and mGluR5 antagonists LY367385 (100 mM) and MTEP (2 mM) eliminated the difference in IPSC rates observed at -35 vs. -45 mV, demonstrating that mGluR activation by self excitation is sufficient to enhance graded subthreshold release.

4.5 DISCUSSION

4.5.1 Summary of findings

We have shown that AOB mitral cells release glutamate from their dendrites in response to both sub and suprathreshold depolarization. The rate of subthreshold release is low under control circumstances, but can be enhanced several-fold by activation of group I metabotropic glutamate receptors, which are expressed highly in the olfactory bulb, thalamus, hippocampus, and cortex (Martin et al., 1992;Sahara et al., 2001). These observations have important implications for both the analysis of mechanisms of neuronal signaling, and also for our understanding of functional circuitry within the olfactory system.

Recently, there has been considerable interest in how subthreshold activity contributes to neuronal output. Studies by Shu et al (2006), and Alle and Geiger (2006)in neocortex and hippocampus have demonstrated that action-potential mediated transmitter release can be modulated by subthreshold changes in presynaptic voltage occuring before a spike is initiated. Similar phenomena have also been described in invertebrate neurons (Shapiro et al., 1980a;Shapiro et al., 1980b), as well as in the auditory brainstem (Awatramani et al., 2005). This basic effect, in which action potentials control the timing of pulsatile transmitter release, but the effective pulse size is regulated by subthreshold voltage, has been described as “hybrid” analog-digital signaling (Clark and Hausser, 2006). In contrast, the work described herein describes an example of true dual-mode release, in which a single neuron can generate analog output in the absence of spiking and still generate output in response to action potential stimulation.

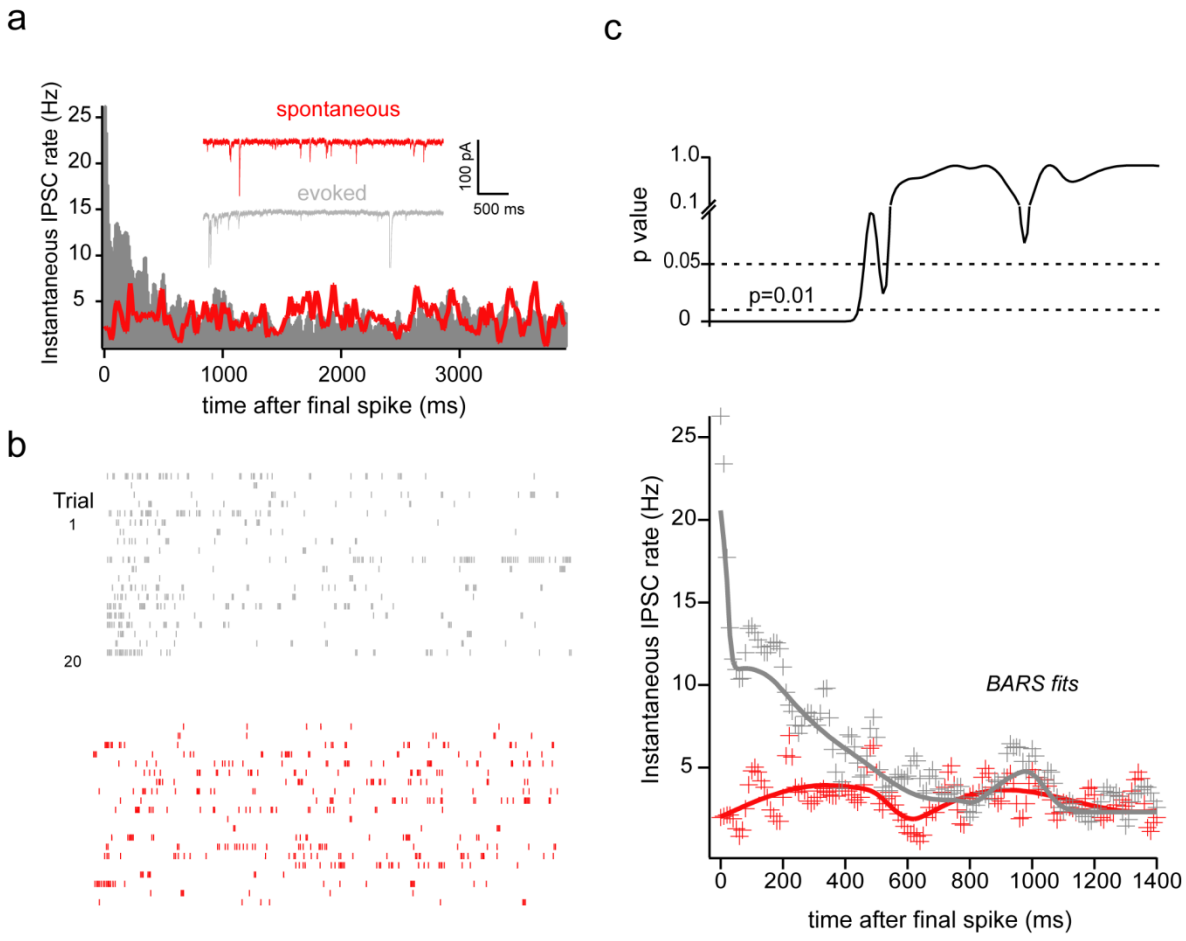
a
b
c
spontaneous
evoked
100 pA
500 ms
Instantaneous IPSC rate (Hz)
time after final spike (ms)
Trial
1
20
p value
p=0.01
BARS fits

Fig. 24. Recurrent IPSCs evoked by action potentials in mitral cells terminate within 500 ms. (a), Plot of instantaneous IPSC rates in mitral cells under spontaneous (red) and spike-evoked (gray) conditions (see *Methods*). Inset traces show example recordings. For the evoked case, 7 spikes at 40 Hz were elicited in current clamped mitral cells, and cells were then rapidly voltage clamped to -80 mV (similar to experiments of figure 23) to ensure that observed IPSCs were not due to release evoked by elevated subthreshold voltage. Recordings were made with KCl–based internal to maximize visibility of IPSCs at hyperpolarized potentials. Data are pooled from 10 cells. (**b),** Rasters of IPSC times from a single example cell for 20 evoked trials (gray, top) and 20 spontaneous trials (red, bottom). **(c),** Bottom, IPSC rate data for the evoked and spontaneous cases were fit using Bayesian Adaptive Regression Splines (BARS) (see *Methods*). Top, p–value for the likelihood ratio test comparing spontaneous and evoked firing at each time point (see *Methods* for details).

4.5.2 Control of dendritic readout

Perhaps the most important finding described above is that mitral cell subthreshold output can be enhanced by activation of mGluRs, including mGluRs activated following endogenous glutamate release from a single AOB mitral cell. In many systems, mGluR activation depends on the total amount of glutamate released from many synapses (Scanziani et al., 1997;De Saint and Westbrook, 2007). In the AOB such a mechanism may allow the sensitivity or gain of recurrent inhibition (mediated by periglomerular or granule cells) to be enhanced when the overall level of mitral cell activity is high, or when inputs to a particular glomerulus are strong. This would allow for dynamic regulation of the selectivity of mitral cell firing and facilitate suppression of inappropriate responses under conditions where many pheromonal stimuli are present. Such a mechanism may occur across the whole of the AOB, or at the level of a few nearby glomeruli. In this case, subthreshold release may be enhanced when nearby glomeruli, which may be innervated by sensory neurons expressing similar receptors, are coactivated, leading to a local and selective recruitment of inhibition.

The subthreshold release we observed is calcium-dependent. However, we did not find a marked enhancement of dendritic subthreshold calcium transients following addition of DHPG. We take this as evidence that dendritic excitability was not substantially altered by mGluRs. Rather, mGluR activation seems to influence the manner in which a particular pattern of dendritic activity is read out. This issue of dendritic "readout" has attracted considerable attention lately, and is central to our understanding of the functional roles of dendritic transmitter release. Dendritic release of endocannabanoids and concomitant expression of depolarization induced suppression of inhibition (DSI), for example, depends on the spatial extent, and possibly source of calcium influx (Brown et al., 2003;Brown et al., 2004;Rancz and Hausser, 2006). Similarly, synaptically evoked calcium responses in the dendrites of olfactory bulb granule cells can be confined to single spines or branches (Zelles et al., 2006), or can propagate throughout the dendritic tree (Egger et al., 2003;Egger et al., 2005). Moreover, these distinct events may result in GABA release over distinct spatial scales. The present work suggests that presynaptic dendrites may allow for two forms of regulation of transmitter release–a local regulation by virtue of the electrical and chemical compartmentalization within dendrites, and a more global, state-dependent form of control that can enhance or diminish the "release efficacy" of a

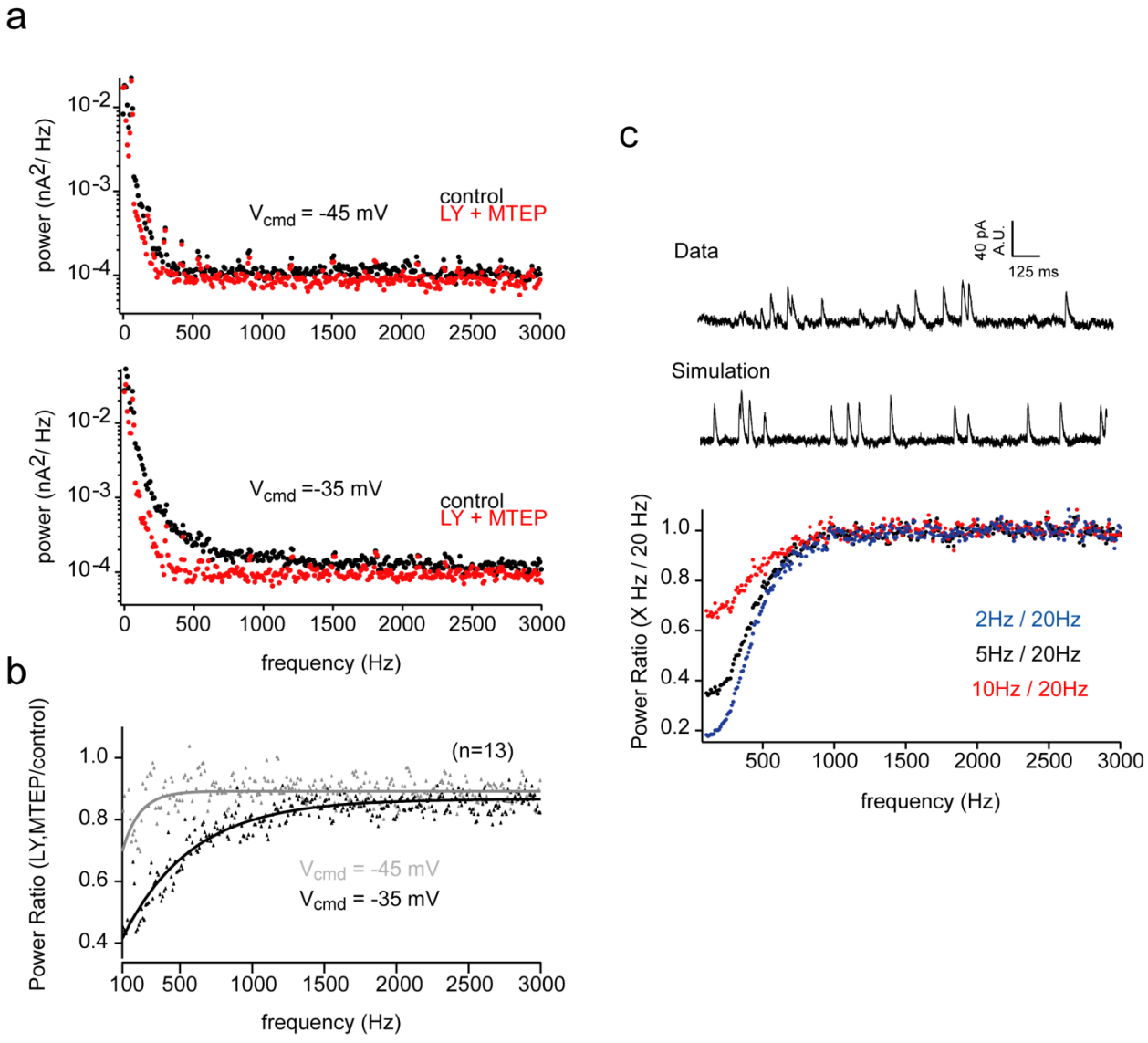
a
power (nA2/ Hz)
10-2
10-3
10-4
Vcmd = -45 mV
control
LY + MTEP
0
500
1000
1500
2000
2500
3000
Vcmd =-35 mV
frequency (Hz)
b
Power Ratio (LY,MTEP/control)
1.0
0.8
0.6
0.4
(n=13)
Vcmd = -45 mV
Vcmd = -35 mV
100
c
Data
40 pA
A.U.
125 ms
Simulation
Power Ratio (X Hz / 20 Hz)
2Hz / 20Hz
5Hz / 20Hz
10Hz / 20Hz

Fig. 25. Spectral analysis of IPSCs. (**a)** Example power spectra of detrended, mean-subtracted current records from experiments described in figure 23 (see also *Methods*). Top, spectra of current records for a cell voltage clamped to -45 mV immediately after 7 spikes at 40 Hz were evoked in current clamp. Control spectrum is shown in black, spectrum following blockade of group I mGluRs by LY367385 and MTEP is shown in red. Bottom, spectra for the same cell in the same experiment, only the cell was voltage clamped to -35 mV following 7 spikes evoked in current clamp. Note that at this more depolarized potential, LY367385 and MTEP strongly attenuate power at lower (< 1000 Hz) frequencies. Power in this lower band corresponds to current fluctuations associated with ongoing synaptic activity (e.g. panel **c**). (**b)** Summary data for experiments described above. For each experiment, the fraction of power reduction by LY367385 and MTEP was calculated across frequencies for holding potentials of both -45 mV and -35 mV. Solid lines are double exponential fits. (**c)** Simulation demonstrating sensitivity of current power spectra to changes in IPSC rate. Top trace, data. Bottom trace, simulation in which IPSCs were modeled as alpha functions (τ=45 ms) occuring at times governed by a poisson process (see *Methods* for details). Bottom graph, power ratios for the indicated IPSC rates.

particular kind of dendritic signal. For the case described here, mGluRs control the efficacy of subthreshold voltage as a trigger of release. One interesting possibility to consider is that subthreshold release may itself also trigger further mGluR activation due to its prolonged timecourse. This may be useful for maintaining the "mode switch" from suprathreshold to subthreshold release.

4.5.3 Significance for AOB function

A number of AOB-mediated behaviors, such as the Bruce and Whitten effects, involve pronounced changes in endocrine state, implying that false-positive responses to stimuli could be behaviorally costly. In contrast to other sensory systems, where ethological demands place a premium on processing speed, the accessory olfactory system may be adapted to for accuracy at the expense of speed. Consistent with this, mitral cells respond to pheromones highly selectively, but with unusually long latencies (on the order of tens of seconds)(Luo et al., 2003).

The ability of mitral cells to switch from a suprathreshold to a subthreshold output mode, as described in the results above, may provide a specialized negative feedback mechanism that enforces selectivity of mitral cell responses, or enhances the dynamic range of pheromone processing. Under this model, the default integration mode of mitral cells would be one of high sensitivity, in which little subthreshold release and recurrent inhibition occur. Thus, even low pheromone concentrations could elicit mitral cell spiking. During periods of high input or activity, subthreshold release mechanisms would come in to operation, resulting in continuous recurrent inhibition that makes spike threshold more difficult to achieve.

5.0 SUMMARY AND GENERAL DISCUSSION

5.1 RELEVANCE AND SUMMARY OF FINDINGS

The earliest mathematical models of neural function treated single neurons as simple integrative, point-like devices (McCulloch and Pitts, 1943). In these models, a neuron's job was simple: collect inputs, and dispatch a message to postsynaptic partners once some minimum net input level was achieved. Useful information processing was assumed to depend on the distributed activity among and connections between many such cells. No single neuron was thought to be sensitive to complex relationships among its inputs, or discerning in the outputs it generated. Although this view is appealing for its simplicity, a wealth of studies point to its inadequacies. Our more modern view of single neurons is that they are highly sophisticated devices, with a host of mechanisms to actively operate on their inputs and influence their targets in subtle ways (Koch and Segev, 2000). In contrast to "point neurons," whose spikes convey specific messages only when pooled, the spikes of single real neurons can be highly informative about specific aspects of the sensory world.

How do single neurons manage such computational feats? A large body of work has studied this question, and a growing consensus is that dendrites play a key role in neural computation and information processing. Although we have gained much insight into how dendritic morphology and active dendritic properties contribute to certain nonlinear aspects of synaptic integration, it has in general been difficult to assign specific computational or even behavioral roles to any particular aspects of dendritic function (Nolan et al., 2004). In this regard,

the olfactory bulb has historically offered a powerful experimental system for forging a stronger link between the physiological properties of dendrites and neuronal computation(Shepherd, 1978;Shepherd, Shepherd, 2004). The main advantages of this system, and the AOB in particular are that inputs to the AOB are well-defined and stereotyped, and outputs from the AOB project to only few brain regions to elicit specific behaviors. Moreover, because the majority of information processing in the AOB occurs via local synaptic interactions between the dendrites of principal neurons and interneurons, it is a superb model system for studying dendritic computation.

Many studies have investigated how the active properties of dendrites enhance the computational power of single neurons. It is known, for example, that active conductances can "boost" synaptic inputs on dendritic trees (Urban et al., 1998), and that backpropagating spikes can enhance the coupling between proximal and distal integrative compartments on dendrites (Larkum et al., 1999). Because the dendrites of AOB mitral cells serve as both pre- and postsynaptic structures, their excitable properties will affect how inputs are integrated, as well how dendritic activity is coupled to output. In **chapter 2** we characterized basic aspects of mitral cell dendritic excitability, and investigated how this excitability influences synaptic integration. We observed that mitral cell dendrites support local regenerative spikes, and that these spikes are triggers of glutamate release. Dendritic spikes have been observed in a number of neuron types, but this is, to our knowledge, the first demonstration of local spikes producing output of classical, fast transmitters. Thus, in addition to contributing to local integrative events, dendritic spikes may allow neurons to independently activate specific subsets of postsynaptic targets.

In many cases, dendritic transmitter output can rapidly and locally affect subsequent dendritic activity via feedback mechanisms. In the AOB, the glutamate released from mitral cell dendrites activates postsynaptic interneurons that in turn inhibit mitral cells via reciprocal dendrodendritic synapses. The presence of these synapses adds considerable complexity and subtlety to dendritic computation. In particular, processes such as dendritic integration and dendritic signal propagation will not depend simply on the biophysical properties of dendrites, but also on the manner and degree to which dendrites activate their local "support circuitry." This could allow for ultra-fine regulation of dendritic processing, since there are multiple loci at which one could alter the relationship between input or spike-evoked dendritic activity and feedback inhibition. In **Chapters 3 and 4**, we studied several ways in which the self-regulation

of dendritic activity can be modified. Specifically, we characterized a previously unknown dependence of mitral cell recurrent inhibition on metabotropic glutamate receptors (**Chapter 3**). Because these receptors are often activated only for vigorous neural activity, this suggests that the magnitude of recurrent inhibition may have a strong history or context dependence. To continue on the analogy above, the available dendritic support circuitry for a single neuron will depend on that neuron's past activity.

By what mechanisms can the recruitment of support circuitry be altered? The most obvious way is by some direct effect on pre or post-synaptic excitability. Plasticity of dendritic excitability has been observed in several cell-types (Yasuda et al., 2003;Frick et al., 2004), and has been shown to affect the boosting and integration of synaptic inputs (Wang et al., 2003). Similarly, we observed that mGluR activation caused a small but significant depolarization of granule cells (**Chapter 3**). Another possibility we investigated was that mGluRs could alter the coupling between neuronal activity and transmitter release – as has been amply described for axonal boutons (Cartmell and Schoepp, 2000). Such modulation is particularly intriguing for mitral cell dendrites, since these structures support many kinds of regenerative and subthreshold activity potentially coupled to release. In **chapter 4**, we describe the effects of mGluRs on transmitter release from mitral cell dendrites, and found that mGluR activation unmasked a capacity for graded, subthreshold glutamate release. This suggests that under conditions of low network activity, in which metabotropic receptors are unlikely to be activated, mitral cells are in some sense disengaged from their feedback circuitry. Following a bout of high activity and concomitant activation of mGluRs, the efficacy of subthreshold membrane potential as a trigger of release is greatly enhanced, allowing for fast and ultrasensitive feedback.

5.2 DIVERSITY OF DENDRITIC SIGNALS

Axons support one type of signal – the action potential – that serves as the exclusive trigger of transmitter release. Although the reliability, amplitude, and time-course of axonal action potentials can be modulated, the stereotypy of action potential waveforms generally ensures that transmitter release is rapid and pulsatile. Dendrites, by contrast, support a range of subthreshold

and regenerative events that can vary considerably in their dynamics and biophysical mechanisms. In presynaptic dendrites, each such event is also a potential output signal, suggesting that dendrites may support multiple (and possibly qualitatively different) signaling modes. Each of these signaling modes may, in turn, be involved in distinct dendritic computations.

Thus, to understand the diverse output modes of transmitter-releasing dendrites, it is important to have a general "catalog" of the evoked events that they support. In this dissertation, we have identified three such events in mitral cell dendrites: backpropagating action potentials, local regenerative spikes in tufts, and sustained, graded calcium transients. These events occur over different spatial and temporal scales, and hence may provide mitral cells dendrites with a broad palette of output options.

5.2.1 Backpropagating action potentials

In **chapter 2**, we described the backpropagation of somatically-evoked action potentials into the principal dendrites of AOB mitral cells. Backpropagating action potentials (BAPs) were first observed directly in paired soma-dendrite recordings by Stuart and Sakmann (1994)[2]. These events demonstrate a striking exception to the classical view that neuronal signaling is unidirectional. Since their discovery, the roles of BAPs have been studied in a number of neuronal functions, including synapse stabilization and plasticity, dendritic integration, and retrograde communication (reviewed in Waters et al., 2005). In many of these studies, the relative attenuation of BAPs along dendrites has been shown to be a critical parameter in determining local plasticity rules and the spatial extent of dendritic transmitter release. Froemke et al (2005), and Letzkus et al (2006) have recently observed a strong dependence of spike-timing dependent plasticity (STDP) rules on dendritic location, with the magnitude of LTP induced being smaller on distal dendrites than proximal ones. Interestingly, this distance dependence was diminished when BAP propagation was enhanced by blockade of A-type

[2] However, the first descriptions of passive, somatofugal conduction of nerve potentials was by Eyzaguirre and Kuffler(EYZAGUIRRE and KUFFLER, 1955). In their classic work on the crustacean stretch receptor, these investigators proposed a "shceme of excitation" in which synaptic prepotentials initiated axonal as well as dendrite-soma impulses.

potassium channels, suggesting that decremental BAP conduction can contribute to the compartmentalization of neuronal function. Other experiments have investigated the role of BAPs as triggers of neurotransmitter release. BAPs in lateral dendrites of MOB mitral cells are known to activate granule cells and can mediate either self-inhibition or lateral inhibition of neighboring mitral cells[3]. Because granule cells are the present along most of the lateral dendrite axis, the properties of BAP propagation in these dendrites determines the distance dependence of lateral inhibition – an operation believed to be critical for sensitively discriminating between closely related stimuli (Urban, 2002;Yokoi et al., 1995). Several reports have shown that BAP conduction in these dendrites is decremental (Margrie et al., 2001), and possibly modulated by a dendritic A-type potassium current (Christie and Westbrook, 2003) as well as local feedback inhibition (Xiong and Chen, 2002;Lowe, 2002). This is still a matter of controversy though, since there are also reports of non-decremental BAP propagation in these same dendrites (Xiong and Chen, 2002).

Regardless of the specific conclusions of these studies, they unequivocally point to BAPs as critical players in dendritic integration and output, and suggest that the relative attenuation of BAPs can strongly influence specific dendritic functions. Conspicuously, there is a marked heterogeneity in how robustly BAPs propagate in different cell types. Although dendritic morphology is a critical parameter in determining the extent of BAP propagation, some of this heterogeneity is also due to differential expression of voltage gated channels along dendrites of different cell types. In CA3 pyramidal cells and Purkinje cells, for example, BAP conduction is highly decremental, and likely due to rapidly decreasing densities of Na+ channels with distance from the soma (Stuart and Hausser, 1994;Migliore and Shepherd, 2002). BAPs are similarly attenuated with distance along CA1 pyramidal cell dendrites, and several studies suggest that this is due to an increased density of dendritic K_A channels along the apical dendrite (Hoffman et al., 1997).

Intriguingly, BAP conduction in MOB mitral cell principal dendrites appears to be robust and non-decremental. This has been verified using calcium imaging techniques, patch clamp recordings, and simulations. Chen et al (1997) and Bischofberger and Jonas (1997) directly

[3] The term "backpropagating action potential" is often applied to axosomatically initiated potentials that propagate into mitral cell lateral dendrites. This may be something of a misnomer though, since somatofugal signal propagation along these dendrites is obligatory for transmitter output (Gordon Shepherd, personal communication).

recorded from the distal dendrites and somata of mitral cells, and observed little dendritic attenuation or broadening of somatically initiated spikes. In fact, under conditions where somatic spikes were suppressed by hyperpolarization or activation of inhibitory inputs, APs could be initiated close to mitral cell tufts (Chen et al., 1997). The unusually robust initiation and propagation of APs in these dendrites is probably due to their high densities of both sodium and potassium channels (Bischofberger and Jonas, 1997). Similarly, somatically-evoked APs appear to propagate even into the most distal, high-order branches of mitral cell tufts (Zhou et al., 2006b;Debarbieux et al., 2003;Ma and Lowe, 2004), though this has typically relied on indirect measurements of dendritic activity since tufts taper to un-patchable diameters within a glomerulus. In the work described above (specifically section **2.4.1**), we investigated many of these same basic aspects of dendritic backpropagation in AOB mitral cells. In agreement with previous work in the MOB, our calcium imaging data indicate that 1) calcium transients propagate nondecrementally into tufts, and 2) branches within a single tuft are activated uniformly by BAPs. A recent study by Ma and Lowe (2004) complements our work nicely, and shows that tuft calcium transients elicited by somatic spikes are blocked by TTX. This strongly indicates that the calcium transients we and others observed are triggered by sodium-mediated action potentials.

In addition to finding homogeneous, non-decremental calcium transients within tuft branches, we and others also observed that (somatic) spike-evoked transients across tufts were of similar amplitude (section **2.4.1**, Fig. 5). This indicates that action potentials can uniformly invade all branches of all tufts, and suggests remarkably robust and high fidelity AP signaling in AOB mitral cell dendrites, reminiscent of axonal signaling. This is particularly intriguing given the known presynaptic role of mitral cell tufts. Indeed, mitral cell dendrites also seem to have the requisite HVA calcium conductances (mostly N and P/Q) for transducing rapid action potentials into transmitter output (Isaacson and Strowbridge, 1998). Several studies have shown that mitral cell action potentials can evoke glutamate release (likely in part from tufts) to mediate self-excitation (Schoppa and Westbrook, 2002), or spillover excitation of neighboring mitral cells (Isaacson, 1999;Urban and Sakmann, 2002). However, surprisingly few studies have examined the activation of glomerular interneurons by mitral cell action potentials (Murphy et al., 2005). In **section 2.4.3** (Fig. 7), we confirmed that backpropagating potentials in AOB mitral cells activate

postsynaptic interneurons by monitoring their activity with the membrane permeable indicator Fura2-AM.

5.2.2 Local spikes

We and others (Murphy et al., 2005) have shown that BAPs in mitral cells and external tufted cells can evoke glutamate release from tufts and activate glomerular interneurons. How might this be relevant for pheromone processing? After all, if a mitral cell has spiked, it has presumably already sent its axonal message to downstream targets. Spike evoked recurrent inhibition of tufts may seem to be a bit after the fact. Of course, one role of mitral cell BAPs may be to affect subsequent integration of VN inputs via feedback inhibiton. This may allow all tufts to be "reset" to a common value, or inhibited in parallel by the same amount. Operating on all tufts simultaneously may thus be important for normalizing activity across tufts, or extending the dynamic range of mitral cell integration. For example, if different tufts are receiving VN inputs of different strengths, BAP evoked self-inhibition would help prevent saturation of any single tuft, while maintaining the relative distribution of activity across tufts.

Another possibility (though not a mutually exclusive one) is that the active processes that allow robust BAP propagation are also involved in mitral cell integration prior to somatic spiking. There is a large literature describing how active dendritic conductances can boost or diminish synaptic inputs, and these conductances are often the same ones underlying the generation action potentials. To test the role of dendritic excitability in synaptic integration, we studied dendritic calcium responses in mitral tufts when VN inputs were activated by extracellular stimulation. We found that individual tufts typically respond to VN stimulation in an all-or-none manner: low levels of inputs evoked no calcium responses, while higher levels of input evoked stereotyped, regenerative calcium spikes comparable in amplitude to transients evoked by backpropagating somatic spikes.

Such dendritic spikes have been observed in many neuron types, and are generally believed to amplify synaptic inputs and contribute to the compartmentalization of dendritic integration. At one extreme, individual dendritic branches or subregions have been proposed to function as binary thresholded units (Wei et al., 2001;Schiller et al., 2000). Under this view, a

terminal dendritic branch is a bistable element whose activation is determined "not by the number of synaptic receptors activated, but by its physical dimensions and the number of its voltage gated channels."(Wei et al., 2001) By extension, axonal output may be sensitive to the number and distribution of active compartments in addition to simply net synaptic input across the dendritic tree.

The bistable dendritic behavior underlying this kind of integrative mode has been best described for the apical and basal branches of pyramidal cells. These dendrites support highly localized spikes mediated by voltage gated calcium and sodium channels (in apical dendrites), and by the regenerative action of NMDA receptors (in basal dendrites). Several models have addressed how this local spiking may increase the computational capacity of single neurons (Archie and Mel, 2000), but these are necessarily abstract since the specific messages conveyed to pyramidal neurons by their synaptic inputs are unknown. By contrast, inputs to AOB mitral cell tufts are highly stereotyped and likely convey a simple message reporting on the presence and concentration of a single, specific ligand. Thus, our work suggests that tufts can function as isolated compartments that report all-or-none signals about specific pheromone compounds.

Several other groups have investigated tuft activity in response to synaptic input, and there are several, sometimes conflicting accounts of the extent to which tufts support local regenerative spikes. The first reports to suggest the presence of regenerative conductances in tufts were by Mori and Shepherd (1982a), who described fast "prepotentials" in mitral cells that accompanied spikes evoked by ON stimulation. In later studies, Shepherd and colleagues explored the regenerative activity of tufts more directly, by simultaneously recording from mitral cell primary dendrites and somata while activating ON inputs (Chen et al., 1997). Although the dendritic membrane close to tufts was highly excitable, isolated spikes were only observed when the soma was hyperpolarized by current injection or activation of inhibitory inputs. Similarly, Yuan and Knopfel have observed that tuft calcium transients in MOB mitral cells evoked by synaptic stimulation tend to be graded, rather than all-or-none, and likely mediated by NMDA receptors and metabotropic glutamate receptors (under conditions of high stimulus intensity or frequency)(Yuan et al., 2004;Yuan and Knopfel, 2006a;Yuan and Knopfel, 2006b). Part of the discrepancy between our results and those above may be due to geometric factors, such as the electrotonic compact-ness of AOB tufts compared to MOB tufts.

5.2.3 Sustained subthreshold calcium signals

The sections above show that AOB mitral cell dendrites support at least two distinct types of evoked activity: backpropagating spikes, and synaptically-evoked local spikes. Since AOB dendrites are presynaptic structures, both of these kinds of activity are candidate triggers of transmitter output. Although local spikes can allow for fine spatial control of dendritic output, the quantity and time-course of this output may be qualitatively similar to that evoked by full blown spikes. After all, the calcium transients we observed for both BAPs and synaptic input were rapid and stereotyped events of comparable amplitude. Are there other forms of dendritic activity that could produce qualitatively different, less stereotyped outputs? In **chapter 4**, we observed that subthreshold depolarizations of mitral cell somata produced sustained elevations of calcium along principal dendrites evident even in the distal tuft (section **4.4.3**, Fig. 22). The amplitude of these sustained transients was proportional to membrane voltage, and analyses of self excitation and recurrent inhibition of mitral cells suggested they mediate a form of graded transmitter output.

Many studies have emphasized that evoked dendritic activity is transient and sterotyped. On closer inspection though, not all dendritic potentials share these attributes. This was evident even in the early dendritic recordings of Llinas and Sugimori (1980). These investigators observed that depolarization of Purkinje cell dendrites evoked long plateau-like potentials mediated by calcium and non-inactivating sodium conductances. Plateau potentials could persist for several hundred milliseconds after depolarizing steps terminated, and both the amplitude and duration of the plateaus were positively correlated with the strength of depolarizing current. Intriguingly, similar, long-lasting dendritic plateau potentials have been observed in a number of cells with dendrites competent for transmitter release, including juxtaglomerular cells (Zhou et al., 2006a;McQuiston and Katz, 2001) and MOB mitral cells (De Saint and Westbrook, 2007;Carlson et al., 2000). In MOB mitral cells, "long-lasting depolarizations" (LLDs) of > 500 ms can be evoked by brief shocks in the glomerular layer, and paired recordings from the principal dendrite and soma suggest that LLDs are initiated in the tuft and allow for extended epochs of synaptic processing by glomerular circuits (Carlson et al., 2000). Intriguing recent work by Westbrook and colleagues suggests that dendritic glutamate output may occur

continuously for the duration of the conspicuously long lasting mitral cell EPSC (De Saint and Westbrook, 2007).

Although the long plateau potentials described above may mediate sustained dendritic transmitter release, they are still typically elicited by brief stimuli. However, there is also evidence that dendrites support sustained, apparently non-inactivating calcium currents that can rapidly "track" subthreshold membrane voltage. Magee and Johnston(1996) observed that resting membrane potential strongly influenced "standing" calcium concentrations in pyramidal cell dendrites via dihydropyridine sensitive channels. There is also evidence for graded calcium transients in MOB mitral cells. In experiments in which mitral cells were patched in-vivo and filled with calcium indicators, Charpak et al (2001) observed odor-evoked subthreshold oscillations of both membrane potential and dendritic calcium. These authors speculated that such calcium transients could mediate a form of graded release, similar to what is observed in hair cells and certain invertebrate neurons.

Our results in **chapter 4** suggest that subthreshold calcium transients are indeed capable of producing transmitter output in response to graded changes in membrane potential. This is supported by several lines of evidence. First, in cases where we enhanced the detectability of self excitatory events in mitral cells with low magnesium, we found that subthreshold current or voltage steps elicited continuous barrages of events blocked by a cocktail of APV, MK801, and CNQX. Second, this ability to release transmitter continuously in the subthreshold regime was diminished by intracellular BAPTA. Third, depolarization evoked calcium transients were directly proportional to membrane voltage. We hypothesize that the sustained, voltage-dependent calcium transients we observe are triggers of graded, continuous neurotransmitter release. Interestingly, the efficacy of these transients as output triggers seems to depend on metabotropic glutamate receptors – this topic is explored in more detail below (section **5.4.1**).

We are currently exploring the mechanisms underlying these slow dendritic calcium influxes. One possibility is that they are mediated by T-type calcium channels. Indeed, T currents have been suggested to mediate a component of transmitter release in granule cell dendrites (Egger et al., 2005), and are responsible for the graded output of retinal bipolar cells (Pan et al., 2001). However, given the marked inactivation of T channels at low voltages (Huguenard, 1996), there may be little T-current available near resting membrane potentials. Our preliminary speculation is that the slow calcium elevation we observe is due to an L-type calcium

conductance. Although L-type channels typically have high activation thresholds, some subtypes, such as CaV1.3 activate rapidly near resting membrane potentials, and are only weakly inactivating (Lipscombe et al., 2004). In addition, L-type channels have been observed in the dendrites of cultured mitral cells(Schild et al., 1995).

5.3 LOCAL DENDRITIC SPIKES AND LOCAL DENDRITIC OUTPUT

Local dendritic spikes are typically poorly propagating, and often fail to trigger axonal action potentials reliably. Are these properties shortcomings or attributes? One advantage to having spatially confined spikes was described above: by functioning as binary-like subunits, individual dendritic compartments could allow single neurons to execute logical operations. Even under this positive view, though, an isolated dendritic spike may seem to contribute little to neural processing. What then, are local spikes good for?

One interesting possibility is that there are local forms of "readout" of dendritic spikes. Several studies have shown, for example, that dendritic spikes can result in local changes in synaptic strength. In recordings from the apical dendrites of CA1 pyramidal neurons, Golding et al (Golding et al., 2002) demonstrated that LTP could be induced in distal dendrites even when TTX was applied locally at the proximal dendrite. Under these conditions, LTP induction was strongly dependent on the occurrence of local spikes, and required both voltage gated calcium channels and NMDARs. This argues that the calcium influx associated with local spikes is sufficient to activate the biochemical machinery required for synaptic strengthening – a form of local, cell-autonomous readout. In related studies, other investigators have observed that LTD in pyramidal and Purkinje cells is expressed presynaptically and requires dendritic release of cannabanoids (Brenowitz and Regehr, 2003), which could presumably be provided by local spikes (Rancz and Hausser, 2006). In **chapter 2**, we described an output role for tuft spikes in mitral cell dendrites: even in the absence of somatic spikes, local spikes were capable of synaptically activating postsynaptic interneurons via glutamate release. Because tufts of AOB

mitral cells are often associated with distinct glomeruli receiving inputs from separate sources, this suggests that single tufts may be local, autonomous output units.

The functions of dendritic spikes as triggers of fast transmitter release have been surmised in a number of cell types, but not directly demonstrated. One of the best studied examples is the axon-lacking granule cell of the olfactory bulb. Similar to mitral cells, granule cells support several types of regenerative dendritic activity. The dendrites of these cells can support full blown sodium spikes (Pinato and Midtgaard, 2005), branch-specific calcium and sodium spikes (Zelles et al., 2006), and even spikes confined to single spines mediated in part by a T-type current (Egger et al., 2005). What is most intriguing about this diversity of dendritic events is that each regulates GABA release over a characteristic spatial scale, and is likely involved in a distinct aspect of neuronal signaling and olfactory computation. Spine or branch-spikes, for example, are likely to amplify recurrent inhibition of single or few mitral cells, while global spikes are well suited to mediate robust lateral inhibition between mitral cells(Willhite et al., 2006).

Similarly, the individual dendritic branches of starburst amacrine cells in the retina have been shown to support local spikes. Intriguingly, the spiking of individual branches is tuned for motion direction even though somatic voltage is relatively nonselective for motion (Euler et al., 2002). Although the output properties of these individual branches have not been examined, they are known to release acetylcholine, and thus may activate specific postsynaptic targets in a direction-selective manner. In addition to our observation of local output of fast transmitters, dendritic calcium spikes have recently been shown to evoke release of endocannabanoids from Purkinje cells (Rancz and Hausser, 2006), allowing for input-specific regulation of synaptic plasticity. Because the spatial extent of Purkinje cell calcium spikes can be modulated by BK channels, these cells may be able to dynamically tune the sizes of their dendritic release compartments.

Our studies and the work described above suggest an updated model of single-neuron processing in which (at least some) neurons are not characterized by a single input-output function, but rather by multiple input output regions defined by the spatial scale of dendritic excitability. Under this view, localized dendritic spikes signal the occurrence or coincidence of particular presynaptic events, and can in turn activate postsynaptic targets in an input specific manner. By having multiple output compartments, a single neuron becomes a more versatile

signaling element, and activates specific sets of postsynaptic cells for specific patterns of afferent activity. Such flexible control of outputs over different dendritic compartments has been described in some detail for thalamic interneurons, which release GABA from their dendrites upon activation of metabotropic glutamate receptors(Cox et al., 1998). Apparently, dendritic GABA release can occur in the absence of dendritic spikes in these cells, and the compartmentalization of release is though to be largely a function of electrical compartmentalization. The mechanism of tuft-spike evoked transmitter release we describe in **chapter 3** extends this view, and suggests that active dendritic conductances may allow neurons to dynamically define release compartments.

5.4 MODULATION OF DENDRODENDRITIC PROCESSING

5.4.1 Obligatory role of mGluRs in reciprocal dendrodendritic inhibition of AOB mitral cells

The results discussed above argue that mitral cell dendrites are highly flexible signaling elements that can produce outputs over several spatial and temporal scales. Intuitively, the efficacy of a particular dendritic signal will depend on whether and how it is coupled to transmitter release (readout), and the extent to which it influences postsynaptic cells (receptivity). There are many potential loci at which readout and receptivity can be modulated, and indeed, many aspects of dendrodendritic signaling are known to be influenced by diverse neuromodulatory systems. Modulation of mitral and granule cell excitability, and synaptic transmission between these cells has been the focus of particular interest. Early studies described strong actions of noradrenaline (NA) on mitral-granule reciprocal signaling (Shipley et al., 1985;McLean et al., 1989), and reported that NA suppressed output of GABA and glutamate from granule cells(Jahr and Nicoll, 1982b) and mitral cells (Trombley and Shepherd, 1992), respectively (but see Araneda and Firestein(2006)). More recent work has described similar alterations of mitral-granule (and

mitral-PG) signaling properties by most known neuromodulators, including serotonin (McLean and Shipley, 1987), acetylcholine (Castillo et al., 1999), and dopamine (Davison et al., 2004).

In many cases, the effects of such neuromodulators on bulb function are diffuse, resulting from physically widespread output from centrifugal fibers. However, there is also evidence that signaling between cells of both the MOB and AOB can be modulated more locally, by the metabotropic actions of glutamate (Schoppa and Westbrook, 1997;Dong et al., 2007;Heinbockel et al., 2007) and GABA(Isaacson and Vitten, 2003). Indeed, expression levels of metabotropic glutamate receptors (mGluRs) in the MOB and AOB are among the highest in the brain (van den Pol, 1995;Martin et al., 1992), and these structures express all of the 8 known mGluRs. Much of the interest in mGluRs in the AOB has centered on the role of mGluR2 in mediating certain forms of olfactory memory. mGluR2 is localized predominantly on granule cell spines, and its activation leads to considerable attenuation of GABA output, with concomitant reduction in recurrent inhibition of mitral cells(Hayashi et al., 1993;Ohishi et al., 1993). Under one model, this reduced inhibition creates conditions favorable for a recently mated female to learn the pheromonal signature of a stud-male (the so-called Bruce effect). Consistent with this, infusion of the group II mGluR agonist DHPG has been shown to facilitate such memory formation (Kaba et al., 1994).

In chapter 3, we described an obligatory role played by mGluR1 in mediating recurrent dendrodendritic inhibition of single AOB mitral cells. Recurrent inhibition was completely eliminated by the mGluR1 antagonist LY367385, and mitral cell mIPSCs were enhanced by the group I agonist DHPG, suggesting at least a partial presynaptic (granule cell) component to the reduced recurrent inhibition. A number of other studies have described effects of group I mGluRs (mGluR1 and mGluR5) on mitral and granule cell excitability and output, though ours is the only one, to our knowledge, demonstrating such a strong dependence of basal transmission on mGluR activation. In the main olfactory bulb, Ennis and coworkers (Heinbockel et al., 2004) observed that mitral cells are directly depolarized by mGluR1 – an effect mediated predominantly by closure of potassium channels and opening of calcium channels. By contrast, we found weak and mixed effects of group I mgluR activation on mitral cell resting potential.

Similar to what we observed, both Heinbockel et al (2004) and Dong et al (2007) have described direct activation of granule cells by group I mGluR agonists. Taken together with our data showing the mGluR1 dependence of recurrent inhibition, this suggests a simple model in

which the gain of recurrent inhibition is potently modulated by direct mGluR effects on granule cell voltage. One interesting question is what patterns of activity are likely to provide the requisite mGluR activation for facilitating granule cell responses. Although we did not test this directly, we speculate that activation of mGluRs on granule cells may be highly sensitive to the firing rate of presynaptic mitral cells, perhaps requiring a certain threshold level of mitral cell activity. Several investigators have suggested that mGluRs are preferentially activated for high levels of presynaptic activity(Scanziani et al., 1997), and in some cases, mGluR-1 mediated EPSPs are only observed when glutamate transporters and ionotropic transmission are blocked (Batchelor and Garthwaite, 1997;Brasnjo and Otis, 2001). In MOB mitral cells, Knopfel and colleagues have shown that group I mediated mGluR responses are evoked only for high (100 Hz) levels of ORN stimulation (Yuan and Knopfel, 2006a). Generally these findings are thought to be consistent with a picture in which high affinity mGluRs located extrasynaptically detect glutamate spillover from distant synapses (Mitchell and Silver, 2000;Isaacson, 2000;Scanziani et al., 1997). Under this view, our data suggest that recurrent inhibition may exhibit a history dependence, such that high levels of mitral cell output tonically depolarize granule cells and "prime" subsequent recurrent inhibition.

5.4.2 mGluRs and the "readout" of dendritic signals

In **chapter 4** we observed that endogenous or exogenous activation of group I mGluRs caused a qualitative change in the "readout" of activity in mitral cell dendrites. Under control conditions, subthreshold depolarization of mitral cells resulted in weak, but detectable dendritic transmitter release. When group I mGluRs were activated, however, these same subthreshold depolarizations elicited sustained, robust, and continuous output of dendritic glutamate that was graded with membrane voltage.

Although most studies have described the actions of mGluRs on intrinsic cellular excitability and spiking behavior (as described above, **5.4.1**), there is also considerable evidence that mGluRs can modulate transmitter release even without changes in action potential waveform or global excitability. Activation of group III mGluRs, for example, diminishes glutamate release from the presynaptic terminals at the calyx of Held by suppressing P/Q type calcium currents

(Takahashi et al., 1996), while mGluR2 (a group II mGluR) agonists are believed to directly suppress GABA release from AOB granule cells (Hayashi et al., 1993;Kaba et al., 1994). Relatively few studies have addressed how activation of group I mGluRs affects transmitter output, presumably because mGluR1 and mGluR5 are generally believed to be localized extrasynaptically in postsynaptic membranes. To date, most physiological investigations of mGluR1 and mGluR5 function have placed more emphasis on their roles in synaptic plasticity. Blockade of mGluR1 with inactivating antibodies, for example, completely eliminates LTD induction of glutamatergic inputs to cultured Purkinje cells, while blockade of mGluR5 diminishes LTP in area CA1(Lu et al., 1997). It should be emphasized, though, that since mitral cell dendrites are both pre and postsynaptic, there are likely to be effects on both dendritic integration and output upon activation of most mGluRs.

What are the mechanisms underlying the switch from phasic to graded transmitter release that we observe? One possibility is that mGluR activation alters the kinetics, voltage dependence, and/or unitary conductances of calcium channels involved in transmitter release, as has been described previously. We feel this is unlikely though, since we saw no effect of mGluR agonists on the amplitude or kinetics of sustained dendritic calcium transients evoked by somatic depolarization (Fig. 22). Another possibility that we favor is that group I mGluR activation may modulate aspects of release downstream of calcium entry, allowing the relatively modest calcium elevations associated with subthreshold voltage to become "unmasked" as potent triggers of subthreshold transmitter release. Such an unmasking could be mediated by changes in vesicle dynamics or fusion-mode (Zakharenko et al., 2002), or changes in the calcium sensitivity of transmitter release(Glitsch, 2006).

In support of this latter possibility, there is growing evidence that the relationship between calcium influx and transmitter release can be modified by second messenger cascades. Lou et al (2005) have recently proposed that the presynaptic calcium sensor for vesicle fusion is modulated by phorbol esters, which target the protein kinase C (PKC)/munc-13 signaling cascade. Under their proposal, phorbol esters enhance the apparent sensitivity of the calcium sensor near basal calcium concentrations, with a concomitant reduction in calcium cooperativity (from ~4^{th} order to ~1^{st} order). Intriguingly, this co-modulation of sensitivity and cooperativity would predict that small elevations of intracellular calcium, normally undetected by the release

machinery, become linearly coupled to transmitter output. This may be sufficient to explain the unmasked regime of graded release that we observe.

Another possibility is that distinct molecular mechanisms mediate sub-and suprathreshold transmitter release from mitral cell dendrites, and that the subthreshold machinery is selectively sensitized by mGluR activation. Although this is somewhat more speculative, recent studies have proposed "dual-sensor" models of transmitter release (Sun et al., 2007), in which a low affinity calcium sensor (most likely synaptotagmin 2 at the calyx of Held) mediates synchronous release, while a higher affinity (and lower cooperativity) calcium sensor supports asynchronous, sustained release for sustained calcium elevations. In axonal release, the basal calcium elevations favorable for asynchronous release are thought to be present only when vigorous spiking results in bulk calcium accumulation(Atluri and Regehr, 1996;Atluri and Regehr, 1998). However, in dendrites these elevations of basal calcium may be achievable without action potentials, and possibly via the sustained plateau-like potentials we describe (Figure 22).

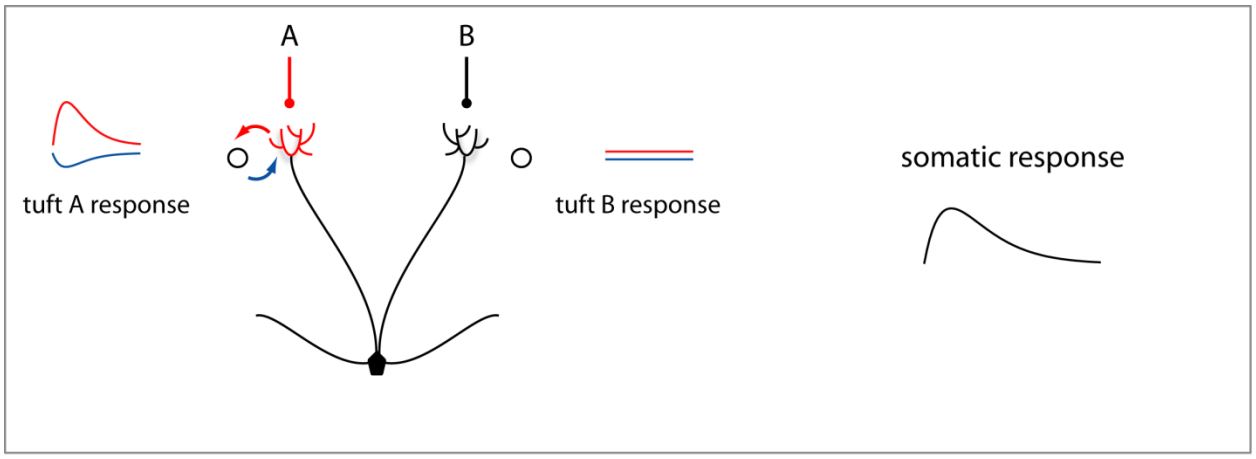
A
B
tuft A response
tuft B response
somatic response

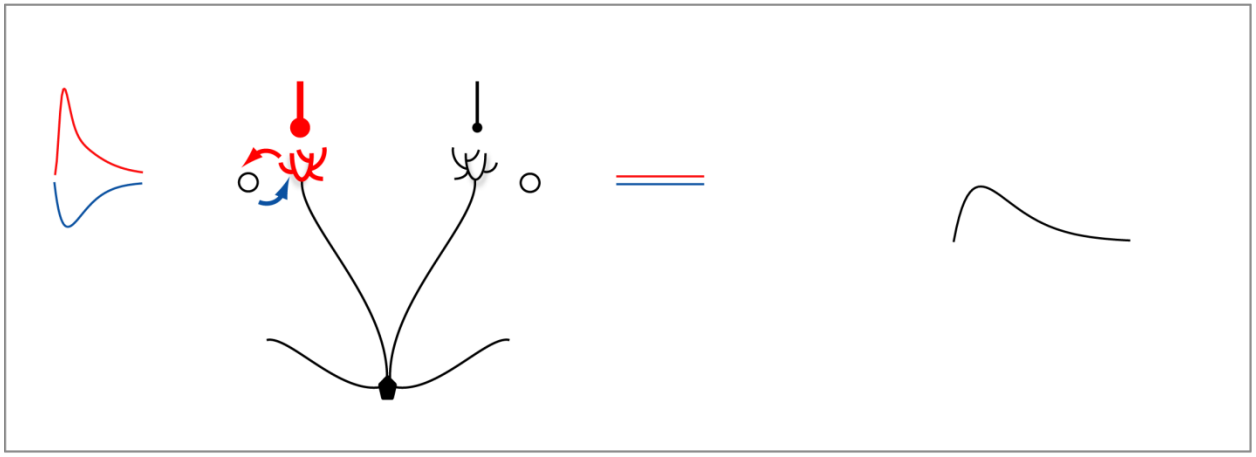

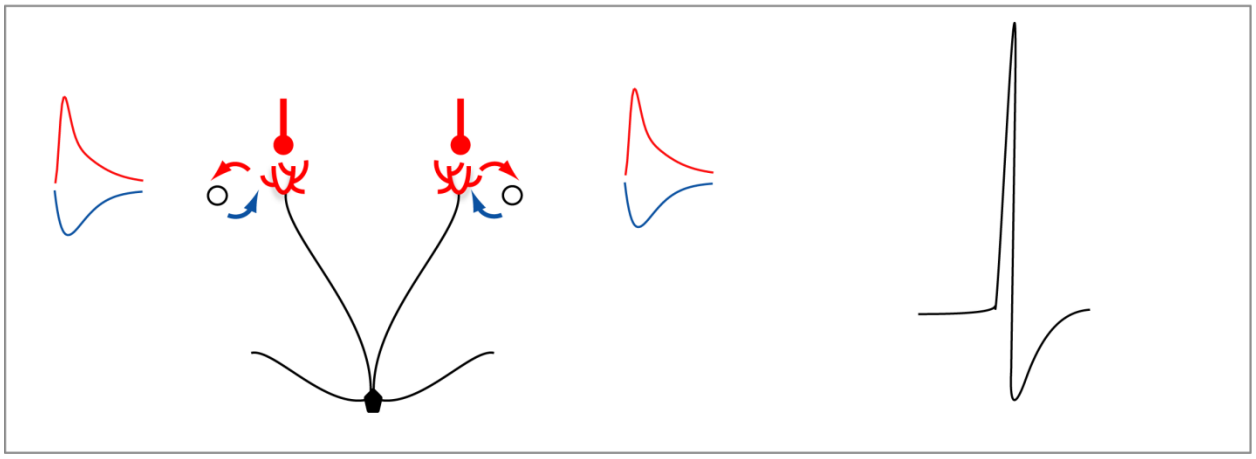

Figure 26. Compartmentalized dendritic integration in single tufts, and pheromone blend detection. Shown are three input regimes for a hypothetical mitral cell selective for the binary compound "AB." Each tuft is assumed to receive input from a distinct population of VRNs (either A or B) Top panel: weak input to the "A tuft" is amplified locally by regenerative conductances (red), while recruiting a small amount of local, recurrent inhibition (blue). This results in a subthreshold EPSP in the mitral cell soma (black trace, right). Middle panel: stronger input to tuft A evokes a stereotyped, regenerative event in the tuft (red), and strongly activates recurrent, tuft-specific inhibition (blue). Despite this larger input, the mitral cell somatic response is still subthreshold (black trace, right). Bottom panel: the mitral cell spikes only when compounds A and B are present.

5.5 DENDRITIC TRANSMITTER RELEASE IN AOB FUNCTION

This thesis has investigated several aspects of dendritic excitability and synaptic processing in AOB circuits that may contribute to the selectivity of pheromone integration. Because the responses of single or few AOB mitral cells are likely to be behaviorally relevant, signaling the presence of highly specific stimuli at the sensory periphery, it is important that the activation and axonal discharge of these cells be regulated. Below we describe how the findings of this thesis – which describe the regulation and modulation of recurrent inhibition over several spatial and temporal scales - may be integrated into an account of pheromone processing.

The responses of at least some AOB mitral cells in vivo are exquisitely selective, firing only for particular combinations of strain and gender-specific molecules that may convey individual identity (Luo et al., 2003). Typically, such highly specific responses are observed in cells many synapses into the CNS. (Imagine finding a face-selective cell in the retina or even V1!) How is this accomplished in the AOB, a relatively peripheral structure, with an economy of synapses and cell-types? Part of this selectivity is certainly due to the specificity of VN sensory neurons and vomeronasal receptors, however additional selectivity may be gained from the active compartmentalization of input processing within distinct regions of the dendritic trees of AOB mitral cells.

In **chapter 2**, we observed that the individual tufts of AOB mitral cells support local calcium spikes. These dendritic spikes amplify local VRN inputs and are also potent triggers of dendritic glutamate release and concomitant recurrent inhibition via glomerular interneurons. This interplay between excitability and inhibition may help enforce an all-or-none activation of individual tufts such that single tufts depolarize the mitral cell soma by a fixed amount. All-or none activation of tufts, in turn, will make mitral cell spiking more sensitive to the total number of tufts activated than to the absolute input to any given tuft. Under the assumption of heterotypic connectivity, in which mitral cells function as detectors of multi-component pheromone “blends,” across their tufts, this would help ensure that mitral cells respond only

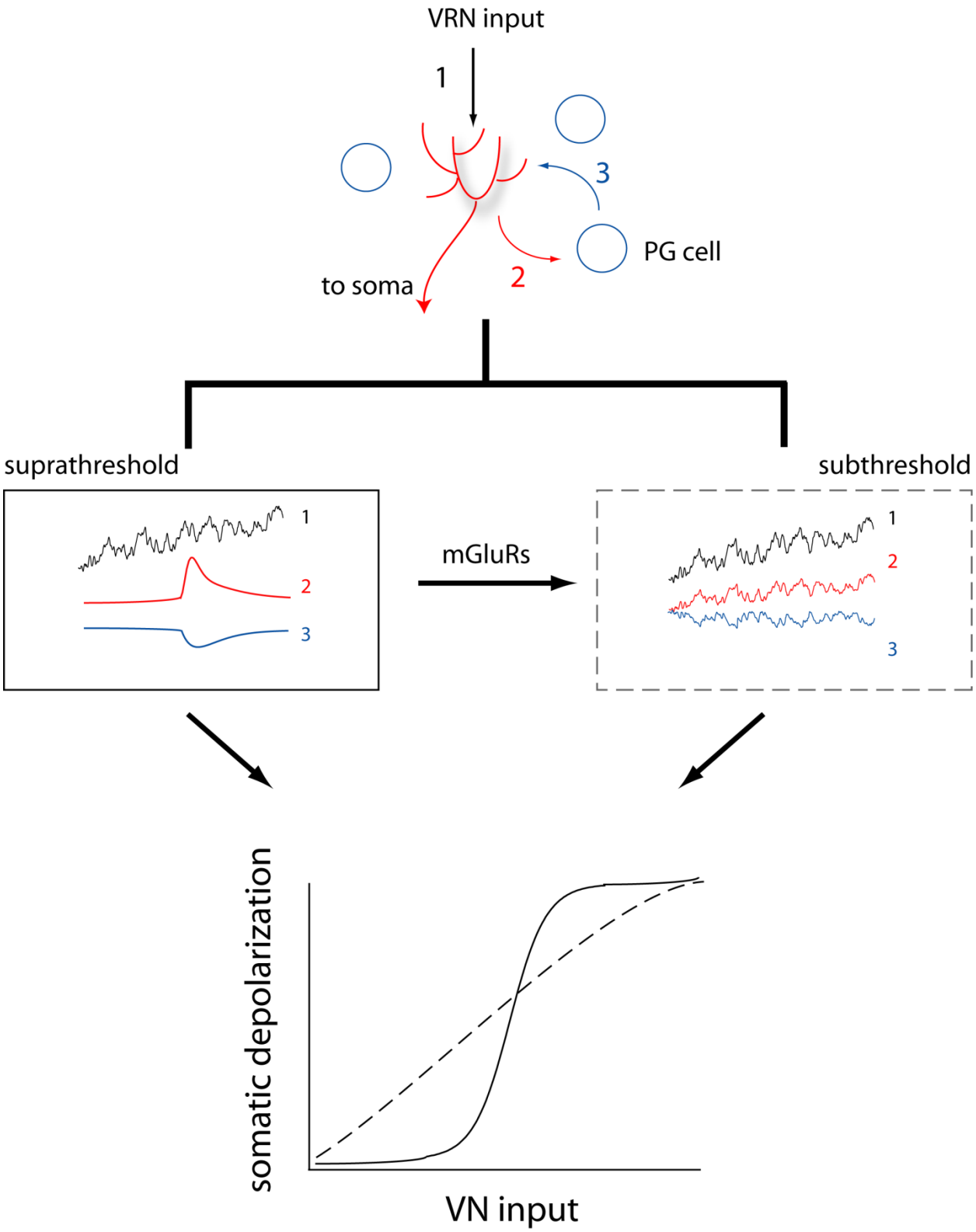
VRN input
1
3
PG cell
2
to soma
suprathreshold
subthreshold
1
2
3
mGluRs
1
2
3
somatic depolarization
VN input

Figure 27. Two modes of mitral cell output. The ***top schematic*** shows integrative and output events occurring at a mitral cell tuft (red branched structure). *(1, black arrow)* sustained VRN input to the tuft; *(2, red arrow)* glutamatergic output from tuft to PG cell (blue circle); *(3 ,blue arrow)* inhibitory feedback from PG cell to tuft. ***Middle panels*** show schematics of tuft input and output during integration. The left box shows the baseline situation: when VRN input (black trace) reaches a threshold level, a tuft spike is triggered (red trace), eliciting feedback inhibition (blue trace). The right dashed box shows the same series of input-output events after the mGluR –induced switch to subthreshold transmitter release. VRN input (*1, black*) is similar to the control case, but now evokes sustained, graded, glutamatergic tuft output (*2, red*). This graded output results in graded feedback from PG cells (*3, blue*). The ***bottom graph*** shows a schematic of how these different release modes may affect the input-output (I-O) function of the mitral cell. Under control conditions (solid line), the I-O relationship is steeply sigmoidal due to the all-or-none nature of tuft spikes. For conditions of graded tuft output, the I-O relationship is substantially linearized.

when multiple blend components are present (Fig. 26). Consider, for example, a hypothetical AOB mitral cell that sensitively reports on the presence of a binary compound "AB" conveying strain and gender specific information (Fig. 26). This cell must respond only to the conjunction of chemicals A and B, yet not produce "false positives" when A or B are present alone, even at high concentrations. Under our proposed model, responses to even low concentrations of A will be sensitively amplified by regenerative conductances in the tuft (Fig. 26, top). When A is present at greater concentration, these same regenerative conductances recruit local, tuft-specific inhibition (Fig. 26, middle), in effect "clamping" the tuft at some maximal level of depolarization. When compound B is present as well, however, both tufts provide a fixed amount of somatic depolarization which may drive mitral cell axonal spiking (Fig. 26, bottom).

Of course, at some sufficiently high level of input, activation of a single tuft is likely to elicit mitral cell spiking. How do mitral cells maintain their dynamic range and tuning to specific pheromone blends when faced with large inputs? One possibility is that the sensitivity or gain of synaptic inputs to the AOB is altered by high activity. This issue has been explored to some degree in the MOB. Wachowiak and colleagues, for example, have shown that OSN inputs are inhibited presynaptically to prevent saturation of inputs to glomeruli (Wachowiak et al., 2005). Another intriguing possibility, which we provide evidence for in chapters 3 and 4, is that high-intensity input to mitral cells alters the efficacy of recurrent inhibition.

This modulation of mitral cell recurrent inhibition appears to have two components. One is the strong regulation of spike evoked recurrent inhibition by metabotropic glutamate receptors (mGluRs). Because activation of mGluR1 is required for mitral cell recurrent inhibition, and mGluRs are typically activated only for vigorous neural activity, this suggests that the potency of recurrent inhibition scales with mitral cell firing rate. Thus, at low levels of spiking, mitral cells may be essentially "disengaged" from their supporting inhibitory interneurons to allow for sensitive responses and robust throughput. By contrast, inhibitory interneurons will be sensitized during high levels of mitral cell spiking to strongly oppose further increases in mitral cell activity.

In addition to these "priming" effects on recurrent inhibition, mGluRs may also change the mechanisms by which mitral cells inhibit themselves (Fig. 27). Under conditions of low mGluR activation (presumably low levels of VN input), mitral cell self-inhibition requires relatively specific types of dendritic activity – backpropagating action potentials, and local tuft

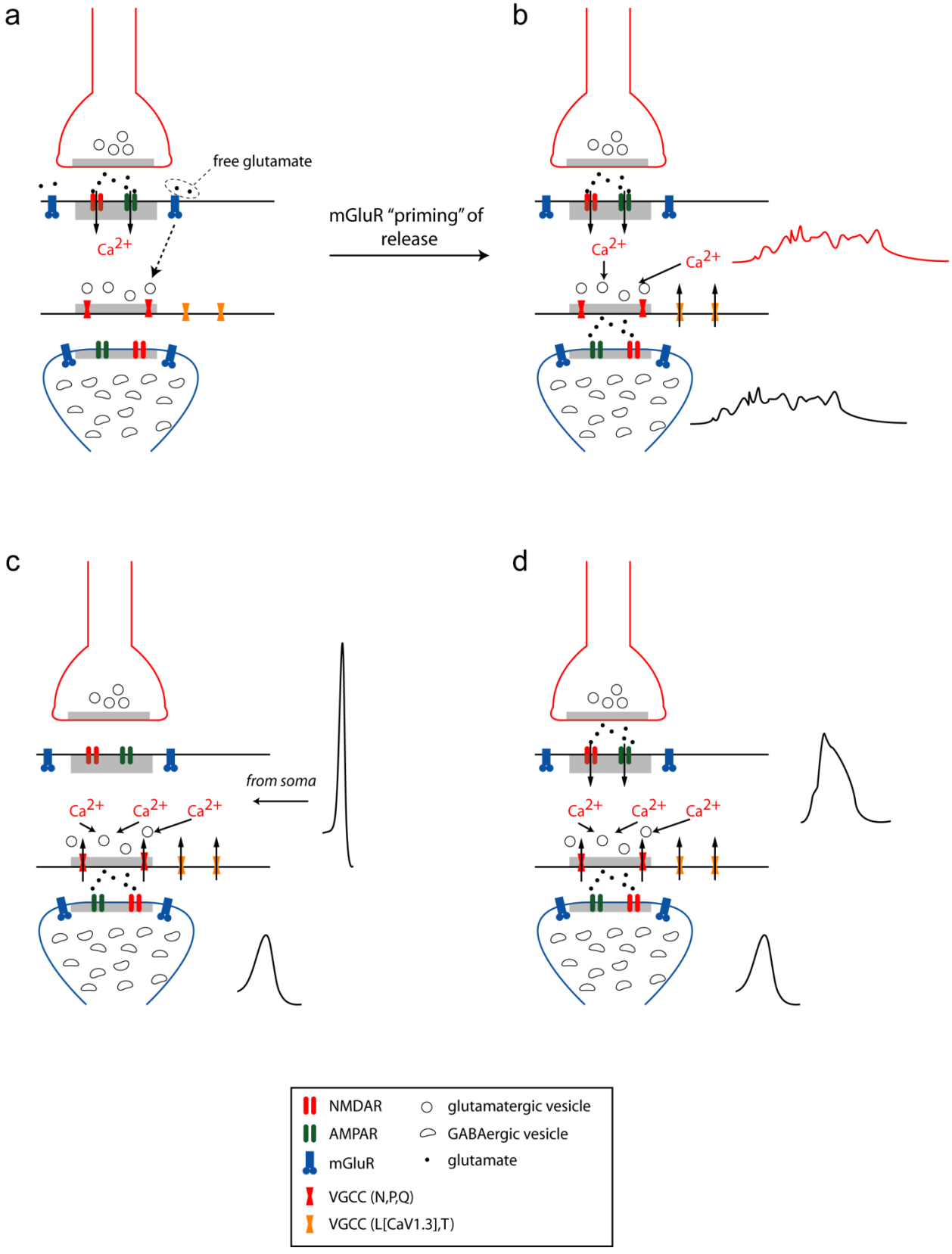
a
free glutamate
Ca2+
mGluR "priming" of release
b
Ca2+
Ca2+
c
from soma
Ca2+
Ca2+
Ca2+
d
Ca2+
Ca2+
Ca2+
NMDAR
AMPAR
mGluR
VGCC (N,P,Q)
VGCC (L[CaV1.3],T)
glutamatergic vesicle
GABAergic vesicle
glutamate

Figure 28. Possible release modes of mitral cell dendrites. a) Following pheromone transduction, glutamate is release from VRN terminals (red) onto mitral cell tufts. This leads to calcium influx via NMDARs and may activate extrasynaptic mGluRs for sufficient presynaptic input. mGluR activation is proposed to facilitate glutamatergic output (onto PG cells (blue, bottom)) by priming vesicle release. b) In the primed state, bulk calcium influx via NMDARs, or "low-voltage" calcium channels (such as the T-type, or CaV1.3) may be sufficient to trigger glutamate exocytosis. The calcium signal observed in mitral cell dendrites (red) will closely mirror subthreshold voltage changes, and will produce sustained glutamatergic output (black). c) Suprathreshold release can occur in mitral cell tufts in response to backpropagating action potentials (BAPs). BAPs likely coordinate glutamate release via a combination of LVA and HVA calcium channels and make use of active zone machinery. d) Local synaptic input can evoke poorly propagating branch spikes that may make use of the same release mechanisms as BAP-coordinated release.

spikes (Fig. 27). Following higher levels of input though, a qualitatively different form of self-inhibition is unmasked in which recurrent inhibition is driven by sustained subthreshold glutamate release from mitral cell dendrites (Fig. 27). This suggests that bouts of vigorous input to mitral cells may induce a mode-switch from spike-evoked inhibitory feedback to continuous inhibitory feedback. Following this mode-switch, recurrent inhibition would be markedly more sensitive, and mitral cell spikes would only be elicited for periods of sustained input.

In summary, mitral cell dendrites appear to support three distinct modes of glutamate output (Fig. 28): subthreshold output (which occurs following activation of group I mGluRs), tuft-spike coupled output, and BAP-coupled output. Subthreshold output is likely to occur only after levels of free or extrasynaptic glutamate are sufficient to activate mGluRs. By a mechanism that is yet not understood, mGluR signaling potentiates exocytosis of glutamatergic vesicles from mitral cell dendrites. In this primed condition, calcium from "low threshold" sources – such as NMDARs or T or L-type (CaV1.3) channels is sufficient to evoke release (Fig. 28b). Calcium influx within ultrastructurally defined active zones may not be necessary for excocytosis, as has been documented at other synapses.

Unless mGluRs have primed release however, mitral cell output will likely occur by either of two "suprathreshold" mechanisms. In one case, somatic action potentials (evoked by synaptic stimulation) can backpropagate into mitral cell tufts and lead to the opening of voltage gated calcium channels. It is likely that these "full blown" spikes will activate both HVA and LVA calcium channels, and that at least a component of release occurs at well-defined active zones (Fig. 28c). The other suprathreshold output from mitral cell dendrites will be the synaptically evoked tuft calcium spikes described in **Chapter 2**. For sufficient levels of input, regenerative branch spikes will be initiated in tufts. Although we have not fully characterized these branch spikes pharmacologically, they are likely to be mediated by combination NMDARs and both LVA and HVA calcium channels.

6.0 BIBLIOGRAPHY

Alle H, Geiger JR (2006) Combined analog and action potential coding in hippocampal mossy fibers. Science 311:1290-1293.

Araneda RC, Firestein S (2006) Adrenergic enhancement of inhibitory transmission in the accessory olfactory bulb. J Neurosci 26:3292-3298.

Archie KA, Mel BW (2000) A model for intradendritic computation of binocular disparity. Nat Neurosci 3:54-63.

Atluri PP, Regehr WG (1996) Determinants of the time course of facilitation at the granule cell to Purkinje cell synapse. J Neurosci 16:5661-5671.

Atluri PP, Regehr WG (1998) Delayed release of neurotransmitter from cerebellar granule cells. J Neurosci 18:8214-8227.

Augustine GJ, Charlton MP, Smith SJ (1985) Calcium entry and transmitter release at voltage-clamped nerve terminals of squid. J Physiol 367:163-181.

Awatramani GB, Price GD, Trussell LO (2005) Modulation of transmitter release by presynaptic resting potential and background calcium levels. Neuron 48:109-121.

Ayali A, Johnson BR, Harris-Warrick RM (1998) Dopamine modulates graded and spike-evoked synaptic inhibition independently at single synapses in pyloric network of lobster. J Neurophysiol 79:2063-2069.

Barnes S (1994) After transduction: response shaping and control of transmission by ion channels of the photoreceptor inner segments. Neuroscience 58:447-459.

Batchelor AM, Garthwaite J (1997) Frequency detection and temporally dispersed synaptic signal association through a metabotropic glutamate receptor pathway. Nature 385:74-77.

Behseta S, Kass RE (2005) Testing equality of two functions using BARS. Stat Med 24:3523-3534.

Behseta S, Kass RE, Moorman DE, Olson CR (2007) Testing equality of several functions: analysis of single-unit firing-rate curves across multiple experimental conditions. Stat Med 26:3958-3975.

Belluscio L, Koentges G, Axel R, Dulac C (1999) A map of pheromone receptor activation in the mammalian brain. Cell 97:209-220.

Berghard A, Buck LB (1996) Sensory transduction in vomeronasal neurons: evidence for G alpha o, G alpha i2, and adenylyl cyclase II as major components of a pheromone signaling cascade. J Neurosci 16:909-918.

Berghard A, Buck LB, Liman ER (1996) Evidence for distinct signaling mechanisms in two mammalian olfactory sense organs. Proc Natl Acad Sci U S A 93:2365-2369.

Besson MJ, Cheramy A, Feltz P, Glowinski J (1969) Release of newly synthesized dopamine from dopamine-containing terminals in the striatum of the rat. Proc Natl Acad Sci U S A 62:741-748.

Best AR, Thompson JV, Fletcher ML, Wilson DA (2005) Cortical metabotropic glutamate receptors contribute to habituation of a simple odor-evoked behavior. J Neurosci 25:2513-2517.

Bhalla US, Bower JM (1993) Exploring parameter space in detailed single neuron models: simulations of the mitral and granule cells of the olfactory bulb. J Neurophys 69:1948-1965.

Bian X, Yanagawa Y, Chen WR, Luo M (2008) Cortical-like functional organization of the pheromone-processing circuits in the medial amygdala. J Neurophysiol 99:77-86.

Bischofberger J, Jonas P (1997) Action potential propagation into the presynaptic dendrites of rat mitral cells. J Physiol (Lond) 504:359-365.

Bjorklund A, Lindvall O (1975) Dopamine in dendrites of substantia nigra neurons: suggestions for a role in dendritic terminals. Brain Res 83:531-537.

Bocskei Z, Findlay JB, North AC, Phillips SE, Somers WS, Wright CE, Lionetti C, Tirindelli R, Cavaggioni A (1991) Crystallization of and preliminary X-ray data for the mouse major urinary protein and rat alpha-2u globulin. J Mol Biol 218:699-701.

Bocskei Z, Groom CR, Flower DR, Wright CE, Phillips SE, Cavaggioni A, Findlay JB, North AC (1992) Pheromone binding to two rodent urinary proteins revealed by X-ray crystallography. Nature 360:186-188.

Boehm U, Zou Z, Buck LB (2005) Feedback loops link odor and pheromone signaling with reproduction. Cell 123:683-695.

Bollmann JH, Sakmann B, Borst JG (2000) Calcium sensitivity of glutamate release in a calyx-type terminal. Science 289:953-957.

Borer KT, Powers JB, Winans SS, Valenstein ES (1974) Influence of olfactory bulb removal on ingestive behaviors, activity levels, and self-stimulation in hamsters. J Comp Physiol Psychol 86:396-403.

Brasnjo G, Otis TS (2001) Neuronal glutamate transporters control activation of postsynaptic metabotropic glutamate receptors and influence cerebellar long-term depression. Neuron 31:607-616.

Brennan PA, Keverne EB (1997) Neural mechanisms of mammalian olfactory learning. Prog Neurobiol 51:457-481.

Brenowitz SD, Regehr WG (2003) Calcium dependence of retrograde inhibition by endocannabinoids at synapses onto Purkinje cells. J Neurosci 23:6373-6384.

Broman I (1920) Die Organon vomero-nasale Jacobsoni-ein Wassergeruchsorgan. Anat Hefte 58:143-191.

Brown SP, Brenowitz SD, Regehr WG (2003) Brief presynaptic bursts evoke synapse-specific retrograde inhibition mediated by endogenous cannabinoids. Nat Neurosci 6:1048-1057.

Brown SP, Safo PK, Regehr WG (2004) Endocannabinoids inhibit transmission at granule cell to Purkinje cell synapses by modulating three types of presynaptic calcium channels. J Neurosci 24:5623-5631.

BRUCE HM, Parrott DM (1960) Role of olfactory sense in pregnancy block by strange males. Science 131:1526.

Butenandt A, BECKMANN R, HECKER E (1961a) [On the sexattractant of silk-moths. I. The biological test and the isolation of the pure sex-attractant bombykol.]. Hoppe Seylers Z Physiol Chem 324:71-83.

Butenandt A, BECKMANN R, STAMM D (1961b) [On the sexattractant of silk-months. II. Constitution and configuration of bombvkol.]. Hoppe Seylers Z Physiol Chem 324:84-87.

Cajal S (1995) Histology of the Nervous System of Man and Vertebrates. Oxford: Oxford University Press.

Carlson GC, Shipley MT, Keller A (2000) Long-lasting depolarizations in mitral cells of the rat olfactory bulb. J Neurosci 20:2011-2021.

Cartmell J, Schoepp DD (2000) Regulation of neurotransmitter release by metabotropic glutamate receptors. J Neurochem 75:889-907.

Castillo PE, Carleton A, Vincent JD, Lledo PM (1999) Multiple and opposing roles of cholinergic transmission in the main olfactory bulb. J Neurosci 19:9180-9191.

Castro JB, Hovis KR, Urban NN (2007) Recurrent dendrodendritic inhibition of accessory olfactory bulb mitral cells requires activation of group I metabotropic glutamate receptors. J Neurosci 27:5664-5671.

Chamero P, Marton TF, Logan DW, Flanagan K, Cruz JR, Saghatelian A, Cravatt BF, Stowers L (2007) Identification of protein pheromones that promote aggressive behaviour. Nature 450:899-902.

Charpak S, Gahwiler BH, Do KQ, Knopfel T (1990) Potassium conductances in hippocampal neurons blocked by excitatory amino-acid transmitters. Nature 347:765-767.

Charpak S, Mertz J, Beaurepaire E, Moreaux L, Delaney K (2001) Odor-evoked calcium signals in dendrites of rat mitral cells. Proc Natl Acad Sci U S A 98:1230-1234.

Chavez AE, Singer JH, Diamond JS (2006) Fast neurotransmitter release triggered by Ca influx through AMPA-type glutamate receptors. Nature 443:705-708.

Chavis P, Ango F, Michel JM, Bockaert J, Fagni L (1998) Modulation of big K+ channel activity by ryanodine receptors and L-type Ca2+ channels in neurons. Eur J Neurosci 10:2322-2327.

Chavis P, Fagni L, Lansman JB, Bockaert J (1996) Functional coupling between ryanodine receptors and L-type calcium channels in neurons. Nature 382:719-722.

Cheetham SA, Thom MD, Jury F, Ollier WE, Beynon RJ, Hurst JL (2007) The genetic basis of individual-recognition signals in the mouse. Curr Biol 17:1771-1777.

Chen WR, Midtgaard J, Shepherd GM (1997) Forward and backward propagation of dendritic impulses and their synaptic control in mitral cells. Science 278:463-467.

Chen WR, Shen GY, Shepherd GM, Hines ML, Midtgaard J (2002) Multiple modes of action potential initiation and propagation in mitral cell primary dendrite. J Neurophysiol 88:2755-2764.

Chen WR, Xiong W, Shepherd GM (2000) Analysis of relations between NMDA receptors and GABA release at olfactory bulb reciprocal synapses. Neuron 25:625-633.

Christie JM, Westbrook GL (2003) Regulation of backpropagating action potentials in mitral cell lateral dendrites by A-type potassium currents. J Neurophysiol 89:2466-2472.

Clancy AN, Macrides F, Singer AG, Agosta WC (1984) Male hamster copulatory responses to a high molecular weight fraction of vaginal discharge: effects of vomeronasal organ removal. Physiol Behav 33:653-660.

Clark B, Hausser M (2006) Neural coding: hybrid analog and digital signalling in axons. Curr Biol 16:R585-R588.

Conn PJ, Pin JP (1997) Pharmacology and functions of metabotropic glutamate receptors. Annu Rev Pharmacol Toxicol 37:205-237.

Coquelin A, Clancy AN, Macrides F, Noble EP, Gorski RA (1984) Pheromonally induced release of luteinizing hormone in male mice: involvement of the vomeronasal system. J Neurosci 4:2230-2236.

Cox CL, Sherman SM (2000) Control of dendritic outputs of inhibitory interneurons in the lateral geniculate nucleus. Neuron 27:597-610.

Cox CL, Zhou Q, Sherman SM (1998) Glutamate locally activates dendritic outputs of thalamic interneurons. Nature 394:478-482.

Davison IG, Boyd JD, Delaney KR (2004) Dopamine inhibits mitral/tufted--> granule cell synapses in the frog olfactory bulb. J Neurosci 24:8057-8067.

De Saint JD, Westbrook GL (2007) Disynaptic amplification of metabotropic glutamate receptor 1 responses in the olfactory bulb. J Neurosci 27:132-140.

Debarbieux F, Audinat E, Charpak S (2003) Action potential propagation in dendrites of rat mitral cells in vivo. J Neurosci 23:5553-5560.

Del Punta K, Leinders-Zufall T, Rodriguez I, Jukam D, Wysocki CJ, Ogawa S, Zufall F, Mombaerts P (2002a) Deficient pheromone responses in mice lacking a cluster of vomeronasal receptor genes. Nature 419:70-74.

Del Punta K, Puche A, Adams NC, Rodriguez I, Mombaerts P (2002b) A divergent pattern of sensory axonal projections is rendered convergent by second-order neurons in the accessory olfactory bulb. Neuron 35:1057-1066.

Del Punta K, Rothman A, Rodriguez I, Mombaerts P (2000) Sequence diversity and genomic organization of vomeronasal receptor genes in the mouse. Genome Res 10:1958-1967.

DEL CJ, KATZ B (1954) Changes in end-plate activity produced by presynaptic polarization. J Physiol 124:586-604.

del RE, McLaughlin M, Downes CP, Nicholls DG (1999) Differential coupling of G-protein-linked receptors to Ca2+ mobilization through inositol(1,4,5)trisphosphate or ryanodine receptors in cerebellar granule cells in primary culture. Eur J Neurosci 11:3015-3022.

Djurisic M, Antic S, Chen WR, Zecevic D (2004) Voltage imaging from dendrites of mitral cells: EPSP attenuation and spike trigger zones. J Neurosci 24:6703-6714.

Dodge FA, Jr., Rahamimoff R (1967) Co-operative action a calcium ions in transmitter release at the neuromuscular junction. J Physiol 193:419-432.

Dong HW, Hayar A, Ennis M (2007) Activation of group I metabotropic glutamate receptors on main olfactory bulb granule cells and periglomerular cells enhances synaptic inhibition of mitral cells. J Neurosci 27:5654-5663.

Dulac C, Axel R (1995) A novel family of genes encoding putative pheromone receptors in mammals. Cell 83:195-206.

Dulac C, Torello AT (2003) Molecular detection of pheromone signals in mammals: from genes to behaviour. Nat Rev Neurosci 4:551-562.

Egger V, Svoboda K, Mainen ZF (2003) Mechanisms of lateral inhibition in the olfactory bulb: efficiency and modulation of spike-evoked calcium influx into granule cells. J Neurosci 23:7551-7558.

Egger V, Svoboda K, Mainen ZF (2005) Dendrodendritic synaptic signals in olfactory bulb granule cells: local spine boost and global low-threshold spike. J Neurosci 25:3521-3530.

Egger V, Urban NN (2006) Dynamic connectivity in the mitral cell-granule cell microcircuit. Seminars in Cell and Developmental Biology 17.

Eisthen HL, Sengelaub DR, Schroeder DM, Alberts JR (1994) Anatomy and forebrain projections of the olfactory and vomeronasal organs in axolotls (Ambystoma mexicanum). Brain Behav Evol 44:108-124.

Euler T, Detwiler PB, Denk W (2002) Directionally selective calcium signals in dendrites of starburst amacrine cells. Nature 418:845-852.

EYZAGUIRRE C, KUFFLER SW (1955) Processes of excitation in the dendrites and in the soma of single isolated sensory nerve cells of the lobster and crayfish. J Gen Physiol 39:87-119.

Fagni L, Chavis P, Ango F, Bockaert J (2000) Complex interactions between mGluRs, intracellular Ca2+ stores and ion channels in neurons. Trends Neurosci 23:80-88.

Falkenburger BH, Barstow KL, Mintz IM (2001) Dendrodendritic inhibition through reversal of dopamine transport. Science 293:2465-2470.

Finch EA, Augustine GJ (1998a) Local calcium signalling by inositol-1,4,5-trisphosphate in Purkinje cell dendrites. Nature 396:753-756.

Finch EA, Augustine GJ (1998b) Local calcium signalling by inositol-1,4,5-trisphosphate in Purkinje cell dendrites. Nature 396:753-756.

Frick A, Magee J, Johnston D (2004) LTP is accompanied by an enhanced local excitability of pyramidal neuron dendrites. Nat Neurosci 7:126-135.

Froemke RC, Poo MM, Dan Y (2005) Spike-timing-dependent synaptic plasticity depends on dendritic location. Nature 434:221-225.

Gall CM, Hendry SH, Seroogy KB, Jones EG, Haycock JW (1987) Evidence for coexistence of GABA and dopamine in neurons of the rat olfactory bulb. J comp Neurol 266:307-318.

Geffen LB, Jessell TM, Cuello AC, Iversen LL (1976) Release of dopamine from dendrites in rat substantia nigra. Nature 260:258-260.

Glitsch M (2006) Selective inhibition of spontaneous but not Ca2+ -dependent release machinery by presynaptic group II mGluRs in rat cerebellar slices. J Neurophysiol 96:86-96.

Golding NL, Spruston N (1998) Dendritic sodium spikes are variable triggers of axonal action potentials in hippocampal CA1 pyramidal neurons. Neuron 21:1189-1200.

Golding NL, Staff NP, Spruston N (2002) Dendritic spikes as a mechanism for cooperative long-term potentiation. Nature 418:326-331.

Govindaiah, Cox CL (2004) Synaptic activation of metabotropic glutamate receptors regulates dendritic outputs of thalamic interneurons. Neuron 41:611-623.

Graubard K, Raper JA, Hartline DK (1980) Graded synaptic transmission between spiking neurons. Proc Natl Acad Sci U S A 77:3733-3735.

Greenwood DR, Comeskey D, Hunt MB, Rasmussen LE (2005) Chemical communication: chirality in elephant pheromones. Nature 438:1097-1098.

Halabisky B, Friedman D, Radojicic M, Strowbridge BW (2000) Calcium influx through NMDA receptors directly evokes GABA release in olfactory bulb granule cells. J Neurosci 20:5124-5134.

Halasz N, Nowycky M, Hokfelt T, Shepherd GM, Markey K, Goldstein M (1982) Dopaminergic periglomerular cells in the turtle olfactory bulb. Brain Res Bull 9:383-389.

Halpern M, Martinez-Marcos A (2003) Structure and function of the vomeronasal system: an update. Prog Neurobiol 70:245-318.

Hausser M, Mel B (2003) Dendrites: bug or feature? Curr Opin Neurobiol 13:372-383.

Hausser M, Spruston N, Stuart GJ (2000) Diversity and dynamics of dendritic signaling. Science 290:739-744.

Hausser M, Stuart G, Racca C, Sakmann B (1995) Axonal initiation and active dendritic propagation of action potentials in substantia nigra neurons. Neuron 15:637-647.

Hayashi JH, Stuart AE (1993) Currents in the presynaptic terminal arbors of barnacle photoreceptors. Vis Neurosci 10:261-270.

Hayashi Y, Momiyama A, Takahashi T, Ohishi H, Ogawa-Meguro R, Shigemoto R, Mizuno N, Nakanishi S (1993) Role of a metabotropic glutamate receptor in synaptic modulation in the accessory olfactory bulb. Nature 366:687-690.

Hefft S, Jonas P (2005) Asynchronous GABA release generates long-lasting inhibition at a hippocampal interneuron-principal neuron synapse. Nat Neurosci 8:1319-1328.

Heinbockel T, Heyward P, Conquet F, Ennis M (2004) Regulation of main olfactory bulb mitral cell excitability by metabotropic glutamate receptor mGluR1. J Neurophysiol 92:3085-3096.

Heinbockel T, Laaris N, Ennis M (2006) Metabotropic Glutamate Receptors in the Main Olfactory Bulb Drive Granule Cell-Mediated Inhibition. J Neurophysiol.

Heinbockel T, Laaris N, Ennis M (2007) Metabotropic glutamate receptors in the main olfactory bulb drive granule cell-mediated inhibition. J Neurophysiol 97:858-870.

Helton TD, Xu W, Lipscombe D (2005) Neuronal L-type calcium channels open quickly and are inhibited slowly. J Neurosci 25:10247-10251.

Hildebrand JG (1995) Analysis of chemical signals by nervous systems. Proc Natl Acad Sci U S A 92:67-74.

Hoffman DA, Magee JC, Colbert CM, Johnston D (1997) K+ channel regulation of signal propagation in dendrites of hippocampal pyramidal neurons. Nature 387:869-875.

Holy TE, Dulac C, Meister M (2000) Responses of vomeronasal neurons to natural stimuli. Science 289:1569-1572.

Huguenard JR (1996) Low-threshold calcium currents in central nervous system neurons. Annu Rev Physiol 58:329-348.

Humphries RE, Robertson DH, Beynon RJ, Hurst JL (1999) Unravelling the chemical basis of competitive scent marking in house mice. Anim Behav 58:1177-1190.

Isaacson JS (1999) Glutamate spillover mediates excitatory transmission in the rat olfactory bulb. Neuron 23:377-384.

Isaacson JS (2000) Spillover in the spotlight. Curr Biol 10:R475-R477.

Isaacson JS (2001) Mechanisms governing dendritic gamma-aminobutyric acid (GABA) release in the rat olfactory bulb. Proc Natl Acad Sci U S A 98:337-342.

Isaacson JS, Strowbridge BW (1998) Olfactory reciprocal synapses: dendritic signaling in the CNS. Neuron 20:749-761.

Isaacson JS, Vitten H (2003) GABA(B) receptors inhibit dendrodendritic transmission in the rat olfactory bulb. J Neurosci 23:2032-2039.

Ito I, Kohda A, Tanabe S, Hirose E, Hayashi M, Mitsunaga S, Sugiyama H (1992) 3,5-Dihydroxyphenyl-glycine: a potent agonist of metabotropic glutamate receptors. Neuroreport 3:1013-1016.

Ivanov AI, Calabrese RL (2006b) Graded inhibitory synaptic transmission between leech interneurons: assessing the roles of two kinetically distinct low-threshold Ca currents. J Neurophysiol 96:218-234.

Ivanov AI, Calabrese RL (2006a) Graded inhibitory synaptic transmission between leech interneurons: assessing the roles of two kinetically distinct low-threshold Ca currents. J Neurophysiol 96:218-234.

Ivanov AI, Calabrese RL (2006c) Spike-mediated and graded inhibitory synaptic transmission between leech interneurons: evidence for shared release sites. J Neurophysiol 96:235-251.

Jahr CE, Nicoll RA (1980) Dendrodendritic inhibition: demonstration with intracellular recording. Science 207:1473-1475.

Jahr CE, Nicoll RA (1982a) An intracellular analysis of dendrodendritic inhibition in the turtle in vitro olfactory bulb. J Physiol (Lond) 326:213-34:213-234.

Jahr CE, Nicoll RA (1982b) Noradrenergic modulation of dendrodendritic inhibition in the olfactory bulb. Nature 297:227-229.

James W (1890) The Principles of Psychology. Harvard University Press.

Jia C, Chen WR, Shepherd GM (1999a) Synaptic organization and neurotransmitters in the rat accessory olfactory bulb. J Neurophysiol 81:345-355.

Jia C, Chen WR, Shepherd GM (1999b) Synaptic organization and neurotransmitters in the rat accessory olfactory bulb. J Neurophysiol 81:345-355.

Jia C, Goldman G, Halpern M (1997) Development of vomeronasal receptor neuron subclasses and establishment of topographic projections to the accessory olfactory bulb. Brain Res Dev Brain Res 102:209-216.

Juusola M, French AS, Uusitalo RO, Weckstrom M (1996) Information processing by graded-potential transmission through tonically active synapses. Trends Neurosci 19:292-297.

Kaba H, Hayashi Y, Higuchi T, Nakanishi S (1994) Induction of an olfactory memory by the activation of a metabotropic glutamate receptor. Science 265:262-264.

Kaba H, Keverne EB (1988) The effect of microinfusions of drugs into the accessory olfactory bulb on the olfactory block to pregnancy. Neuroscience 25:1007-1011.

Kaneko N, Debski EA, Wilson MC, Whitten WK (1980) Puberty acceleration in mice. II. Evidence that the vomeronasal organ isa receptor for the primer pheromone in male mouse urine. Biol Reprod 22:873-878.

KARLSON P, LUSCHER M (1959) Pheromones': a new term for a class of biologically active substances. Nature 183:55-56.

Kasowski HJ, Kim H, Greer CA (1999) Compartmental organization of the olfactory bulb glomerulus. J comp Neurol 407:261-274.

Keverne EB, Brennan PA (1996) Olfactory recognition memory. J Physiol Paris 90:399-401.

Kevetter GA, Winans SS (1981) Connections of the corticomedial amygdala in the golden hamster. I. Efferents of the "vomeronasal amygdala". J Comp Neurol 197:81-98.

Kimchi T, Xu J, Dulac C (2007) A functional circuit underlying male sexual behaviour in the female mouse brain. Nature 448:1009-1014.

Kobayakawa K, Kobayakawa R, Matsumoto H, Oka Y, Imai T, Ikawa M, Okabe M, Ikeda T, Itohara S, Kikusui T, Mori K, Sakano H (2007) Innate versus learned odour processing in the mouse olfactory bulb. Nature 450:503-508.

Koch C, Segev I (2000) The role of single neurons in information processing. Nat Neurosci 3 Suppl:1171-1177.

Konig P, Engel AK, Singer W (1996) Integrator or coincidence detector? The role of the cortical neuron revisited. Trends Neurosci 19:130-137.

Korf J, Zieleman M, Westerink BH (1976) Dopamine release in substantia nigra? Nature 260:257-258.

Kosaka K, Hama K, Nagatsu I, Wu JY, Kosaka T (1988) Possible coexistence of amino acid (gamma-aminobutyric acid), amine (dopamine) and peptide (substance P); neurons containing immunoreactivities for glutamic acid decarboxylase, tyrosine hydroxylase and substance P in the hamster main olfactory bulb. Exp Brain Res 71:633-642.

Kreitzer AC, Regehr WG (2001) Cerebellar depolarization-induced suppression of inhibition is mediated by endogenous cannabinoids. J Neurosci 21:RC174.

Kudoh SN, Taguchi T (2002b) A simple exploratory algorithm for the accurate and fast detection of spontaneous synaptic events. Biosens Bioelectron 17:773-782.

Kudoh SN, Taguchi T (2002a) A simple exploratory algorithm for the accurate and fast detection of spontaneous synaptic events. Biosens Bioelectron 17:773-782.

Landisman CE, Connors BW (2005) Long-term modulation of electrical synapses in the mammalian thalamus. Science 310:1809-1813.

Larkum ME, Zhu JJ, Sakmann B (1999) A new cellular mechanism for coupling inputs arriving at different cortical layers. Nature 398:338-341.

Leinders-Zufall T, Lane AP, Puche AC, Ma W, Novotny MV, Shipley MT, Zufall F (2000) Ultrasensitive pheromone detection by mammalian vomeronasal neurons. Nature 405:792-796.

Letzkus JJ, Kampa BM, Stuart GJ (2006) Learning rules for spike timing-dependent plasticity depend on dendritic synapse location. J Neurosci 26:10420-10429.

Lewis RS, Hudspeth AJ (1983) Voltage- and ion-dependent conductances in solitary vertebrate hair cells. Nature 304:538-541.

Leypold BG, Yu CR, Leinders-Zufall T, Kim MM, Zufall F, Axel R (2002) Altered sexual and social behaviors in trp2 mutant mice. Proc Natl Acad Sci U S A 99:6376-6381.

Liman ER, Corey DP (1996) Electrophysiological characterization of chemosensory neurons from the mouse vomeronasal organ. J Neurosci 16:4625-4637.

Liman ER, Corey DP, Dulac C (1999) TRP2: a candidate transduction channel for mammalian pheromone sensory signaling. Proc Natl Acad Sci U S A 96:5791-5796.

Lin DM, Wang F, Lowe G, Gold GH, Axel R, Ngai J, Brunet L (2000) Formation of precise connections in the olfactory bulb occurs in the absence of odorant-evoked neuronal activity. Neuron 26:69-80.

Lin DY, Zhang SZ, Block E, Katz LC (2005) Encoding social signals in the mouse main olfactory bulb. Nature 434:470-477.

Lipscombe D, Helton TD, Xu W (2004) L-type calcium channels: the low down. J Neurophysiol 92:2633-2641.

Llinas R, Nicholson C, Freeman JA, Hillman DE (1968) Dendritic spikes and their inhibition in alligator Purkinje cells. Science 160:1132-1135.

Llinas R, Steinberg IZ, Walton K (1981) Relationship between presynaptic calcium current and postsynaptic potential in squid giant synapse. Biophys J 33:323-351.

Llinas R, Sugimori M (1980) Electrophysiological properties of in vitro Purkinje cell dendrites in mammalian cerebellar slices. J Physiol (Lond) 305:197-213:197-213.

Llinas R, Sugimori M, Silver RB (1992) Microdomains of high calcium concentration in a presynaptic terminal. Science 256:677-679.

Llinas RR, Sugimori M, Silver RB (1994) Localization of calcium concentration microdomains at the active zone in the squid giant synapse. Adv Second Messenger Phosphoprotein Res 29:133-137.

Lloyd-Thomas, Keverne B (1982) Role of the brain and accessory olfactory system in the block to pregnancy in mice. Neuroscience 7:907-913.

Lou X, Scheuss V, Schneggenburger R (2005) Allosteric modulation of the presynaptic Ca2+ sensor for vesicle fusion. Nature 435:497-501.

Lowe G (2002) Inhibition of backpropagating action potentials in mitral cell secondary dendrites. J Neurophysiol 88:64-85.

Lu YM, Jia Z, Janus C, Henderson JT, Gerlai R, Wojtowicz JM, Roder JC (1997) Mice lacking metabotropic glutamate receptor 5 show impaired learning and reduced CA1 long-term potentiation (LTP) but normal CA3 LTP. J Neurosci 17:5196-5205.

Lucas P, Ukhanov K, Leinders-Zufall T, Zufall F (2003) A diacylglycerol-gated cation channel in vomeronasal neuron dendrites is impaired in TRPC2 mutant mice: mechanism of pheromone transduction. Neuron 40:551-561.

Ludwig M, Pittman QJ (2003) Talking back: dendritic neurotransmitter release. Trends Neurosci 26:255-261.

Luo M, Fee MS, Katz LC (2003) Encoding pheromonal signals in the accessory olfactory bulb of behaving mice. Science 299:1196-1201.

Luo M, Katz LC (2004) Encoding pheromonal signals in the mammalian vomeronasal system. Curr Opin Neurobiol 14:428-434.

Ma J, Lowe G (2004) Action potential backpropagation and multiglomerular signaling in the rat vomeronasal system. J Neurosci 24:9341-9352.

Magee JC, Avery RB, Christie BR, Johnston D (1996) DIHYDROPYRIDINE-SENSITIVE, VOLTAGE-GATED CA2+ CHANNELS CONTRIBUTE TO THE RESTING INTRACELLULAR CA2+ CONCENTRATION OF HIPPOCAMPAL CA1 PYRAMIDAL NEURONS. J Neurophys 76:3460-3470.

Maher BJ, Westbrook GL (2008) Co-transmission of dopamine and GABA in periglomerular cells. J Neurophysiol.

Margrie TW, Sakmann B, Urban NN (2001) Action potential propagation in mitral cell lateral dendrites is decremental and controls recurrent and lateral inhibition in the mammalian olfactory bulb. Proc Natl Acad Sci U S A 98:319-324.

Markram H, Sakmann B (1994) Calcium transients in dendrites of neocortical neurons evoked by single subthreshold excitatory postsynaptic potentials via low- voltage-activated calcium channels. Proceedings of the National Academy of Sciences of the United States of America 91:5207-5211.

Martin LJ, Blackstone CD, Huganir RL, Price DL (1992) Cellular localization of a metabotropic glutamate receptor in rat brain. Neuron 9:259-270.

Masu M, Tanabe Y, Tsuchida K, Shigemoto R, Nakanishi S (1991) Sequence and expression of a metabotropic glutamate receptor. Nature 349:760-765.

Matsui K, Jahr CE (2003) Ectopic release of synaptic vesicles. Neuron 40:1173-1183.

Matsui K, Jahr CE (2004) Differential control of synaptic and ectopic vesicular release of glutamate. J Neurosci 24:8932-8939.

McCulloch W, Pitts W (1943) Bulletin of Mathematical Biophysics 5:115-133.

McLean JH, Shipley MT (1987) Serotonergic afferents to the rat olfactory bulb: I. Origins and laminar specificity of serotonergic inputs in the adult rat. J Neurosci 7:3016-3028.

McLean JH, Shipley MT, Nickell WT, ston-Jones G, Reyher CK (1989) Chemoanatomical organization of the noradrenergic input from locus coeruleus to the olfactory bulb of the adult rat. J Comp Neurol 285:339-349.

McQuiston AR, Katz LC (2001) Electrophysiology of interneurons in the glomerular layer of the rat olfactory bulb. J Neurophysiol 86:1899-1907.

Meisami E, Bhatnagar KP (1998) Structure and diversity in mammalian accessory olfactory bulb. Microsc Res Tech 43:476-499.

Mel BW (1993) Synaptic integration in an excitable dendritic tree. J Neurophys 70:1086-1101.

Meredith M (1998) Vomeronasal, olfactory, hormonal convergence in the brain. Cooperation or coincidence? Ann N Y Acad Sci 855:349-361.

Meredith M, O'Connell RJ (1979) Efferent control of stimulus access to the hamster vomeronasal organ. J Physiol 286:301-316.

Migliore M, Shepherd GM (2002) Emerging rules for the distributions of active dendritic conductances. Nat Rev Neurosci 3:362-370.

Mitchell SJ, Silver RA (2000) Glutamate spillover suppresses inhibition by activating presynaptic mGluRs. Nature 404:498-502.

Mombaerts P (2004) Odorant receptor gene choice in olfactory sensory neurons: the one receptor-one neuron hypothesis revisited. Curr Opin Neurobiol 14:31-36.

Mori K, Nowycky MC, Shepherd GM (1981) Electrophysiological analysis of mitral cells in the isolated turtle olfactory bulb. J Physiol (Lond) 314:281-94:281-294.

Mori K, Nowycky MC, Shepherd GM (1982a) Impulse activity in presynaptic dendrites: analysis of mitral cells in the isolated turtle olfactory bulb. J Neurosci 2:497-502.

Mori K, Nowycky MC, Shepherd GM (1982b) Impulse activity in presynaptic dendrites: analysis of mitral cells in the isolated turtle olfactory bulb. J Neurosci 2:497-502.

Murphy GJ, Darcy DP, Isaacson JS (2005) Intraglomerular inhibition: signaling mechanisms of an olfactory microcircuit. Nat Neurosci 8:354-364.

Neher E, Sakaba T (2001) Estimating transmitter release rates from postsynaptic current fluctuations. J Neurosci 21:9638-9654.

Nicoll RA, Jahr CE (1982) Self-excitation of olfactory bulb neurones. Nature 296:441-444.

Nolan MF, Malleret G, Dudman JT, Buhl DL, Santoro B, Gibbs E, Vronskaya S, Buzsaki G, Siegelbaum SA, Kandel ER, Morozov A (2004) A behavioral role for dendritic integration: HCN1 channels constrain spatial memory and plasticity at inputs to distal dendrites of CA1 pyramidal neurons. Cell 119:719-732.

Novotny M, Harvey S, Jemiolo B, Alberts J (1985) Synthetic pheromones that promote inter-male aggression in mice. Proc Natl Acad Sci U S A 82:2059-2061.

Novotny M, Schwende FJ, Wiesler D, Jorgenson JW, Carmack M (1984) Identification of a testosterone-dependent unique volatile constituent of male mouse urine: 7-exo-ethyl-5-methyl-6,8-dioxabicyclo[3.2.1]-3-octene. Experientia 40:217-219.

Ohishi H, Shigemoto R, Nakanishi S, Mizuno N (1993) Distribution of the mRNA for a metabotropic glutamate receptor (mGluR3) in the rat brain: an in situ hybridization study. J comp Neurol 335:252-266.

Ozaki M, Wada-Katsumata A, Fujikawa K, Iwasaki M, Yokohari F, Satoji Y, Nisimura T, Yamaoka R (2005) Ant nestmate and non-nestmate discrimination by a chemosensory sensillum. Science 309:311-314.

Pan ZH, Hu HJ, Perring P, Andrade R (2001) T-type Ca(2+) channels mediate neurotransmitter release in retinal bipolar cells. Neuron 32:89-98.

PHILLIPS CG, Powell TP, Shepherd GM (1963) RESPONSES OF MITRAL CELLS TO STIMULATION OF THE LATERAL OLFACTORY TRACT IN THE RABBIT. J Physiol 168:65-88.

Pinato G, Midtgaard J (2003) Regulation of granule cell excitability by a low-threshold calcium spike in turtle olfactory bulb. J Neurophysiol 90:3341-3351.

Pinato G, Midtgaard J (2005) Dendritic sodium spikelets and low-threshold calcium spikes in turtle olfactory bulb granule cells. J Neurophysiol 93:1285-1294.

Pinching AJ, Powell TP (1971a) The neuron types of the glomerular layer of the olfactory bulb. J Cell Sci 9:305-345.

Pinching AJ, Powell TP (1971b) The neuropil of the glomeruli of the olfactory bulb. J Cell Sci 9:347-377.

Pinching AJ, Powell TP (1971c) The neuropil of the periglomerular region of the olfactory bulb. J Cell Sci 9:379-409.

Pinching AJ, Powell TP (1972) Experimental studies on the axons intrinsic to the glomerular layer of the olfactory bulb. J Cell Sci 10:637-655.

Poirazi P, Brannon T, Mel BW (2003) Pyramidal neuron as two-layer neural network. Neuron 37:989-999.

Polsky A, Mel BW, Schiller J (2004) Computational subunits in thin dendrites of pyramidal cells. Nat Neurosci 7:621-627.

Pow DV, Morris JF (1989) Dendrites of hypothalamic magnocellular neurons release neurohypophysial peptides by exocytosis. Neuroscience 32:435-439.

Powers JB, Winans SS (1973) Sexual behavior in peripherally anosmic male hamsters. Physiol Behav 10:361-368.

Powers JB, Winans SS (1975) Vomeronasal organ: critical role in mediating sexual behavior of the male hamster. Science 187:961-963.

Prescott ED, Zenisek D (2005) Recent progress towards understanding the synaptic ribbon. Curr Opin Neurobiol 15:431-436.

Price JL, Powell TP (1970a) The morphology of the granule cells of the olfactory bulb. J Cell Sci 7:91-123.

Price JL, Powell TP (1970b) The synaptology of the granule cells of the olfactory bulb. J Cell Sci 7:125-155.

Rall W, Shepherd GM (1968) Theoretical reconstruction of field potentials and dendrodendritic synaptic interactions in olfactory bulb. J Neurophys 31:884-915.

Rall W, Shepherd GM, Reese TS, Brightman MW (1966) Dendrodendritic synaptic pathway for inhibition in the olfactory bulb. Experimental Neurology 14:44-56.

Rancz EA, Hausser M (2006) Dendritic calcium spikes are tunable triggers of cannabinoid release and short-term synaptic plasticity in cerebellar Purkinje neurons. J Neurosci 26:5428-5437.

Reed RR (1992) Signaling pathways in odorant detection. Neuron 8:205-209.

Regehr WG, Connor JA, Tank DW (1989) Optical imaging of calcium accumulation in hippocampal pyramidal cells during synaptic activation. Nature 341:533-536.

Rodriguez I, Feinstein P, Mombaerts P (1999) Variable patterns of axonal projections of sensory neurons in the mouse vomeronasal system. Cell 97:199-208.

Ronnett GV, Cho H, Hester LD, Wood SF, Snyder SH (1993) Odorants differentially enhance phosphoinositide turnover and adenylyl cyclase in olfactory receptor neuronal cultures. J Neurosci 13:1751-1758.

Ronnett GV, Snyder SH (1992) Molecular messengers of olfaction. Trends Neurosci 15:508-513.

Ryba NJ, Tirindelli R (1997) A new multigene family of putative pheromone receptors. Neuron 19:371-379.

Sabatini BL, Svoboda K (2000) Analysis of calcium channels in single spines using optical fluctuation analysis. Nature 408:589-593.

Sahara Y, Kubota T, Ichikawa M (2001) Cellular localization of metabotropic glutamate receptors mGluR1, 2/3, 5 and 7 in the main and accessory olfactory bulb of the rat. Neurosci Lett 312:59-62.

Sam M, Vora S, Malnic B, Ma W, Novotny MV, Buck LB (2001) Neuropharmacology. Odorants may arouse instinctive behaviours. Nature 412:142.

Scanziani M, Salin PA, Vogt KE, Malenka RC, Nicoll RA (1997) Use-dependent increases in glutamate concentration activate presynaptic metabotropic glutamate receptors. Nature 385:630-634.

Schaal B, Coureaud G, Langlois D, Ginies C, Semon E, Perrier G (2003) Chemical and behavioural characterization of the rabbit mammary pheromone. Nature 424:68-72.

Schaefer ML, Young DA, Restrepo D (2001) Olfactory fingerprints for major histocompatibility complex-determined body odors. J Neurosci 21:2481-2487.

Schild D, Geiling H, Bischofberger J (1995) Imaging of L-type Ca2+ channels in olfactory bulb neurones using fluorescent dihydropyridine and a styryl dye. J Neurosci Methods 59:183-190.

Schiller J, Helmchen F, Sakmann B (1995) Spatial profile of dendritic calcium transients evoked by action potentials in rat neocortical pyramidal neurones. Journal of Physiology 487:583-600.

Schiller J, Major G, Koester HJ, Schiller Y (2000) NMDA spikes in basal dendrites of cortical pyramidal neurons. Nature 404:285-289.

Schiller J, Schiller Y (2001) NMDA receptor-mediated dendritic spikes and coincident signal amplification. Curr Opin Neurobiol 11:343-348.

Schiller J, Schiller Y, Stuart G, Sakmann B (1997) Calcium action potentials restricted to distal apical dendrites of rat neocortical pyramidal neurons. J Physiol (Lond) 505:605-616.

Schneggenburger R, Neher E (2000) Intracellular calcium dependence of transmitter release rates at a fast central synapse. Nature 406:889-893.

Schoppa NE, Kinzie JM, Sahara Y, Segerson TP, Westbrook GL (1998) Dendrodendritic inhibition in the olfactory bulb is driven by NMDA receptors. J Neurosci 18:6790-6802.

Schoppa NE, Urban NN (2003) Dendritic processing within olfactory bulb circuits. Trends Neurosci 26:501-506.

Schoppa NE, Westbrook GL (1997) Modulation of mEPSCs in olfactory bulb mitral cells by metabotropic glutamate receptors. J Neurophysiol 78:1468-1475.

Schoppa NE, Westbrook GL (2001) Glomerulus-specific synchronization of mitral cells in the olfactory bulb. Neuron 31:639-651.

Schoppa NE, Westbrook GL (2002) AMPA autoreceptors drive correlated spiking in olfactory bulb glomeruli. Nat Neurosci 5:1194-1202.

Schuman EM, Madison DV (1991) A requirement for the intercellular messenger nitric oxide in long-term potentiation. Science 254:1503-1506.

Serulle Y, Sugimori M, Llinas RR (2007) Imaging synaptosomal calcium concentration microdomains and vesicle fusion by using total internal reflection fluorescent microscopy. Proc Natl Acad Sci U S A 104:1697-1702.

Shapiro E, Castellucci VF, Kandel ER (1980a) Presynaptic inhibition in Aplysia involves a decrease in the Ca2+ current of the presynaptic neuron. Proc Natl Acad Sci U S A 77:1185-1189.

Shapiro E, Castellucci VF, Kandel ER (1980b) Presynaptic membrane potential affects transmitter release in an identified neuron in Aplysia by modulating the Ca2+ and K+ currents. Proc Natl Acad Sci U S A 77:629-633.

Shepherd GM (1963) NEURONAL SYSTEMS CONTROLLING MITRAL CELL EXCITABILITY. J Physiol 168:101-117.

Shepherd GM (1978) Microcircuits in the nervous system. Sci Am 238:93-103.

Shepherd G (1991) Foundations of the Neuron Doctrine. New York: Oxford University Press.

Shepherd G (2004) The Synaptic Organization of the Brain. New York: Oxford University Press.

Sherborne AL, Thom MD, Paterson S, Jury F, Ollier WE, Stockley P, Beynon RJ, Hurst JL (2007) The genetic basis of inbreeding avoidance in house mice. Curr Biol 17:2061-2066.

Sherrington C (1906) The Integrative Action of the Nervous System. New York: Charles Scribner's Sons.

Shigemoto R, Nakanishi S, Mizuno N (1992) Distribution of the mRNA for a metabotropic glutamate receptor (mGluR1) in the central nervous system: an in situ hybridization study in adult and developing rat. J comp Neurol 322:121-135.

Shipley MT, Halloran FJ, de la TJ (1985) Surprisingly rich projection from locus coeruleus to the olfactory bulb in the rat. Brain Res 329:294-299.

Shu Y, Hasenstaub A, Duque A, Yu Y, McCormick DA (2006) Modulation of intracortical synaptic potentials by presynaptic somatic membrane potential. Nature 441:761-765.

Singer AG, Agosta WC, O'Connell RJ, Pfaffmann C, Bowen DV, Field FH (1976) Dimethyl disulfide: an attractant pheromone in hamster vaginal secretion. Science 191:948-950.

Singer AG, Macrides F, Clancy AN, Agosta WC (1986b) Purification and analysis of a proteinaceous aphrodisiac pheromone from hamster vaginal discharge. J Biol Chem 261:13323-13326.

Singer AG, Macrides F, Clancy AN, Agosta WC (1986a) Purification and analysis of a proteinaceous aphrodisiac pheromone from hamster vaginal discharge. J Biol Chem 261:13323-13326.

Spencer WA, Kandel ER (1968) Cellular and integrative properties of the hippocampal pyramidal cell and the comparative electrophysiology of cortical neurons. Int J Neurol 6:266-296.

Sterling P, Matthews G (2005) Structure and function of ribbon synapses. Trends Neurosci 28:20-29.

Stowers L, Holy TE, Meister M, Dulac C, Koentges G (2002) Loss of sex discrimination and male-male aggression in mice deficient for TRP2. Science 295:1493-1500.

Stuart G, Hausser M (1994) Initiation and spread of sodium action potentials in cerebellar Purkinje cells. Neuron 13:703-712.

Stuart G, Schiller J, Sakmann B (1997) Action potential initiation and propagation in rat neocortical pyramidal neurons. J Physiol 505 (Pt 3):617-632.

Stuart G, Spruston N (1995) Probing dendritic function with patch pipettes. Curr Opin Neurobiol 5:389-394.

Stuart GJ, Sakmann B (1994) Active propagation of somatic action potentials into neocortical pyramidal cell dendrites. Nature 367:69-72.

Sun J, Pang ZP, Qin D, Fahim AT, Adachi R, Sudhof TC (2007) A dual-Ca2+-sensor model for neurotransmitter release in a central synapse. Nature 450:676-682.

Takahashi T, Forsythe ID, Tsujimoto T, Barnes-Davies M, Onodera K (1996) Presynaptic calcium current modulation by a metabotropic glutamate receptor. Science 274:594-597.

Takami S, Graziadei PP (1990) Morphological complexity of the glomerulus in the rat accessory olfactory bulb--a Golgi study. Brain Res 510:339-342.

Takami S, Graziadei PP (1991) Light microscopic Golgi study of mitral/tufted cells in the accessory olfactory bulb of the adult rat. J Comp Neurol 311:65-83.

Takechi H, Eilers J, Konnerth A (1998) A new class of synaptic response involving calcium release in dendritic spines. Nature 396:757-760.

Taniguchi M, Kaba H (2001) Properties of reciprocal synapses in the mouse accessory olfactory bulb. Neuroscience 108:365-370.

Teicher MH, Stewart WB, Kauer JS, Shepherd GM (1980) Suckling pheromone stimulation of a modified glomerular region in the developing rat olfactory bulb revealed by the 2-deoxyglucose method. Brain Res 194:530-535.

Tirindelli R, Mucignat-Caretta C, Ryba NJ (1998) Molecular aspects of pheromonal communication via the vomeronasal organ of mammals. Trends Neurosci 21:482-486.

Toida K, Kosaka K, Aika Y, Kosaka T (2000) Chemically defined neuron groups and their subpopulations in the glomerular layer of the rat main olfactory bulb--IV. Intraglomerular synapses of tyrosine hydroxylase-immunoreactive neurons. Neuroscience 101:11-17.

Trinh K, Storm DR (2003) Vomeronasal organ detects odorants in absence of signaling through main olfactory epithelium. Nat Neurosci 6:519-525.

Trinh K, Storm DR (2004) Detection of odorants through the main olfactory epithelium and vomeronasal organ of mice. Nutr Rev 62:S189-S192.

Trombley PQ, Shepherd GM (1992) Noradrenergic inhibition of synaptic transmission between mitral and granule cells in mammalian olfactory bulb cultures. J Neurosci 12:3985-3991.

Urban NN (2002) Lateral inhibition in the olfactory bulb and in olfaction. Physiol Behav 77:607-612.

Urban NN, Barrionuevo G (1998) Active summation of excitatory postsynaptic potentials in hippocampal CA3 pyramidal neurons. Proc Natl Acad Sci U S A 95:11450-11455.

Urban NN, Castro JB (2005) Tuft calcium spikes in accessory olfactory bulb mitral cells. J Neurosci 25:5024-5028.

Urban NN, Henze DA, Barrionuevo G (1998) Amplification of perforant-path EPSPs in CA3 pyramidal cells by LVA calcium and sodium channels. J Neurophysiol 80:1558-1561.

Urban NN, Sakmann B (2002) Reciprocal intraglomerular excitation and intra- and interglomerular lateral inhibition between mouse olfactory bulb mitral cells. J Physiol 542:355-367.

van den Pol AN (1995) Presynaptic metabotropic glutamate receptors in adult and developing neurons: autoexcitation in the olfactory bulb. J comp Neurol 359:253-271.

Vandenbergh JG, Whitsett JM, Lombardi JR (1975) Partial isolation of a pheromone accelerating puberty in female mice. J Reprod Fertil 43:515-523.

Vassar R, Ngai J, Axel R (1993) Spatial segregation of odorant receptor expression in the mammalian olfactory epithelium. Cell 74:309-318.

Wachowiak M, McGann JP, Heyward PM, Shao Z, Puche AC, Shipley MT (2005) Inhibition [corrected] of olfactory receptor neuron input to olfactory bulb glomeruli mediated by suppression of presynaptic calcium influx. J Neurophysiol 94:2700-2712.

Wagner S, Gresser AL, Torello AT, Dulac C (2006a) A Multireceptor Genetic Approach Uncovers an Ordered Integration of VNO Sensory Inputs in the Accessory Olfactory Bulb. Neuron 50:697-709.

Wagner S, Gresser AL, Torello AT, Dulac C (2006b) A multireceptor genetic approach uncovers an ordered integration of VNO sensory inputs in the accessory olfactory bulb. Neuron 50:697-709.

Wang Z, Xu NL, Wu CP, Duan S, Poo MM (2003) Bidirectional changes in spatial dendritic integration accompanying long-term synaptic modifications. Neuron 37:463-472.

Waters J, Helmchen F (2004) Boosting of action potential backpropagation by neocortical network activity in vivo. J Neurosci 24:11127-11136.

Waters J, Larkum M, Sakmann B, Helmchen F (2003) Supralinear Ca2+ influx into dendritic tufts of layer 2/3 neocortical pyramidal neurons in vitro and in vivo. J Neurosci 23:8558-8567.

Waters J, Schaefer A, Sakmann B (2005) Backpropagating action potentials in neurones: measurement, mechanisms and potential functions. Prog Biophys Mol Biol 87:145-170.

Wei DS, Mei YA, Bagal A, Kao JP, Thompson SM, Tang CM (2001) Compartmentalized and binary behavior of terminal dendrites in hippocampal pyramidal neurons. Science 293:2272-2275.

Willhite DC, Nguyen KT, Masurkar AV, Greer CA, Shepherd GM, Chen WR (2006) Viral tracing identifies distributed columnar organization in the olfactory bulb. Proc Natl Acad Sci U S A.

Williams JH, Errington ML, Lynch MA, Bliss TV (1989) Arachidonic acid induces a long-term activity-dependent enhancement of synaptic transmission in the hippocampus. Nature 341:739-742.

Wilson RI, Nicoll RA (2001) Endogenous cannabinoids mediate retrograde signalling at hippocampal synapses. Nature 410:588-592.

Woolf TB, Shepherd GM, Greer CA (1991) Local information processing in dendritic trees: subsets of spines in granule cells of the mammalian olfactory bulb. J Neurosci 11:1837-1854.

Wu TJ, Gibson MJ, Rogers MC, Silverman AJ (1997) New observations on the development of the gonadotropin-releasing hormone system in the mouse. J Neurobiol 33:983-998.

Xiong W, Chen WR (2002) Dynamic gating of spike propagation in the mitral cell lateral dendrites. Neuron 34:115-126.

Xu F, Schaefer M, Kida I, Schafer J, Liu N, Rothman DL, Hyder F, Restrepo D, Shepherd GM (2005) Simultaneous activation of mouse main and accessory olfactory bulbs by odors or pheromones. J Comp Neurol 489:491-500.

Yamazaki K (1982) [Distinctive odors governed by the major histocompatibility locus of the mouse (author's transl)]. Tanpakushitsu Kakusan Koso 27:535-548.

Yamazaki K, Beauchamp GK (2007) Genetic basis for MHC-dependent mate choice. Adv Genet 59:129-145.

Yamazaki K, Beauchamp GK, Kupniewski D, Bard J, Thomas L, Boyse EA (1988) Familial imprinting determines H-2 selective mating preferences. Science 240:1331-1332.

Yamazaki K, Beauchamp GK, Thomas L, Boyse EA (1984) Chemosensory identity of H-2 heterozygotes. J Mol Cell Immunol 1:79-82.

Yasuda R, Sabatini BL, Svoboda K (2003) Plasticity of calcium channels in dendritic spines. Nat Neurosci 6:948-955.

Yokoi M, Mori K, Nakanishi S (1995) Refinement of odor molecule tuning by dendrodendritic synaptic inhibition in the olfactory bulb. Proc Natl Acad Sci U S A 92:3371-3375.

Yoon H, Enquist LW, Dulac C (2005) Olfactory inputs to hypothalamic neurons controlling reproduction and fertility. Cell 123:669-682.

Yuan Q, Knopfel T (2006a) Olfactory nerve stimulation-evoked mGluR1 slow potentials, oscillations, and calcium signaling in mouse olfactory bulb mitral cells. J Neurophysiol 95:3097-3104.

Yuan Q, Knopfel T (2006b) Olfactory nerve stimulation-induced calcium signaling in the mitral cell distal dendritic tuft. J Neurophysiol 95:2417-2426.

Yuan Q, Mutoh H, Debarbieux F, Knopfel T (2004) Calcium signaling in mitral cell dendrites of olfactory bulbs of neonatal rats and mice during olfactory nerve Stimulation and beta-adrenoceptor activation. Learn Mem 11:406-411.

Zakharenko SS, Zablow L, Siegelbaum SA (2002) Altered presynaptic vesicle release and cycling during mGluR-dependent LTD. Neuron 35:1099-1110.

Zelles T, Boyd JD, Hardy AB, Delaney KR (2006) Branch-specific Ca2+ influx from Na+-dependent dendritic spikes in olfactory granule cells. J Neurosci 26:30-40.

Zhou Z, Xiong W, Masurkar AV, Chen WR, Shepherd GM (2006a) Dendritic Calcium Plateau Potentials Modulate Input-Output Properties of Juxtaglomerular Cells in the Rat Olfactory Bulb. J Neurophysiol.

Zhou Z, Xiong W, Zeng S, Xia A, Shepherd GM, Greer CA, Chen WR (2006b) Dendritic excitability and calcium signalling in the mitral cell distal glomerular tuft. Eur J Neurosci 24:1623-1632.

Zilberter Y (2000) Dendritic release of glutamate suppresses synaptic inhibition of pyramidal neurons in rat neocortex. J Physiol 528:489-496.

Zilberter Y, Kaiser KM, Sakmann B (1999) Dendritic GABA release depresses excitatory transmission between layer 2/3 pyramidal and bitufted neurons in rat neocortex. Neuron 24:979-988.